UNIVERSIDADE FEDERAL DE MINAS GERAIS
Escola de Engenharia
Programa de Pós-Graduação em Engenharia Elétrica

Jonatan Mota Campos

ON THE OPTIMAL NONLINEAR ADAPTIVE CONTROL OF EULER-LAGRANGE SYSTEMS

Belo Horizonte, Brazil
2024

Jonatan Mota Campos

ON THE OPTIMAL NONLINEAR ADAPTIVE CONTROL OF EULER-LAGRANGE SYSTEMS

Dissertation submitted to the Graduate Program in Electrical Engineering of Universidade Federal de Minas Gerais, in partial fulfillment of the requirements for the degree of Master in Electrical Engineering.

Advisor: Prof. Dr. Guilherme Vianna Raffo
Co-advisor: Prof. Dr. Daniel Neri Cardoso

Belo Horizonte, Brazil
2024

Campos, Jonatan Mota.
C198o On the optimal nonlinear adaptive control of Euler-Lagrange Systems [recurso eletrônico] / Jonatan Mota Campos. – 2024.
1 recurso online (117 f. : il., color.) : pdf.

Orientadores: Guilherme Vianna Raffo, Daniel Neri Cardoso.

Dissertação (mestrado) – Universidade Federal de Minas Gerais, Escola de Engenharia.

Inclui bibliografia.

1. Engenharia elétrica – Teses. 2. Incerteza – Modelos matemáticos – Teses. 3. Controle robusto – Teses. 4. Lagrange, Equações de – Teses. 5. Números de Euler – Teses. I. Raffo, Guilherme Vianna. II. Cardoso, Daniel Neri. III. Universidade Federal de Minas Gerais. Escola de Engenharia. IV. Título.

CDU: 621.3(043)

Ficha catalográfica elaborada pelo bibliotecário Marcio A. A. Gomes CRB/6 2812
Biblioteca Prof. Mário Werneck, Escola de Engenharia da UFMG

UNIVERSIDADE FEDERAL DE MINAS GERAIS
ESCOLA DE ENGENHARIA
PROGRAMA DE PÓS-GRADUAÇÃO EM ENGENHARIA ELÉTRICA
FOLHA DE APROVAÇÃO

"On The Optimal Nonlinear Adaptive Control Of Euler-Lagrange Systems"

Jonatan Mota Campos

Dissertação de Mestrado submetida à Banca Examinadora designada pelo Colegiado do Programa de Pós-Graduação em Engenharia Elétrica da Escola de Engenharia da Universidade Federal de Minas Gerais, como requisito para obtenção do grau de Mestre em Engenharia Elétrica.

Aprovada em 04 de setembro de 2024.

Por:

Prof. Dr. Guilherme Vianna Raffo
DELT (UFMG) - Orientador

Prof. Dr. Daniel Neri Cardoso
PPGEE (UFMG) - Coorientador

Prof. Dr. Luis Antonio Aguirre
DELT (UFMG)

Prof. Dr. Leonardo Antônio Borges Torres
DELT (UFMG)

Prof. Dr. Víctor Costa da Silva Campos
DELT (UFMG)

Documento assinado eletronicamente por **Leonardo Antonio Borges Torres**, **Professor do**

Magistério Superior, em 04/09/2024, às 20:07, conforme horário oficial de Brasília, com fundamento no art. 5º do Decreto nº 10.543, de 13 de novembro de 2020.

Documento assinado eletronicamente por **Guilherme Vianna Raffo**, **Professor do Magistério Superior**, em 04/09/2024, às 20:15, conforme horário oficial de Brasília, com fundamento no art. 5º do Decreto nº 10.543, de 13 de novembro de 2020.

Documento assinado eletronicamente por **Luis Antonio Aguirre**, **Professor do Magistério Superior**, em 04/09/2024, às 21:02, conforme horário oficial de Brasília, com fundamento no art. 5º do Decreto nº 10.543, de 13 de novembro de 2020.

Documento assinado eletronicamente por **Victor Costa da Silva Campos**, **Professor do Magistério Superior**, em 04/09/2024, às 21:14, conforme horário oficial de Brasília, com fundamento no art. 5º do Decreto nº 10.543, de 13 de novembro de 2020.

Documento assinado eletronicamente por **Daniel Neri Cardoso**, **Professor Magistério Superior-Substituto**, em 05/09/2024, às 11:35, conforme horário oficial de Brasília, com fundamento no art. 5º do Decreto nº 10.543, de 13 de novembro de 2020.

A autenticidade deste documento pode ser conferida no site https://sei.ufmg.br/sei/controlador_externo.php?acao=documento_conferir&id_orgao_acesso_externo=0, informando o código verificador **3525933** e o código CRC **03C55FB9**.

Referência: Processo nº 23072.248154/2024-18 SEI nº 3525933

To my parents,
This achievement is as much yours as it is mine...

Acknowledgments

First and foremost, I would like to express my deepest gratitude to my parents for their support and for instilling in me the importance of critical thinking from an early age. Their influence has been profound, both in shaping my intellectual curiosity and in supporting me through the challenges of this Masters degree. As I navigate the complexities of scientific research, I find myself ever more appreciative of the sacrifices they made and the challenges they overcame during their own academic pursuits.

I am also profoundly grateful to my advisors, Guilherme Raffo and Daniel Neri. To Guilherme, thank you for the guidance, even when it came with necessary and constructive critique. To Daniel, your patience, encouragement, and those much-needed motivational chats have been a lifeline during the toughest moments of this journey. I would also like to acknowledge the incredible support of my colleagues at MACRO. Each of you has contributed to my growth as a researcher and a scholar, and for that, I am truly grateful.

I would like to offer my special thanks for the aid of the Brazilian public agencies CNPq, CAPES, FAPEMIG, and FAPESP as well as acknowledge the INCT (National Institute of Science and Technology) for Cooperative Autonomous Systems Applied to Security and Environment. Without their commitment to funding research, this work would not have been possible. Finally, I would like to extend my special thanks to all the Brazilian Universities and research centers, especially UFMG, for their unwavering support of the national research and their commitment with offering a free and high quality education for their students.

Resumo

Um dos principais desafios nas aplicações modernas de controle é lidar com sistemas que apresentam incertezas. O projeto de controle geralmente se baseia em modelos matemáticos que não podem descrevem completamente os fenômenos do mundo real, resultando em modelos com dinâmicas não modeladas e incertezas nos parâmetros. Além disso, os sistemas reais frequentemente enfrentam distúrbios externos e ruído de sensores, complicando ainda mais o projeto do controlador para manter o desempenho em meio às incertezas. Abordagens de controle robusto e adaptativo oferecem soluções viáveis para esses desafios. Estratégias de controle robusto, particularmente os controles ótimos $\mathcal{H}_2$ e $\mathcal{H}_\infty$, têm sido amplamente utilizados para lidar com as incertezas do sistema. Tradicionalmente formuladas no domínio da frequência para sistemas monovariáveis (SISO, do inglês single-input-single-output), essas estratégias se concentram em minimizar a energia da resposta ao impulso do sistema a distúrbios ou o ganho máximo do sistema em malha fechada aos sinais de distúrbio. Apesar de seu sucesso, as estratégias de controle $\mathcal{H}_2$ e $\mathcal{H}_\infty$ apresentam limitações, particularmente no controle do comportamento transitório. Para lidar com essa questão, abordagens recentes envolvem a formulacão desses controladores em espacos de Sobolev $\mathcal{W}_{m,p}$, melhorando o desempenho transitório ao considerar a norma $\mathcal{W}_{m,2}$ em vez da norma $\mathcal{L}_2$. Esses problemas de controle são comunmente tratados por meio de programacão dinâmica, envolvendo a solução complexa da equacão de Hamilton-Jacobi (HJ). O método de Extensão e Mistura do Regressor Dinâmico (DREM) apresenta um avanço significativo ao fornecer uma condição para a convergência dos parâmetros sem depender da condição de PE. Nesse contexto, esta dissertação de mestrado propõe controladores adaptativos robustos para gerenciar incertezas em sistemas de Euler-Lagrange. O controlador não linear $\mathcal{H}_\infty$ é estendido para uma formulação adaptativa, incorporando leis de adaptação baseadas na técnica DREM para garantir robustez contra distúrbios externos e alcançar a estimativa exata dos parâmetros sob condições menos rigorosas que a PE. Além disso, um controlador adaptativo não linear $\mathcal{W}_\infty$ é proposto para melhorar a resposta transitória.

Palavras-chave: controle robusto; controle adaptativo; controle não linear; controle ótimo; estimação de parâmetros..

Abstract

One of the primary challenges in modern control applications is managing systems with uncertainties. Control design typically relies on mathematical models that do not fully discreve real-world phenomena, resulting in models with unmodeled dynamics and parameter uncertainties. Additionally, real systems often face external disturbances and sensor noise, further complicating controller design to maintain performance amidst uncertainties. Robust and adaptive control approaches offer viable solutions to these challenges. Robust control strategies, particularly $\mathcal{H}_2$ and $\mathcal{H}_\infty$ optimal control, have been extensively used to address system uncertainties. Traditionally formulated in the frequency domain for single-input-single-output (SISO) systems, these strategies focus on minimizing the energy of the system's impulse response to disturbances or the maximum gain of the closed-loop system to disturbance signals. Despite their success, $\mathcal{H}_2$ and $\mathcal{H}_\infty$ control strategies have limitations, particularly in controlling transient behavior. To address this, recent approaches involve formulating these controllers in Sobolev spaces $\mathcal{W}_{m,p}$, enhancing transient performance by considering the $\mathcal{W}_{m,2}$-norm instead of the $\mathcal{L}_2$-norm. These control problems are often tackled through dynamic programming, involving the complex solution of the Hamilton-Jacobi (HJ) equation. The Dynamic Regressor Extension and Mixing (DREM) method presents a significant advancement by providing a necessary and sufficient condition for parameter convergence without relying on the PE condition. In this context, this Master thesis proposes robust adaptive controllers to manage uncertainties in Euler-Lagrange systems. The nonlinear $\mathcal{H}_\infty$ controller is extended to an adaptive formulation, incorporating update laws based on the DREM technique to ensure robustness against external disturbances and achieve exact parameter estimation under less stringent conditions than PE. Furthermore, an adaptive nonlinear $\mathcal{W}_\infty$ controller is proposed to enhance transient response.

Keywords: robust control; adaptive control; nonlinear control; optimal control; parameter estimation..

List of Figures

Acronyms

AC Adaptive Control.

CLRC Composite Learning Robot Control.

DOF Degrees of Freedom.

DREM Dynamic Regressor Extension and Mixing.

HJ Hamilton-Jacobi.

HJB Hamilton-Jacobi-Bellman.

HJBI Hamilton-Jacobi-Bellman-Isaacs.

IE Interval Excitation.

LMI Linear Matrix Inequality.

MIMO Multiple-Input Multiple-Output.

MPC Model Predictive Control.

MRAC Model Reference Adaptive Control.

MREM Memory Regressor Extension and Mixing.

NN Neural Network.

PDE Partial Differential Equation.

PE Persistency of Excitation.

PID Proportional Integral Derivative.

RL Reinforcement Learning.

SISO Single-Input Single-Output.

Notation

a	italic lower case letters denote scalars.
$\mathbb{N}$	the set of natural numbers, $\mathbb{N} \triangleq \{1, 2, 3...\}$.
$\mathbb{C}$	the set of complex numbers.
$\mathbb{Z}$	the set of integers, $\mathbb{Z} \triangleq \{..., -3, -2, -1, 0, 1, 2, 3, ...\}$.
$\mathbb{R}$	the set of real numbers, $\mathbb{R} \triangleq (-\infty, \ \infty)$.
$\mathbb{R}_{>0}$	the set of positive real numbers, $\mathbb{R}_{>0} \triangleq (0, \ \infty)$.
$\mathbb{R}_{\geq 0}$	the set of positive real numbers including zero, $\mathbb{R}_{\geq 0} \triangleq [0, \ \infty)$.
$\mathbb{R}^n$	the set of real vectors with dimension n, $\mathbb{R}^n \triangleq \{\boldsymbol{r} = [r_1 \ ... \ r_n]' : r_i \in \mathbb{R}, i \in \{1, ..., n\}\}$.
$\mathbb{R}^{n \times m}$	the set of real matrices with dimension $n \times m$, $\mathbb{R}^{n \times m} \triangleq \{\boldsymbol{R} = [\boldsymbol{r}_1 \ ... \ \boldsymbol{r}_m] : \boldsymbol{r}_i \in \mathbb{R}^n, i \in \{1, ..., m\}\}$.
$a \in \Omega$	a is an element of the set Ω.
$\Omega_1 \times \Omega_2$	denotes the Cartesian product between the sets Ω_1 and Ω_2.
$(.)'$	denotes the transpose of (.).
$(.)^{-1}$	denotes the inverse of the square matrix (.).
$\text{Trace}(\boldsymbol{A})$	Trace of A.
diag()	Diagonal matrix whose diagonal elements are given in the parentheses.
blkdiag(.)	represents a block diagonal matrix whose diagonal elements are the matrices or vectors given in the parentheses, and all off-diagonal blocks are zero matrices..
$\mathbf{0}$	zeros matrix with appropriate dimension.
$\boldsymbol{I}$	identity matrix with appropriate dimension.
$\mathbf{1}$	ones matrix with appropriate dimension.

$\boldsymbol{z}(\cdot) : \Omega \to \Gamma$	a function that maps the domain space Ω to the image space Γ.
$\mathcal{U} : \Omega \to \Gamma$	the set of functions that maps the space Ω to Γ.
$\dot{\boldsymbol{z}}(t)$	the time-derivative of the function $\boldsymbol{z}(t) : \mathbb{R}_{\geq 0} \to \mathbb{R}^{n_z}$, in which $t \in \mathbb{R}_{\geq 0}$ is the time variable.
$\lvert\lvert \boldsymbol{z}(t) \rvert\rvert_{\mathcal{L}_p}$	the Lebesgue $\mathcal{L}_p$ – norm of $\boldsymbol{z}(t)$.
$\lvert\lvert \boldsymbol{z}(t) \rvert\rvert_{\mathcal{W}_{m,p}}$	the Sobolev $\mathcal{W}_{m,p}$ – norm of $\boldsymbol{z}(t)$.
$\lvert\lvert \boldsymbol{z}(t) \rvert\rvert_{\mathcal{W}_{m,p,\boldsymbol{\sigma}}}$	the weighted Sobolev $\mathcal{W}_{m,p,\boldsymbol{\sigma}}$ – norm of $\boldsymbol{z}(t)$.
$\boldsymbol{z}(t) \in \mathcal{L}_p[0, \infty)$	the function $\boldsymbol{z}(t)$ belongs to the $\mathcal{L}_p$-space, i.e. $\lvert\lvert \boldsymbol{z}(t) \rvert\rvert_{\mathcal{L}_p} < \infty$.
$\boldsymbol{z}(t) \in \mathcal{W}_{m,p}[0, \infty)$	the function $\boldsymbol{z}(t)$ belongs to the Sobolev $\mathcal{W}_{m,p}$-space, i.e. $\lvert\lvert \boldsymbol{z}(t) \rvert\rvert_{\mathcal{W}_{m,p}} < \infty$.
$\boldsymbol{z}(t) \in \mathcal{W}_{m,p,\boldsymbol{\sigma}}[0, \infty)$	the function $\boldsymbol{z}(t)$ belongs to the weighted Sobolev $\mathcal{W}_{m,p,\boldsymbol{\sigma}}$-space, i.e. $\lvert\lvert \boldsymbol{z}(t) \rvert\rvert_{\mathcal{W}_{m,p,\boldsymbol{\sigma}}} < \infty$.
$\inf S$	infimum of set S, i.e. $s \in S$, $s \leq s_0$, $\forall s_0 \in S$..

Contents

1
Introduction

This chapter motivates the design of optimal nonlinear adaptive control strategies for Euler-Lagrange systems and exposes the objectives of this research endeavour.

1.1 Motivation

One of the main challenges faced by modern control applications is handling systems that posses uncertainties. In general, control design is conducted based on mathematical models which are not capable of fully represent real-world phenomena. Models are by definition approximations of the system introducing unmodeled dynamics and parameter uncertainties. In addition, real systems are often affected by external disturbances and sensor noise which contributes even further to the challenge of designing a controller capable of mantaining performance in the presence of uncertainties. In this context, the robust and adaptive control approaches emerge as suitable alternatives.

Regarding robust controllers, two usual approaches to tackle these issues in the control design stage are the $\mathcal{H}_2$ (Johansson, 1990) and $\mathcal{H}_\infty$ (Van Der Schaft, 1992) optimal control strategies. These strategies have been originally formulated in the frequency domain in order to cope with single-input-single-output (SISO) systems represented by transfer functions (Doyle et al., 2013). In this domain, the $\mathcal{H}_2$ controller seeks to minimize the energy of the system impulse response from the disturbance to the output (Geromel et al., 1999), while the $\mathcal{H}_\infty$ controller minimizes the maximum gain given by the closed-loop system to a disturbance signal (Francis and Doyle, 1987). For multiple-input-multiple-output (MIMO) systems represented in the state-space domain, the $\mathcal{H}_\infty$ control formulation has been firstly introduced in Doyle et al. (1989), which has received considerable attention in the past decades, which was an initial point to the development of $\mathcal{H}_2$ and $\mathcal{H}_\infty$ controllers based on Linear Matrix inequalities (LMIs) (Nguang and Shi, 2003; Hu et al., 2003). Concerning nonlinear systems, the $\mathcal{H}_\infty$ control strategy has been first introduced in Van der Schaft (1991), where the problem is formulated in the $\mathcal{L}_2$ space using the theory of dissipative systems (Willems, 2007).

Although the $\mathcal{H}_2$ and $\mathcal{H}_\infty$ control strategies have been successfully applied to a wide range of systems and their effectiveness has been experimentally verified (Van der Linden and Lambrechts, 1993; Nichols et al., 1993; Sedhom et al., 2020), these methods have certain drawbacks. According to Chilali and Gahinet (1996), $\mathcal{H}_2$ and $\mathcal{H}_\infty$ control strategies primarily focus on stabilization and disturbance attenuation, offering limited control over transient behavior. To address this issue, an alternative approach involves formulating both $\mathcal{H}_2$ and $\mathcal{H}_\infty$ controllers in Sobolev spaces $\mathcal{W}_{m,p}$. These are function spaces in $\mathcal{L}_p$ space where generalized derivatives up to order m are also in $\mathcal{L}_p$ space (Treves, 2016). In control engineering, Sobolev space properties have been effectively used for tasks such as designing state observers (Alessandri and Sanguineti, 2007; Zemouche and Boutayeb, 2008). For control design, Aliyu and Boukas (2011a) have proposed reformulating the $\mathcal{H}_2$ and $\mathcal{H}_\infty$ control approaches in a Sobolev space to enhance transient performance. In this formulation, the $\mathcal{W}_{1,2}$-norm of the cost variable is considered instead of the $\mathcal{L}_2$-norm.[1]. The control problems are addressed through dynamic programming, requiring the solution of a hard to solve Hamilton-Jacobi (HJ) equation to obtain the resulting controllers.

An alternative to handle uncertainties is the adaptive control framework, which is an approach designed to automatically adjust the parameters of a controller in execution-time to improve the control system performance. Results in Lin and Kanellakopoulos (1998) have indicated that exact parameter estimation enhances the overall stability and robustness of closed-loop adaptive systems. In addition, by accurately estimating the parameters deviations in estimated parameters from expected values can serve as early indicators of component degradation or failure. This capability enables the detection of faults or inefficiencies caused by aging, allowing for timely maintenance or intervention before more severe failures occur, thereby enhancing system reliability and lifespan. Nevertheless, parameter convergence to their true values is hindered by the requirement of satisfying a particularly strict condition known as the Persistence of Excitation (PE) condition. Relaxing the PE condition poses a challenging theoretical problem and many research works have been devoted to addressing this issue. In Pan and Yu (2018), the concept of interval excitation (IE) has been proposed. In this study, an approach known as Composite

[1]The Sobolev $\mathcal{W}_{m,p}-$norm of a function $\boldsymbol{z}(t) : \mathbb{R}_{\geq 0} \to \mathbb{R}$, for $m \in \mathbb{N}$ and $p \in \mathbb{N} \cup \{\infty\}$, is defined as $||\boldsymbol{z}(t)||_{\mathcal{W}_{m,p}} = \big(\sum_{\alpha=0}^{m} ||\frac{d^\alpha \boldsymbol{z}(t)}{dt^\alpha}||_{\mathcal{L}_p}^p\big)^{1/p}$, where $||\cdot||_{\mathcal{L}_p}$ stands for the $\mathcal{L}_p -$ norm, $\mathbb{N} = \{1, 2, 3...\}$.

Learning Robot Control (CLRC) has been designed to achieve fast and accurate parameter estimation under the less stringent IE condition. Within this context, one particularly technique has garnered attention, the Dynamic Regressor Extension and Mixing (DREM) method (Aranovskiy et al., 2017), which involves the generation of an augmented regressor through the application of dynamic operators to the original regression matrix. The DREM technique allows to obtain a necessary and sufficient condition for parameter convergence that does not rely on the PE one.

Also, in Egardt (1979), it has been noticed that adaptive schemes could easily become unstable when exposed to small disturbances. The lack of robustness in adaptive control has become highly controversial, as additional examples of instabilities have been published, highlighting the lack of robustness in the presence of unmodeled dynamics and bounded disturbances (Ioannou and Kokotovic, 1983; Rohrs et al., 1985). Thus, the research on robust adaptive control has began focusing on proposing several robustness modifications such as Leakage, Projetion methods and Dynamic Normalization (Egardt, 1979; Ioannou and Sun, 1988).

In this context, this master thesis proposes robust adaptive controllers to handle uncertainties in Euler-Lagrange systems. The nonlinear $\mathcal{H}_\infty$ controller is extended to its adaptive formulation and improved by using update laws based on the DREM technique. This ensures robustness against external disturbances and, under conditions that are less stringent than the PE condition, the achievement of exact parameter estimation. To enhance transient response, the adaptive nonlinear $\mathcal{W}_\infty$ controller is proposed. Additionally, a method to generate vector regressors from matrix regressors based on the Euler-Lagrange first integral is introduced to facilitate the straightforward application of DREM-based techniques.

1.2 Literature Review

This section presents a literature review on the main topics of interest of this master thesis, which is concerned with the following topics: (i) adaptive control; (ii) the $\mathcal{H}_2$ and $\mathcal{H}_\infty$ control frameworks; and (iii) the $\mathcal{W}_2$ and $\mathcal{W}_\infty$ control frameworks.

1.2.1 Adaptive Control

The field of adaptive control has its history characterized by significant debates regarding its precise definition and proofs of stability and robustness. Beginning in the early 1950s, the development of autopilots for high-performance aircraft has spurred substantial research in adaptive control (Ioannou and Sun, 1996). These aircraft experience drastic changes in dynamics when transitioning between operating points, which constant-gain feedback control cannot manage. This has motivated the design of an adaptive controller, capable of learning and adapting to changes in aircraft dynamics. In this context, Model Reference Adaptive Control (MRAC) has been suggested to address the autopilot control issue in Osburn and Kezer (1961) and Whitaker et al. (1958) . The sensitivity method and the MIT rule (Mareels et al., 1987) have been employed to design the adaptive laws for various adaptive control schemes. Additionally, in Kalman (1958), an adaptive pole placement scheme based on the optimal linear quadratic problem has been proposed.

State space techniques and stability theory based on Lyapunov in the context of adaptive systems have been then introduced. In Parks (1966) for example, a method has been developed to redesign the MIT rule-based adaptive laws used in the 1950s MRAC schemes by applying the Lyapunov design approach. Although their work was limited to a specific class of LTI plants, it laid the groundwork for more rigorous stability proofs in adaptive control for broader classes of plant models. Following their lead, MRAC schemes using the Lyapunov design approach have been developed and analyzed in several studies (Morse, 1980; Narendra et al., 1980). The concepts of positivity and hyperstability have been employed to create a broad range of MRAC schemes with well-established stability properties (Landau, 1984). Concurrently, efforts for discrete-time plants in both deterministic and stochastic environments have led to the creation of several adaptive control schemes with rigorous stability proofs (Goodwin et al., 1980; Goodwin and Sin, 1984).

Around that time, as part of the NASA X-15 program, three hypersonic planes X-15-1, X-15-2, and X-15-3 have been subjected to flight tests. The X-15-1 and X-15-2 have featured a fixed-gain stability augmentation system, whereas the X-15-3 has been among the first aircraft to implement an adaptive control scheme. The Honeywell MH-96 self-adaptive controller in the X-15-3 adjusted parameters online to maintain the aircraft's performance throughout the flight envelope. Nevertheless, no stability proof of such adaptive system had been proposed and, as of consequence, a fatal accident occurred (Dydek et al., 2010). The X-15-3 accident reminds us of the importance of rigorous stability proofs and analysis of the properties of the control scheme in the context of control engineering.

Recent efforts have been directed to mix Learning based techniques and adaptive control. In the works Lewis and Vrabie (2009); Vrabie et al. (2009); Kamalapurkar et al. (2016), tracking performance has been enhanced by using stored input-output data along the system trajectory, which contains sufficient information about the unknown system and control parameters. In Annaswamy et al. (2023), a combination of a reinforcement learning (RL)-based policy in the outer loop, chosen to ensure stability and optimality for the nominal dynamics, along with adaptive control (AC) in the inner loop has been proposed. The AC-RL controllers have led to online policies that ensure stability through a high-order tuner and accommodate parametric uncertainties and input magnitude limits.

Regarding adaptive controllers in the context of Euler-Lagrange systems, the equations of motion present a structural characteristic that allows the representation of the model as a product of a matrix, referred to as the 'regressor', and a vector of constant unknown parameters. Leveraging this structural feature and based on Johansson (1990), the authors in Chen et al. (1997) have formulated the nonlinear adaptive $\mathcal{H}_2$ and $\mathcal{H}_\infty$ controllers respectively for mechanical systems. Nonetheless, it fails to achieve parameter estimation convergence due to the restrictive requirement of satisfying the PE condition (Ioannou and Sun, 1996). To ensure parameter convergence, parameter drift must be prevented by guaranteeing that the regressor vector is persistently excited. In Petronilho et al. (2005), a nonlinear adaptive neural network tracking control method has been proposed ensuring guaranteed $\mathcal{H}_\infty$ performance for a constrained robot manipulator with uncertain plant dynamics, where the neural network employs an adaptive algorithm to learn these unknown dynamics

In Loría et al. (2005), it has been demonstrated that the necessary and sufficient condition to guarantee the convergence of the parameters is that the regressor matrix presents the PE condition along the reference trajectories, allowing the a priori verification. In Boyd and Sastry (1986) and Boyd and Sastry (1983), it has been demonstrated that the persistent excitation (PE) condition on the regressor requires that the reference input contains as many spectral lines as there are unknown parameters. Although restrictive, this requirement provides a method to enforce the PE condition. However, adding perturbation to the external reference input to satisfy the PE condition can significantly degrade control performance. Furthermore, enforcing the PE condition through the exogenous reference is often impractical, and monitoring whether a signal will remain PE online is challenging, as it depends on the signal's future behavior. Therefore, finding a practical solution for parameter convergence and transient response improvement remains a longstanding research issue (Loria, 2004; Datta and Ioannou, 1994; Huang, 2003; Cao and Hovakimyan, 2008). Additionally, some works (Slotine and Li, 1989; Lavretsky, 2009; Duarte and Narendra, 1989) have focused on a class of adaptive control known as Combined/Composite techniques, which utilize prediction error alongside tracking error to design the parameter update law. These Combined/Composite designs lead to improved transient response and reduced steady-state parameter estimation error compared to classical adaptive designs that rely only on tracking error, while still require the PE assumption for parameter convergence.

Efforts to mitigate the persistent excitation requirement, such as adopting IE, have gained momentum recently, as highlighted by Pan and Yu (2018) where a CLRC has been designed to achieve fast and accurate parameter estimation under the less stringent IE condition. Another key development in the context of adaptive systems is the DREM technique, developed in Aranovskiy et al. (2017). This technique involves the generation of an augmented regressor through the application of dynamic operators to the original regression matrix. Conventional parameter estimation techniques can then be applied considering this newly generated matrix. In Arteaga (2023), a composite scheme that combines the standard gradient adaptive law with a DREM-based additional term has been proposed and applied to a robotic manipulator. It has proposed a new condition for which, if achieved, exact parameter estimation occurs. In addition, it is capable of performing trajectory tracking with asymptotic convergence, regardless of whether exact parameter estimation has been achieved. In Arteaga (2024), a similar DREM-based adaptive scheme has been proposed, which has enabled to take a predefined amount of excitation and increase it to a level where finite-time exact parameter estimation happens.

1.2.2 The $\mathcal{H}_2$ and $\mathcal{H}_\infty$ Optimal Control

As previously mentioned, classic $\mathcal{H}_2$ and $\mathcal{H}_\infty$ control strategies (Van Der Schaft, 1992) inherently provide disturbance attenuation for the closed-loop system. These strategies have been initially developed in the frequency domain to address SISO systems represented by transfer functions (Doyle et al., 2013). In this context, the $\mathcal{H}_2$ controller aims to minimize the energy of the disturbance impulse response (Geromel et al., 1999), whereas the $\mathcal{H}_\infty$ controller focuses on minimizing the maximum gain of the closed-loop system in response to a disturbance signal (Francis and Doyle, 1987).

The need to address MIMO systems has led to the extension of $\mathcal{H}_2$ and $\mathcal{H}_\infty$ control strategies to state-space representations, first introduced in Doyle et al. (1989). Over the past decades, these strategies have garnered significant attention as a foundation for developing $\mathcal{H}_\infty$ controllers through convex optimization problems with Linear Matrix Inequalities (LMI) constraints (Gahinet and Apkarian, 1994; Hu et al., 2003). In the context of state-space systems, the multi-objective linear mixed $\mathcal{H}_2/\mathcal{H}_\infty$ controller (Khargonekar and Rotea, 1991) has been formulated to integrate $\mathcal{H}_2$ performance within the $\mathcal{H}_\infty$ control framework.

Regarding the nonlinear $\mathcal{H}_\infty$ control, it has been first introduced in Van der Schaft (1991). The control problem has been formulated based on the $\mathcal{L}_2$-space using the theory of dissipative systems (Willems, 2007). As to the developing of nonlinear $\mathcal{H}_2$ controllers for Euler-Lagrange systems, a seminal work is Johansson (1990). This work has formulated the nonlinear $\mathcal{H}_2$ control problem using dynamic programming for a specific class of fully actuated systems, providing an analytical solution to the resulting Hamilton-Jacobi (HJ) equation. Building on this foundational solution, numerous subsequent studies have emerged. For instance, Chen et al. (1994b) has formulated a nonlinear $\mathcal{H}_\infty$ control strategy for the same class of systems, while Siqueira et al. (2006) has developed a nonlinear mixed $\mathcal{H}_2/\mathcal{H}_\infty$ control strategy for mechanical systems with actuation redundancy. In Feng and Postlethwaite (1993), a similar approach for robotic systems has been proposed, where the cost variable considers the coupling between the controlled variables and the control inputs, giving more degrees of freedom to the control design.

Building on these initial methodologies for mechanical systems, several significant contributions have emerged. Chen et al. (1996) have introduced a method for designing an $\mathcal{H}_\infty$ controller focused on robust tracking for perturbed nonholonomic mechanical systems Aguilar et al. (2003) have expanded the $\mathcal{H}_\infty$ framework to accommodate nonsmooth, time-varying mechanical systems with friction. Ortega et al. (2005) has advanced the nonlinear $\mathcal{H}_\infty$ control strategy by adding an integral action to the error vector and defining conditions to express the controller as a nonlinear PID. In Sage et al. (1999), a survey on robust control for robot manipulators, which includes an overview of nonlinear $\mathcal{H}_\infty$ control techniques has been developed.

Regarding underactuated mechanical systems, the design of $\mathcal{H}_2$ and $\mathcal{H}_\infty$ controllers often leverages the intrinsic characteristics of these systems. For instance, in Siqueira and Terra (2004) and Siqueira et al. (2006), a nonlinear $\mathcal{H}_\infty$ controller has been developed specifically for underactuated manipulators. These studies have exploited the passive-active properties of mechanical systems, where the active degrees of freedom are directly actuated by control inputs, and the passive ones are unactuated. The control design accounts for the dynamic coupling between passive and active degrees of freedom, assuming the passive joints are equipped with brakes. The strategy involves controlling the passive joints to reach their desired positions by applying torques to the active ones, then engaging the brakes. Subsequently, all active joints are controlled as if the manipulator were fully actuated. Similarly, Raffo et al. (2011a) have explored the passive-active property in designing a cascade controller for a quadrotor UAV. In their work, a nonlinear $\mathcal{H}_\infty$ controller manages the active degrees of freedom, while a model predictive controller (MPC) generates references for the active degrees to guide the passive ones along the desired trajectory.

In Raffo et al. (2011b), a nonlinear $\mathcal{H}_\infty$ control methodology is introduced to address underactuated mechanical systems exhibiting input coupling (Olfati-Saber, 2001). The system dynamics are segmented into controlled and stabilized degrees of freedom. The controller is crafted to ensure trajectory tracking for the controlled degrees of freedom, while stabilizing the remaining ones. The effectiveness of this control approach is validated through numerical experiments involving a quadrotor UAV. To introduce input coupling into the system dynamics, the authors suggest a modification in the quadrotor UAV's mechanical structure by slightly tilting the thrusters towards the aircraft's geometric center. This small tilt ensures complete controllability of the quadrotor UAV. In a similar vein, Raffo et al. (2015) employs a nonlinear $\mathcal{H}_\infty$ controller for a two-wheeled self-balancing vehicle. The goal is to control the pendulum's inclination angle (controlled degrees of freedom) to reach the upright vertical position, while setting the angular velocity of the wheels (time derivative of the remaining degrees of freedom) to a desired reference value.

Nonlinear $\mathcal{H}_2$ and $\mathcal{H}_\infty$ control strategies have been successfully implemented in various systems through numerous experiments. However, these approaches come with notable limitations. As discussed in Chen et al. (1994a); Raffo et al. (2011b), the standard formulation of nonlinear $\mathcal{H}_\infty$ control, and consequently nonlinear $\mathcal{H}_2$ control, for Euler-Lagrange systems has a drawback on how the cost variable is weighted. Specifically, the weighting matrices must be considered as positive real scalars multiplied by the identity matrix, restricting the adaptability of the control law for systems with multiple degrees of freedom and different dynamics. Additionally, as highlighted in Chilali and Gahinet (1996), the $\mathcal{H}_\infty$ control strategy primarily focuses on addressing the maximum gain of disturbances, offering limited control over the transient behavior of the system.

To address the first limitation, Raffo (2011) has proposed an approach based on the diagonalization of the inertia matrix, which enhances the flexibility in tuning the nonlinear $\mathcal{H}_\infty$ controller. Conversely, there is a scarcity of work addressing the second limitation in the context of designing control strategies for nonlinear systems

1.2.3 The $\mathcal{W}_2$ and $\mathcal{W}_\infty$ Optimal Control

Sobolev spaces $\mathcal{W}_{m,p}$ and weighted Sobolev spaces $\mathcal{W}_{m,p,\sigma}$ are normed vector spaces, characterized by functions in $\mathcal{L}_p$ with generalized derivatives up to order m also belonging to the $\mathcal{L}_p$ space (Adams and Fournier, 2003; Dlotko, 2014; Maz'ya, 2013; Treves, 2016; Kufner, 1985; Goldshtein and Ukhlov, 2009). These spaces play a crucial role in the analysis of partial differential equations. For example, Pavel (2013) has explored the global classical solvability of mixed initial-boundary value problems for semilinear hyperbolic systems involving nonlinear reaction coupling of the Lotka-Volterra type. The results formulated within Sobolev spaces have provided a basis for developing further boundary control techniques for these systems. In another study, González De Paz (2009) has proposed a variational principle to address several free boundary value problems via a relaxation method, proving the equivalence between the solutions of the relaxed and the original problems. Moreover, Kilpeläinen (1994) has examined various inequality properties within weighted Sobolev spaces.

The properties of Sobolev spaces have found significant applications in the design of state observers within the control domain. For instance, Alessandri and Sanguineti (2007) have investigated optimal estimation problems for nonlinear systems, utilizing the Luenberger observer as a case study. This study adopts $\mathcal{L}_p$ and Sobolev optimality criteria, defining the optimality criterion based on the norm of the estimation error within a function space, influenced by a chosen innovation function. It explores the connections between internal stability (asymptotic and exponential) and input-output stability, providing upper bounds for the estimation error. Conversely, Zemouche and Boutayeb (2008) have tackled an unknown input observer design for nonlinear systems, considering disturbances in both the state and output equations. A significant outcome of this work is the definition of a new robustness criterion using Sobolev norms, termed the modified $\mathcal{H}_\infty$ criterion. This approach diverges from the standard $\mathcal{H}_\infty$ filtering method (Simon, 2006) by addressing the unknown input observer synthesis problem within noisy contexts.

Additionally, Aliyu and Boukas (2011b) have extended the classical $\mathcal{H}_2$ and $\mathcal{H}_\infty$ optimization problems by proposing $\mathcal{W}_{1,2}$ and $\mathcal{W}_{1,\infty}$ estimation problems. They have introduced proportional, proportional-derivative, and proportional-integral (PI) filters for each problem type, and provide sufficient conditions for the existence of optimal filter gains based on new Hamilton-Jacobi-Bellman (HJB) and Hamilton-Jacobi-Bellman-Isaacs (HJBI) equations

To address the limitations of the nonlinear $\mathcal{H}_2$ and $\mathcal{H}_\infty$ control strategies, Aliyu and Boukas (2011a) have reframed these control approaches within the Sobolev space. Their work has considered the $\mathcal{W}_{1,2}$-norm of the cost variable instead of the $\mathcal{L}_2$-norm. The control problems have been formulated using dynamic programming, which involves solving the Hamilton-Jacobi partial differential equation (HJ PDE). Specifically, Aliyu and Boukas (2011a) have noted that solving the HJ PDE derived from the nonlinear $\mathcal{H}_\infty$ control approach in Sobolev space is extremely challenging and computationally infeasible, labeling it as horrendous and impossible to compute the solution. As a solution, they have proposed using the backstepping technique to simplify the problem. However, the approach does not consider the rate of change of the cost variable in the cost functional, thus failing to improve transient performance. Additionally, the methods proposed in Aliyu and Boukas (2011a) do not differentiate between the effects of the cost variable and its time derivatives on the control objectives

In Cardoso et al. (2021a), the nonlinear $\mathcal{W}_2$ and $\mathcal{W}_\infty$ controllers, have been designed to address two types of underactuated mechanical systems: those with a reduced number of degrees of freedom (DOF), and fully underactuated mechanical systems with input coupling. The formulation allows tuning component-wise the influences of the cost variable and its time derivative in the cost functional. The optimal control problems have been formulated using dynamic programming, and specific solutions to the resulting Hamilton-Jacobi equations have been provided, along with the corresponding stability analysis.

1.3 Research Objectives

Specifically, the research objectives are:

1. To propose robust adaptive controllers based on the $\mathcal{H}_\infty$ formalism alongside the DREM technique to handle uncertainties in Euler-Lagrange systems.

2. To explore different estimation laws based on the DREM technique.

3. To extend the $\mathcal{W}_\infty$ control framework to its adaptive formulation.

4. To propose stability proofs for all the robust adaptive controllers developed.

1.4 List of publications

During this research the following scientific works were prepared.

Journal papers:

- Campos et al. (2024a) J. M. Campos, D. N. Cardoso, S. Esteban, and G. V. Raffo. **Enhanced Robust Adaptive Flight Control for a Convertible VTOL UAV**. Journal of the Franklin Institute - 2024.

Conference papers:

- Campos et al. (2023b) J. M. Campos, D. N. Cardoso, and G. V. Raffo. **Adaptive Nonlinear $\mathcal{W}_\infty$ Control for Fully Actuated Mechanical Systems**. Simposio Brasileiro de Automacao Inteligente - 2023 (SBAI).
- Campos et al. (2023a) J. M. Campos, D. N. Cardoso, and G. V. Raffo. **A Robust Nonlinear Flight Control in the Weighted Sobolev Space for a Quadtiltrotor UAV**. International Conference Series on Climbing and Walking Robots and the Support Technologies for Mobile Machines - 2023 (CLAWAR).
- Campos et al. (2024c) J. M. Campos, D. N. Cardoso, and G. V. Raffo. **An Adaptive Nonlinear $\mathcal{H}_\infty$ Control with Exact Parameter Estimation for Mechanical Systems**. European Control Conference - 2024 (ECC).
- Campos et al. (2024b) J. M. Campos, D. N. Cardoso, and G. V. Raffo. **A Nonlinear Adaptive $\mathcal{H}_\infty$ Control with Finite-Time Exact Parameter Estimation**. Conference on Decision and Control - 2024 (CDC).

1.5 Thesis Structure

The following chapters are structured as:

- **Chapter 2** presents the mathematical background that includes the derivation of the Euler-Lagrange equations using a variational approach and discusses some properties of such systems, interesting properties of the $\mathcal{W}_2$ and $\mathcal{W}_\infty$ control approaches, the concept of Persistency of Excitation and the Dynamic Regressor Extension and Mixing technique.
- **Chapter 3** is concerned with the development of a general method to obtain vector regressor forms from matrix regressor forms using the notion of the Euler-Lagrange first integral, the proposition of variations of the nonlinear adaptive $\mathcal{H}_\infty$ controller using the DREM technique, and the demonstration of the stability proofs of the controllers using Lyapunov theory of stability.

- **Chapter 4** is concerned with the extension of the nonlinear $\mathcal{W}_\infty$ controller to its adaptive formulation using the DREM technique and its stability proof using Lyapunov theory of stability.
- **Chapter 5** summarizes the contributions and suggests future works.

2

Mathematical Preliminaries

This chapter presents some preliminary concepts and definitions necessary to the development of this master thesis. The following topics are discussed: (i) the Euler-Lagrange equations; (ii) properties of Euler-Lagrange systems; (iii) properties of the nonlinear $\mathcal{W}_2$ and $\mathcal{W}_\infty$ control strategies; (iv) the persistency of excitation condition; and (v) the Dynamic Regressor Extension and Mixing (DREM) technique.

2.1 The Euler-Lagrange Equation

This section presents the Euler-Lagrange equations of motion, which describes the time evolution of a system subjected to holonomic constraints[1]. There are at least two ways of deriving these equations. The first one uses the method of virtual work and D'Alembert's principle and can be found, for example, in Spong et al. (2020). The second one bases on Hamilton's principle of least action, which is the method employed in this section.

The Euler-Lagrange equation is derived in Appendix A.1 based on Hamilton's principle of least action. It is shown how to take into account external forces into the Hamilton's formulation.

To obtain the canonical form of the Euler-Lagrange equation, it is considered that: (i) the kinetic energy can be written as a quadratic function of the generalized velocities, and (ii) the potential energy is a function only of the generalized coordinates.

[1]Nonholonomic constraints in general cannot be expressed by variational principles except when considering semi-holonomic constraints (Goldstein et al., 2002).

As presented in the Appendix A.1, the Euler-Lagrange equation is given by

$$\frac{d}{dt}\left[\frac{\partial \boldsymbol{\mathcal{L}}(\boldsymbol{q},\dot{\boldsymbol{q}})}{\partial \dot{\boldsymbol{q}}}\right] - \left[\frac{\partial \boldsymbol{\mathcal{L}}(\boldsymbol{q},\dot{\boldsymbol{q}})}{\partial \boldsymbol{q}}\right] = \boldsymbol{\vartheta}(\boldsymbol{q},\dot{\boldsymbol{q}},\boldsymbol{u}). \tag{2.1}$$

For several systems, the Lagrangian function can be written as

$$\boldsymbol{\mathcal{L}}(\boldsymbol{q},\dot{\boldsymbol{q}}) = \mathcal{K}(\boldsymbol{q},\dot{\boldsymbol{q}}) - \mathcal{P}(\boldsymbol{q}), \tag{2.2}$$

where $\mathcal{K}(\boldsymbol{q},\dot{\boldsymbol{q}})$ and $\mathcal{P}(\boldsymbol{q})$ are, respectively, the kinetic and potential energies.

For mechanical systems for instance, the total kinetic energy can be computed as

$$\mathcal{K}(\boldsymbol{q},\dot{\boldsymbol{q}}) = \sum_{i=1}^{k} \frac{1}{2} m_i \boldsymbol{v}_i' \boldsymbol{v}_i + \frac{1}{2}\boldsymbol{\omega}_i' \boldsymbol{I}_i^{\mathcal{I}} \boldsymbol{\omega}_i, \tag{2.3}$$

where m_i, $\boldsymbol{v}_i$, $\boldsymbol{\omega}_i$, and $\boldsymbol{I}^{\mathcal{I}}$ are, respectively, the mass, the linear velocity vector, the angular velocity vector, and the inertia tensor matrix of the i-th body, all taken with respect to an inertial reference frame.

Recall it is possible to express $\boldsymbol{v}_i$ and $\boldsymbol{\omega}_i$ using Jacobian matrices (for details see Appendix A.1)

$$\boldsymbol{v}_i = \boldsymbol{J}_{v_i}\dot{\boldsymbol{q}}, \tag{2.4}$$

$$\boldsymbol{\omega}_i = \boldsymbol{J}_{\omega_i}\dot{\boldsymbol{q}}, \tag{2.5}$$

Therefore, by replacing expressions (2.4) and (2.5) into (2.3), the kinetic energy is written as

$$\begin{aligned}
\mathcal{K}(\boldsymbol{q},\dot{\boldsymbol{q}}) &= \sum_{i=1}^{k} \frac{1}{2} m_i (\boldsymbol{J}_{\boldsymbol{v}_i}\dot{\boldsymbol{q}})'(\boldsymbol{J}_{v_i}\dot{\boldsymbol{q}}) + \frac{1}{2}(\boldsymbol{J}_{\boldsymbol{\omega}_i}\dot{\boldsymbol{q}})'\boldsymbol{I}_i^{\mathcal{I}}(\boldsymbol{J}_{\omega_i}\dot{\boldsymbol{q}}),\\
&= \sum_{i=1}^{k} \frac{1}{2} m_i \dot{\boldsymbol{q}}' \boldsymbol{J}_{v_i} \boldsymbol{J}_{v_i}\dot{\boldsymbol{q}} + \frac{1}{2}\dot{\boldsymbol{q}}'\boldsymbol{J}_{\omega_i}'\boldsymbol{I}_i^{\mathcal{I}}\boldsymbol{J}_{\omega_i}\dot{\boldsymbol{q}},\\
&= \frac{1}{2}\dot{\boldsymbol{q}}' \underbrace{\left(\sum_{i=1}^{k} m_i (\boldsymbol{J}_{\boldsymbol{v}_i})'\boldsymbol{J}_{\boldsymbol{v}_i} + (\boldsymbol{J}_{\omega_i})'\boldsymbol{I}_i^{\mathcal{I}}\boldsymbol{J}_{\omega_i}\right)}_{\boldsymbol{M}(\boldsymbol{q})}\dot{\boldsymbol{q}},\\
&= \frac{1}{2}\dot{\boldsymbol{q}}'\boldsymbol{M}(\boldsymbol{q})\dot{\boldsymbol{q}},
\end{aligned} \tag{2.6}$$

where $\boldsymbol{M}(\boldsymbol{q})$ is the so called Inertia Matrix, which is symmetric and positive definite.

Similarly to the kinetic energy, the total potential energy of a mechanical system can be computed by the summing up the potential energies of each rigid body,

$$\begin{aligned}\mathcal{P}(\boldsymbol{q}) &= \sum_{i=1}^{k} \mathcal{P}_i(\boldsymbol{q}) \\ &= -\sum_{i=1}^{k} m_i \boldsymbol{g}_{\boldsymbol{r}}' \boldsymbol{r}_i(\boldsymbol{q}),\end{aligned} \tag{2.7}$$

where $\boldsymbol{g}_{\boldsymbol{r}}$ is the gravity acceleration vector, taken with respect to the inertial reference frame, and $\boldsymbol{r}_i(\boldsymbol{q})$ is the position of the center of mass of the i-th body of the mechanical system.

Taking into account (2.6) and (2.7), the Lagrangian can be written as

$$\mathcal{L}(\boldsymbol{q}, \dot{\boldsymbol{q}}) = \frac{1}{2}\dot{\boldsymbol{q}}'(t)\boldsymbol{M}(\boldsymbol{q})\dot{\boldsymbol{q}}(t) - \mathcal{P}(\boldsymbol{q}). \tag{2.8}$$

Consequently, by replacing equation (2.8) in (2.1), yields

$$\begin{aligned}\frac{d}{dt}\left(\frac{\partial}{\partial \dot{\boldsymbol{q}}}\left(\frac{1}{2}\dot{\boldsymbol{q}}'\boldsymbol{M}(\boldsymbol{q})\dot{\boldsymbol{q}}\right)\right) - \left(\frac{\partial}{\partial \boldsymbol{q}}\left(\frac{1}{2}\dot{\boldsymbol{q}}'\boldsymbol{M}(\boldsymbol{q})\dot{\boldsymbol{q}}\right)\right) + \frac{\partial \mathcal{P}(\boldsymbol{q})}{\partial \boldsymbol{q}} &= \boldsymbol{\vartheta}, \\ \dot{\boldsymbol{M}}(\boldsymbol{q})\dot{\boldsymbol{q}} + \boldsymbol{M}(\boldsymbol{q})\ddot{\boldsymbol{q}} - \frac{1}{2}\dot{\boldsymbol{q}}'\frac{\partial \boldsymbol{M}(\boldsymbol{q})}{\partial \boldsymbol{q}}\dot{\boldsymbol{q}} + \frac{\partial \mathcal{P}(\boldsymbol{q})}{\partial \boldsymbol{q}} &= \boldsymbol{\vartheta}. \\ \sum_{j=1}^{n}\frac{dM_{lj}}{dt}\dot{q}_j + \sum_{j=1}^{n} M_{lj}\ddot{q}_j - \frac{1}{2}\sum_{s=1}^{n}\sum_{j=1}^{n}\frac{\partial M_{sj}}{\partial q_l}\dot{q}_s\dot{q}_j + \frac{\partial \mathcal{P}}{\partial q_l} &= \vartheta_l, \forall l = 1, ..., n.\end{aligned} \tag{2.9}$$

Next, consider the first term in (2.9) and take the total derivative of the components of the inertia matrix.

$$dM_{lj} = \sum_{s=1}^{n}\frac{\partial M_{lj}}{\partial q_s}dq_s. \tag{2.10}$$

Hence, by taking the limit of (2.10) with respect to dt to obtain the time derivative of the Inertia Matrix, and by replacing the expression onto (2.9), yields

$$\begin{aligned}\sum_{s=1}^{n}\sum_{j=1}^{n}\frac{\partial M_{lj}}{\partial q_s}\dot{q}_s\dot{q}_j + \sum_{j=1}^{n} M_{lj}\ddot{q}_j - \frac{1}{2}\sum_{s=1}^{n}\sum_{l=1}^{n}\frac{\partial M_{sj}}{\partial q_l}\dot{q}_s\dot{q}_j + \frac{\partial \mathcal{P}}{\partial q_l} &= \vartheta_l, \\ \sum_{j=1}^{n} M_{lj}\ddot{q}_j + \sum_{s=1}^{n}\sum_{j=1}^{n}\left\{\frac{\partial M_{lj}}{\partial q_s} - \frac{1}{2}\frac{\partial M_{sj}}{\partial q_l}\right\}\dot{q}_s\dot{q}_j + \frac{\partial \mathcal{P}}{\partial q_l} &= \vartheta_l.\end{aligned} \tag{2.11}$$

The term involving the double sum can be rewritten as,

$$\sum_{s=1}^{n}\sum_{j=1}^{n}\left\{\frac{\partial M_{lj}}{\partial q_s} - \frac{1}{2}\frac{\partial M_{sj}}{\partial q_l}\right\}\dot{q}_s\dot{q}_j = \sum_{s=1}^{n}\sum_{j=1}^{n}\overbrace{\frac{1}{2}\left\{\frac{\partial M_{lj}}{\partial q_s} + \frac{\partial M_{ls}}{\partial q_j} - \frac{\partial M_{sj}}{\partial q_l}\right\}}^{c_{sjl}}\dot{q}_s\dot{q}_j, \tag{2.12}$$

where c_{sjl} is the Christoffel symbols of the first kind. Then by defining $g_l \triangleq \frac{\partial \mathcal{P}}{\partial q_l}$, the specialized Euler-Lagrange equations can be given by

$$\sum_{j=1}^{n} M_{lj}(q)\ddot{q}_j + \sum_{s=1}^{n}\sum_{j=1}^{n} c_{sjl}(q)\dot{q}_s\dot{q}_j + g_l(q) = \vartheta_l, \forall l = 1, ..., n,$$

$$\boldsymbol{M}(\boldsymbol{q})\ddot{\boldsymbol{q}} + \boldsymbol{C}(\boldsymbol{q}, \dot{\boldsymbol{q}})\dot{\boldsymbol{q}} + \boldsymbol{G}(\boldsymbol{q}) = \boldsymbol{\vartheta}(\boldsymbol{q}, \dot{\boldsymbol{q}}, \boldsymbol{u}, \boldsymbol{\zeta}). \tag{2.13}$$

Moreover, the terms of the Coriolis matrix, $\boldsymbol{C}(\boldsymbol{q}, \dot{\boldsymbol{q}})$, are given by

$$C_{lj} = \sum_{s=1}^{n} c_{sjl}(q)\dot{q}_s. \tag{2.14}$$

Expression (2.13) is the so-called Euler-Lagrange equation in its canonical form.

2.2 Properties of Euler-Lagrange Systems

Lyapunov-based controllers rely on several properties that allow convenient controller design. Some of these properties are often assumed without rigorous proof. Specifically, the boundedness of the inertia matrix and the skew-symmetric nature of the Inertia matrix are straightforward to establish for single rigid bodies and standard robotic manipulators with 1-DoF Euclidean joints. However, proving these properties becomes more intricate for general multibody systems (Johan et al., 2014, p.285). This practice can undermine the rigor of stability proofs. To ensure formal correctness, it is essential to establish these properties rigorously for the specific system and parameterization under consideration.

For instance, following the arguments in Johan et al. (2014), for a single rigid body, the inertia matrix must always remain bounded, as an unbounded inertia matrix indicates the presence of singularities in the formulation. These singularities stem from the choice of state variables used in the system's representation, rather than from the inherent dynamic properties of the system itself. When a small change in velocity results in a disproportionately large change in kinetic energy, this suggests the presence of a representation singularity rather than reflecting the true behavior of the system. Such singularities must be avoided in control and modeling. In the case of robotic manipulators, whether on a fixed base or in vehicle-manipulator systems, the inertia matrix can become unbounded in two scenarios. The first is similar to single rigid bodies, where singularities arise from the chosen representation. A given robotic structure may have one representation for which the inertia matrix remains bounded and another where it does not. Notably, in the commonly used mathematical representations of vehicle-manipulator systems, the inertia matrix often does not remain bounded, as demonstrated in Johan et al. (2014).

The second case is when the geometry of the robotic arm allows for singular configurations. In this case the problem cannot be solved by choosing a different set of variables because the singularities arise as a result of the physical properties of the manipulator.

Any controller and stability proof requiring the boundedness of the inertia matrix remain valid as long as we ensure the current configuration maintains a certain distance from this point.

In this context, equation (2.13), for suitable parametrizations, possesses the following properties (Spong et al., 2020)

Property 1. *The inertia matrix* $\boldsymbol{M}(\boldsymbol{q})$ *is symmetric and positive definite for every* $\boldsymbol{q}(t) \in \mathbb{R}^n$.

Property 2. *There exist constants* λ_m, $\lambda_M \in \mathbb{R}$, *such that the inequality* $\lambda_m||\tilde{\boldsymbol{x}}||^2 \leq \tilde{\boldsymbol{x}}'\boldsymbol{M}\tilde{\boldsymbol{x}} \leq \lambda_M||\tilde{\boldsymbol{x}}||^2$ *holds* $\forall \boldsymbol{q}(t) \in \mathbb{R}^n, \tilde{\boldsymbol{x}} \in \mathbb{R}^n$, *and* $0 < \lambda_m \leq \lambda_M < \infty$.

Property 3. *The Coriolis and centripetal forces and the gravity vector are bounded as* $\|\boldsymbol{C}(\dot{\boldsymbol{q}}, \boldsymbol{q})\dot{\boldsymbol{q}}(t)\| \leq \gamma_1\|\dot{\boldsymbol{q}}(t)\|^2$ *and* $\|\boldsymbol{G}(\boldsymbol{q})\| \leq \gamma_2$ *respectively, with* $\gamma_1, \gamma_2 \in \mathbb{R}_{>0}$.

Property 4. *Defining matrix* $\boldsymbol{C}$ *using Christoffel symbols of the first kind yields* $\dot{\boldsymbol{M}}(\boldsymbol{q}) - 2\boldsymbol{C} = \boldsymbol{N}$ *in which* $\boldsymbol{N} \in \mathbb{R}^{n\times n}$, *is skew-symmetric.*

Property 5. *The Euler-Lagrange equation* (2.13) *is linear in the parameters for a suitable selection of the vector of parameters* $\boldsymbol{\theta} \in \mathbb{R}^p$, *allowing to write*

$$\boldsymbol{M}(\boldsymbol{q}, \boldsymbol{\theta})\ddot{\boldsymbol{q}}(t) + \boldsymbol{C}(\boldsymbol{q}, \dot{\boldsymbol{q}}, \boldsymbol{\theta})\dot{\boldsymbol{q}}(t) + \boldsymbol{G}(\boldsymbol{q}, \boldsymbol{\theta}) = \mathcal{Y}(\boldsymbol{q}, \dot{\boldsymbol{q}}, \ddot{\boldsymbol{q}})\boldsymbol{\theta}, \tag{2.15}$$

where $\mathcal{Y}(\boldsymbol{q}, \dot{\boldsymbol{q}}, \ddot{\boldsymbol{q}}) : \mathbb{R}^n \times \mathbb{R}^n \times \mathbb{R}^n \to \mathbb{R}^{n\times p}$ *is called the regressor matrix.*

For a more in-depth discussion about properties of Euler-Lagrange systems see Kelly et al. (2005).

2.3 The $\mathcal{H}_2$ and $\mathcal{H}_\infty$ Control Approaches

Consider the following linear time invariant system represented in state-space

$$\mathcal{F} : \begin{cases} \dot{\boldsymbol{x}}(t) = \boldsymbol{A}\boldsymbol{x}(t) + \boldsymbol{B}_\tau\boldsymbol{\tau}(t) + \boldsymbol{B}_{\tau_l}\boldsymbol{\tau}_l(t), \\ \boldsymbol{y}(t) = \boldsymbol{Q}\boldsymbol{x}(t) + \boldsymbol{R}\boldsymbol{\tau}(t), \end{cases} \tag{2.16}$$

with $\boldsymbol{x}(t) : \mathbb{R}_{\geq 0} \to \mathbb{R}^{n_x}$ being the state vector, $\boldsymbol{\tau}(t) : \mathbb{R}_{\geq 0} \to \mathbb{R}^{n_\tau}$ the input vector, $\boldsymbol{\tau}_l(t) : \mathbb{R}_{\geq 0} \to \mathbb{R}^{n_w}$ the disturbance vector, $\boldsymbol{y}(t) : \mathbb{R}_{\geq 0} \to \mathbb{R}^{n_x}$ the output vector, $\boldsymbol{A} \in \mathbb{R}^{n_x \times n_x}$, $\boldsymbol{B}_\tau \in \mathbb{R}^{n_x\times n_\tau}$, and $\boldsymbol{B}_{\tau_l} \in \mathbb{R}^{n_x\times n_w}$ matrices with appropriate dimensions, and $\boldsymbol{Q} > 0$ and $\boldsymbol{R} > 0$ weighting matrices.

For the system described by (2.16), the classical $\mathcal{H}_2$ control strategy is formulated in the frequency domain to derive a control law that minimizes the energy of the output vector $\boldsymbol{y}(t)$ under an impulsive disturbance $\boldsymbol{\tau}_l(t)$. In this context, the $\mathcal{H}_2$ control problem can be expressed as the following optimization problem (Dullerud and Paganini, 2013):

$$\min_{\tau\in\mathbb{C}} \frac{1}{2\pi}\int_{-\infty}^{\infty} \text{trace}\left[\boldsymbol{H}^*(j\omega)\boldsymbol{H}(j\omega)\right] d\omega, \tag{2.17}$$

where $\boldsymbol{H}(j\omega)$ is the transfer function of $\mathcal{F}$ from $\boldsymbol{\tau}_l(t)$ to $\boldsymbol{y}(t)$.

This work focuses on the formulation of the $\mathcal{H}_2$ controller in the time domain. By using Parseval's Theorem and assuming $\boldsymbol{\tau}_l(t) \in \mathcal{L}_2[0,\infty)$, the optimization problem (2.17) can be reformulated as follows (Trofino et al., 2003):

$$\begin{aligned} &\min_{\tau\in\mathcal{L}_2} \int_0^{\infty} \text{trace}\left[\boldsymbol{y}'(t)\boldsymbol{y}(t)\right] dt, \\ &s.t.\ \ \mathcal{F}. \end{aligned} \tag{2.18}$$

Interestingly, Khalaf et al. (2006) have demonstrated that if $\boldsymbol{x}(0) = \boldsymbol{0}$, $\boldsymbol{y}(t) = \boldsymbol{S}\begin{bmatrix}\boldsymbol{x}(t)\\ \boldsymbol{\tau}(t)\end{bmatrix}$, with $\boldsymbol{S} \triangleq [\boldsymbol{Q}\ \ \boldsymbol{R}]$, and $\boldsymbol{\tau}_l(t) = \boldsymbol{\delta}(t)$, in which $\boldsymbol{\delta}(t)$ is a vector with appropriate dimension composed of delta Dirac functions, the classic $\mathcal{H}_2$ control problem can be equivalently posed for $\mathcal{F}$ as

$$\begin{aligned} &\min_{\tau(t)\in\mathcal{L}_2} \frac{1}{2}||\boldsymbol{y}(t)||^2_{\mathcal{L}_2}, \\ &s.t.\ \ \mathcal{F}, \end{aligned} \tag{2.19}$$

which is the formulation of the $\mathcal{H}_2$ controller in the space of quadratically integrable functions.

Similarly to the $\mathcal{H}_2$ controller, the $\mathcal{H}_\infty$ controller is initially formulated in the frequency domain to derive a control law that minimizes the maximum ratio between the norm of the performance output signal and the norm of the disturbance signal. For the LTI system (2.16), this control problem can be shown to be equivalent to

$$\min_{\tau\in\mathbb{C}} M\{\boldsymbol{H}(j\omega)\}, \tag{2.20}$$

where $M\{\boldsymbol{H}(j\omega)\}$ denotes the maximum singular value of $\boldsymbol{H}(j\omega)$, in which $\boldsymbol{H}(j\omega)$ is the transfer function of $\mathcal{F}$ from $\boldsymbol{\tau}_l(t)$ to $\boldsymbol{y}(t)$.

Parseval's theorem yields

$$||\boldsymbol{y}(t)||^2_{\mathcal{L}_2} = \frac{1}{2\pi}\int_{-\infty}^{\infty} \boldsymbol{Z}'(j\omega)\boldsymbol{Z}(j\omega)d\omega, \tag{2.21}$$

and

$$||\boldsymbol{\tau}_l(t)||^2_{\mathcal{L}_2} = \frac{1}{2\pi}\int_{-\infty}^{\infty} \boldsymbol{W}'(j\omega)\boldsymbol{W}(j\omega)d\omega, \tag{2.22}$$

where $\boldsymbol{Z}(j\omega)$ and $\boldsymbol{W}(j\omega)$ are, respectively, the signals $\boldsymbol{y}(t)$ and $\boldsymbol{\tau}_l(t)$ represented in the frequency domain. Thus,

$$\begin{aligned}
||\boldsymbol{y}(t)||^2_{\mathcal{L}_2} &= \frac{1}{2\pi}\int_{-\infty}^{\infty} \boldsymbol{W}'(j\omega)\boldsymbol{H}'(j\omega)\boldsymbol{H}(j\omega)\boldsymbol{W}(j\omega)d\omega,\\
&\leq \sup_{\omega} M\{\boldsymbol{H}(j\omega)\}^2 \frac{1}{2\pi}\int_{-\infty}^{\infty} \boldsymbol{W}'(j\omega)\boldsymbol{W}(j\omega)d\omega,\\
&\leq \sup_{\omega} M\{\boldsymbol{H}(j\omega)\}^2 ||\boldsymbol{\tau}_l(t)||^2_{\mathcal{L}_2},\\
&\leq \gamma^2 ||\boldsymbol{\tau}_l(t)||^2_{\mathcal{L}_2},
\end{aligned} \tag{2.23}$$

in which $\gamma = \sup_\omega M\{\boldsymbol{H}(j\omega)\}$ is the $\mathcal{H}_\infty$ attenuation level.

Remark 2.1. In (2.23), the $\mathcal{H}_\infty$ attenuation level γ represents the maximum gain ratio that system (2.16) allows between the energy of the performance output and the energy of the disturbance signal. Q.E.D

Accordingly, the $\mathcal{H}_\infty$ controller can be formulated in the time-domain as

$$\begin{aligned}
&\min_{\tau\in\mathcal{L}_2} \gamma, \\
s.t.\quad &||\boldsymbol{y}(t)||^2_{\mathcal{L}_2} - \gamma^2||\boldsymbol{\tau}_l(t)||^2_{\mathcal{L}_2} \leq 0.
\end{aligned} \tag{2.24}$$

The control problem (2.24) represents the $\mathcal{H}_\infty$ control formulation in the space of quadratically integrable functions.

2.4 The $\mathcal{W}_2$ and $\mathcal{W}_\infty$ Control Approaches

This section presents some properties of the $\mathcal{W}_2$ and $\mathcal{W}_\infty$ control formulations within the context of weighted Sobolev spaces.

The control problem (2.19) can be for instance used to synthesize $\mathcal{W}_2$ controller for the nonlinear system

$$\Pi : \begin{cases} \dot{\boldsymbol{x}}(t) = \boldsymbol{f}(\boldsymbol{x}(t),t) + \boldsymbol{g}(\boldsymbol{x}(t),t)\boldsymbol{\tau}(t) + \boldsymbol{k}(\boldsymbol{x}(t),t)\boldsymbol{\tau}_l(t), \\ \boldsymbol{y}(t) = \boldsymbol{S}\begin{bmatrix}\boldsymbol{x}(t)\\ \boldsymbol{\tau}(t)\end{bmatrix}, \end{cases} \tag{2.25}$$

where $\boldsymbol{x}(t)$, $\boldsymbol{\tau}(t)$, $\boldsymbol{\tau}_l(t)$, and $\boldsymbol{y}(t)$ are defined as in (2.16), and $\boldsymbol{f}(\boldsymbol{x}(t),t)$, $\boldsymbol{g}(\boldsymbol{x}(t),t)$, and $\boldsymbol{k}(\boldsymbol{x}(t),t)$, with $\boldsymbol{f}(0,t) = 0$, are matrices with appropriate dimension.

In the Sobolev spaces, such control problem is posed as

$$\begin{aligned} &\min_{\tau(t)\in\mathbb{U}} \frac{1}{2}||\boldsymbol{z}(t)||^2_{\mathcal{W}_{1,2,\boldsymbol{\Psi}}}, \\ &s.t. \quad \Pi, \end{aligned} \tag{2.26}$$

where $\mathbb{U} : \mathbb{R}_{\geq 0} \to \mathbb{R}^{n_\tau}$, with the output variable given by $\boldsymbol{z}(t) = \boldsymbol{x}(t)$, and $\boldsymbol{\Psi} = (\boldsymbol{\Psi}_0, \boldsymbol{\Psi}_1)$, in which $\boldsymbol{\Psi}_0, \boldsymbol{\Psi}_1$ are weighting matrices.

Remark 2.2. Sobolev Spaces can be seen as a special case of Lebesgue spaces when $m = 0$, i.e., $\mathcal{W}_{m=0,p} = \mathcal{L}_p$. On the other hand, Sobolev spaces constrain the Lebesgue spaces by including conditions on derivatives, thus forming a more comprehensive framework for function spaces. In addition, smoothness conditions are imposed due to the inclusion of derivatives, so functions in Sobolev spaces tend to be smoother. Q.E.D

Remark 2.3. The optimal control problem (2.26) takes into account for the energy of the output vector and its rate of change in the optimization index. Consequently, the resulting controller tends to produce less oscillatory behavior and offers a faster response to disturbances compared to the $\mathcal{H}_2$ controller. Q.E.D

Note that, in the $\mathcal{H}_2$ control problem (2.19) the cost functional can be expanded as

$$\begin{aligned} \mathcal{J}_{\mathcal{L}} &= \frac{1}{2}||\boldsymbol{y}(t)||^2_{\mathcal{L}_2}, \\ &= \frac{1}{2}\int_0^\infty \boldsymbol{y}'(t)\boldsymbol{y}(t)dt, \\ &= \frac{1}{2}\int_0^\infty \left(\begin{bmatrix} \boldsymbol{x}'(t) & \boldsymbol{u}'(t) \end{bmatrix} \boldsymbol{S}'\boldsymbol{S} \begin{bmatrix} \boldsymbol{x}(t) \\ \boldsymbol{u}(t) \end{bmatrix} \right) dt, \end{aligned} \tag{2.27}$$

while in the $\mathcal{W}_2$ control problem (2.26) one has that

$$\begin{aligned} \mathcal{J}_{\mathcal{W}} &= \frac{1}{2}||\boldsymbol{z}(t)||^2_{\mathcal{W}_{1,2}}, \\ &= \frac{1}{2}||\boldsymbol{z}(t)||^2_{\mathcal{L}_2,\boldsymbol{\Psi}_0} + \frac{1}{2}||\dot{\boldsymbol{z}}(t)||^2_{\mathcal{L}_2,\boldsymbol{\Psi}_1}, \\ &= \frac{1}{2}\int_0^\infty \left(\begin{bmatrix} \boldsymbol{x}'(t) & \dot{\boldsymbol{x}}'(t) \end{bmatrix} \begin{bmatrix} \boldsymbol{\Psi}_0 & \boldsymbol{0} \\ \boldsymbol{0} & \boldsymbol{\Psi}_1 \end{bmatrix} \begin{bmatrix} \boldsymbol{x}(t) \\ \dot{\boldsymbol{x}}(t) \end{bmatrix} \right) dt. \end{aligned} \tag{2.28}$$

From (2.27) and (2.28), it is evident that the $\mathcal{H}_2$ approach requires that $\boldsymbol{x}(t), \boldsymbol{u}(t) \in \mathcal{L}_2[0, \infty)$, while the $\mathcal{W}_2$ approach necessitates that $\boldsymbol{x}(t), \dot{\boldsymbol{x}}(t) \in \mathcal{L}_2[0, \infty)$. This characteristic of the $\mathcal{W}_2$ approach is particularly noteworthy, as it relaxes the requirement for $\boldsymbol{u}(t) \in \mathcal{L}2[0, \infty)$, and consequently, $\lim_{t\to\infty} \boldsymbol{u}(t) = 0$.

This feature enables the design of a $\mathcal{W}_2$ controller for the system (2.25) even when $\boldsymbol{f}(0, t) \neq 0$. To maintain such a system at the origin of the state space, the controller must inject energy indefinitely, even in the steady state, requiring a control signal that is not in the $\mathcal{L}_2$ space to achieve asymptotic stability.

Remark 2.4. In the case where $\boldsymbol{f}(0,t) \neq 0$ in system (2.25), it is common practice to decompose $\boldsymbol{f}(x(t),t)$ into $\bar{\boldsymbol{f}}(x(t),t) + \hat{\boldsymbol{f}}(x(t),t)$, with $\bar{\boldsymbol{f}}(0,t) = 0$ and $\hat{\boldsymbol{f}}(0,t) \neq 0$. Then, a change of variables is performed in the control input vector: $\boldsymbol{u}(t) = \hat{\boldsymbol{f}}(x(t),t) + \boldsymbol{v}(t)$. The controller is subsequently designed using the new input vector $\boldsymbol{v}(t)$. Q.E.D

In the Sobolev spaces, the control problem is posed as

$$\begin{aligned} &\min_{\tau(t)\in\mathbb{U}} \gamma, \\ &s.t. \;\; \frac{1}{2}||\boldsymbol{z}(t)||^2_{\mathcal{W}_{1,2,\boldsymbol{\Psi}}} - \gamma^2||\boldsymbol{\tau}_l(t)||^2_{\mathcal{L}_2} \leq 0, \end{aligned} \tag{2.29}$$

for all $\boldsymbol{\tau}_l(t) \in \mathcal{L}_2[0,\infty)$, where γ is the $\mathcal{W}_\infty$ attenuation level. Besides, $\mathbb{U} : \mathbb{R}_{\geq 0} \to \mathbb{R}^{n_\tau}$, $\boldsymbol{z}(t) = \boldsymbol{x}(t)$, and $\boldsymbol{\Psi} = (\boldsymbol{\Psi}_0, \boldsymbol{\Psi}_1)$, in which $\boldsymbol{\Psi}_0, \boldsymbol{\Psi}_1$ are weighting matrices.

Remark 2.5. Remarks 2.3 also applies to the $\mathcal{W}_\infty$ control problem (2.29). Q.E.D

Remark 2.6. In the control problem (2.29), the $\mathcal{W}_\infty$ attenuation level γ can be seen as the maximum gain in terms of energy that a disturbance signal induces on the output variable and its time derivative. Q.E.D

Note that the control problem (2.29) considers both the cost variables and their time derivatives. Consequently, minimizing γ leads to controllers that offer faster attenuation of disturbances. This is the primary characteristic of the $\mathcal{W}_\infty$ control formulation in the weighted Sobolev space.

2.5 Persistency of Excitation Condition

In this section, some definitions regarding excitation of a bounded regressor function $\boldsymbol{m}(t) : \mathbb{R}_{\geq 0} \to \mathbb{R}^p$ are presented.

Definition 2.7 (Excitation over a time interval (Tao, 2003))**.** A bounded function $\boldsymbol{m}(t) \in \mathbb{R}^n$, where $t \in [t_0, \infty)$, is considered exciting over a time interval $[t, t+T]$, with $T \in \mathbb{R}_{\geq 0}$ and $t \geq t_0$, if there exists $\delta \in \mathbb{R}_{>0}$ such that the following condition is met:

$$\int_t^{t+T} \boldsymbol{m}(\tau)\boldsymbol{m}(\tau)' d\tau \geq \delta \boldsymbol{I}, \tag{2.30}$$

where δ is called the degree of excitation. Q.E.D

Definition 2.8 (Persistency of excitation (Tao, 2003))**.** A bounded function $\boldsymbol{m}(t) \in \mathbb{R}^n$, where $t \in [t_0, \infty)$, is considered persistently exciting, if there exists $T \in \mathbb{R}_{\geq 0}$ and $\delta \in \mathbb{R}_{>0}$ such that the following condition is met:

$$\int_t^{t+T} \boldsymbol{m}(\tau)\boldsymbol{m}(\tau)' d\tau \geq \delta \boldsymbol{I}, \;\; \forall t \geq t_0. \tag{2.31}$$

Q.E.D

In adaptive estimation and identification algorithms, where the regressor typically depends only on time, Definition 2.8 is sufficient to describe the persistent excitation (PE) condition for the regressor. However, in adaptive control, the PE condition must be applied to the regressor matrix, which depends on both the state and time. To account for the regressor's dependence on initial conditions, the concept of uniform persistent excitation (u-PE) is introduced in Panteley et al. (2001). This definition pertains to a pair $(\varphi, \boldsymbol{f})$, where $\varphi(\boldsymbol{x}, t)$ is a general function of time t and state $\boldsymbol{x}$, with $\varphi : \mathbb{R}^n \times \mathbb{R}_{\geq 0} \to \mathbb{R}^p$, serving as the regressor in the context of adaptive control, and $\boldsymbol{f}(\boldsymbol{x}, t)$ represents the function governing the system's dynamics i.e

$$\dot{\boldsymbol{x}} = \boldsymbol{f}(\boldsymbol{x}, t).$$

The definition of u-PE in Panteley et al. (2001) is restated below for the function $\varphi(\boldsymbol{x}, t)$ with respect to the dynamics.

Definition 2.9. (Panteley et al., 2001): The pair $(\varphi, \boldsymbol{f})$ is called uniformly persistently exciting (μ-PE) if, for each $r > 0$, there exist $T \in \mathbb{R}_{\geq 0}$, $\mu \in \mathbb{R}_{\geq 0}$, such that, for all $(\boldsymbol{x}_0, t_0) \in \mathbb{B}_r \times \mathbb{R}_{\geq 0}$, with $\mathbb{B}_r \triangleq \{\boldsymbol{x} \in \mathbb{R}^n : ||\boldsymbol{x}|| < r\}$ all corresponding solutions satisfy

$$\int_t^{t+T} \boldsymbol{\varphi}\left(\boldsymbol{x}\left(\boldsymbol{x}_0, t_0, s\right), s\right) \boldsymbol{\varphi}\left(\boldsymbol{x}\left(\boldsymbol{x}_0, t_0, s\right), s\right)' ds \geq \mu \boldsymbol{I}, \quad \forall t \geq t_0. \tag{2.32}$$

Q.E.D

The definition above indicates that the parameters μ and T are not influenced by the initial conditions $\boldsymbol{x}_0$ and t_0, meaning they are consistent across different initial conditions. If μ and T were dependent on the initial conditions, such signal would exhibit non-uniform persistency of excitation.

One possible relaxation of Definition 2.9 is its interval excitation condition shown in the following.

Definition 2.10. (Panteley et al., 2001): The pair (φ, f) is called interval persistently exciting $\left(\left(t_1,\mu\right)\text{-PE}\right)$ if, for each $r > 0$, there exist $t_1 \in \mathbb{R}_{\geq 0}$, $T \in \mathbb{R}_{\geq 0}$, $\mu > 0$, such that, for all $\boldsymbol{x}_0 \in \mathbb{B}_r$, with $\mathbb{B}_r \triangleq \{\boldsymbol{x} \in \mathbb{R}^n : ||\boldsymbol{x}|| < r\}$, all corresponding solutions satisfy

$$\int_{t_1}^{t_1+T} \boldsymbol{\varphi}\left(\boldsymbol{x}\left(\boldsymbol{x}_0, t_0, s\right), s\right) \boldsymbol{\varphi}\left(\boldsymbol{x}\left(\boldsymbol{x}_0, t_0, s\right), s\right)' ds \geq \mu \boldsymbol{I}. \tag{2.33}$$

Q.E.D

Note that contrary to Definition 2.9, the interval excitation condition in Definition 2.10 is not uniform in time and holds for a particular interval starting at t_1. The interval excitation condition is also called initial excitation condition (Pan and Yu, 2018).

2.6 The Dynamic Regressor Extension and Mixing (DREM)

Consider the estimation of constant parameters in the p-dimensional linear regression

$$y(t) = \boldsymbol{m}'(t)\boldsymbol{\theta}, \tag{2.34}$$

where $y : \mathbb{R}_{\geq 0} \to \mathbb{R}$ and $\boldsymbol{m} : \mathbb{R}_{\geq 0} \to \mathbb{R}^p$ denote time-dependent known, bounded functions, and $\boldsymbol{\theta} \in \mathbb{R}^p$ represents a constant vector of unknown parameters. By employing the classic gradient estimator

$$\dot{\hat{\boldsymbol{\theta}}}(t) = -\boldsymbol{\Psi}\boldsymbol{m}(t)\left(\boldsymbol{m}'(t)\hat{\boldsymbol{\theta}}(t) - y(t)\right), \tag{2.35}$$

with $\boldsymbol{\Psi} \in \mathbb{R}^{p\times p}$ being a given positive definite adaptation gain matrix, the following parameter error equation is obtained:

$$\dot{\tilde{\boldsymbol{\theta}}}(t) = -\boldsymbol{\Psi}\boldsymbol{m}(t)\boldsymbol{m}'(t)\tilde{\boldsymbol{\theta}}(t), \tag{2.36}$$

where $\tilde{\boldsymbol{\theta}}(t) \triangleq \hat{\boldsymbol{\theta}}(t) - \boldsymbol{\theta}$ is the parameter estimation error vector. It is well-known that the zero equilibrium point of the time-varying linear system (2.36) is uniformly globally exponentially stable iff the regressor vector $\boldsymbol{m}(t)$ meet the PE condition (Sastry et al., 1990)

$$\int_t^{t+T} \boldsymbol{m}(\tau)\boldsymbol{m}(\tau)'d\tau \geq \delta\boldsymbol{I}, \tag{2.37}$$

for T, $\delta > 0$ and for all $t \geq 0$. However, in practical scenarios, this condition is often unfulfilled, and consequently, very little can be inferred about the parameter estimation error convergence.

Given the challenge in fulfilling the PE condition, the DREM method (Aranovskiy et al., 2017) offers an innovative solution. The DREM generates p new, one-dimensional, regression models to independently estimate each of the parameters under conditions on the regressor $\boldsymbol{m}(t)$ that differ from the PE condition (2.37). The methodology involves the introduction $p-1$ linear stable $\mathcal{L}_\infty$ operators denoted as $H_i : \mathcal{L}_\infty \to \mathcal{L}_\infty$, for $i \in \{1, 2, p-1\}$. These operators can be defined, for example, as exponentially stable linear filters

$$\dot{y}_{f_i}(t) = -b_i y_{f_i}(t) + a_i y(t), \tag{2.38}$$

with $a_i \neq 0$ and $b_i > 0$. This configuration yields $p-1$ filtered outputs

$$y_{f_i}(t) = \boldsymbol{m}'_{f_i}\boldsymbol{\theta}. \tag{2.39}$$

Stacking up the original linear regression (2.34) with the $p-1$ filtered regressors (2.39), we obtain the augmented regressor system

$$\boldsymbol{y}_f(t) = \boldsymbol{Y}_f(t)\boldsymbol{\theta}, \tag{2.40}$$

where $\boldsymbol{y}_f = [y \; y_{f_1} \; \dots \; y_{f_{p-1}}]'$, and $\boldsymbol{Y}_f = [\boldsymbol{m}' \;\; \boldsymbol{m}'_{f_1} \;\; \dots \;\; \boldsymbol{m}'_{f_{p-1}}]'$. Using the fact that

$$\mathrm{adj}(\boldsymbol{Y}_f)\boldsymbol{Y}_f = \boldsymbol{Y}_f\mathrm{adj}(\boldsymbol{Y}_f) = \phi\boldsymbol{I}, \tag{2.41}$$

in which $\phi \triangleq \det(\boldsymbol{Y}_f)$, and $\mathrm{adj}(\cdot)$ is the adjugate matrix of $(\cdot)$, we multiply both sides of (2.40) by the adjugate matrix $\mathrm{adj}(\boldsymbol{Y}_f)$ of $\boldsymbol{Y}_f \in \mathbb{R}^{p\times p}$ leading to p decoupled equations of the form $y_{e_j} = \phi\theta_j, \;\; \forall j \in \{1, 2, ..., p\}$, with $\boldsymbol{y}_e = \mathrm{adj}(\boldsymbol{Y}_f)\boldsymbol{y}_f$, where $(\cdot)_j$ is the j-th element of the vector $(\cdot)$. As a consequence, p-decoupled estimators of the form

$$\dot{\hat{\theta}}_j = -\gamma_j\phi(t)\left(\phi(t)\hat{\theta}_j - y_e\right) \tag{2.42}$$

are obtained with $\gamma_j > 0$, which leads to the parameter error dynamics

$$\dot{\tilde{\theta}}_j = -\gamma_j\phi^2(t)\tilde{\theta}_j, \tag{2.43}$$

where $\tilde{\theta}_j$ is the j-th element of the error vector of unknown parameters. Therefore, from (2.43), one can deduce

$$\phi \notin \mathcal{L}_2 \implies \lim_{t\to\infty}\tilde{\theta}_j = 0, \;\; \forall j \in \{1, 2, ..., p\}. \tag{2.44}$$

Note that the solution of the time-varying linear system defined in (2.43) is given by

$$\tilde{\theta}_j(t) = e^{-\gamma_j\int_{t_0}^{t}\phi^2(s)ds}\tilde{\theta}_j(t_0), \;\; \forall j = 1, ..., p. \tag{2.45}$$

From (2.45), it is noteworthy that the DREM technique, alongside the gradient estimator, provides some interesting properties stated in the following Lemma

Lemma 2.11 (Stability of the solution of (2.43))**.** *Suppose that*

$$\dot{\tilde{\theta}}_j(t) = -\gamma_j\phi^2(t)\tilde{\theta}_j(t),$$

where $\gamma_j \in \mathbb{R}_{>0}$, $\phi(t) : \mathbb{R}_{\geq 0} \to \mathbb{R}$, and $\tilde{\theta}_j(t)$ is the j-th element of the error vector of unknown parameters. Therefore, the following are true

(i) (Asymptotic Stability) $\phi(t) \notin \mathcal{L}_2 \implies \lim_{t\to\infty}\tilde{\theta}_j(t) = 0$;

(ii) (Exponential Stability) $\phi(t)$ is PE $\implies \tilde{\theta}_j(t) \to 0$ exponentially fast;

(iii) (Elementwise monotonicity) for any $t_2 \geq t_1 \geq 0$ and $j = 1, ..., p$, it holds that

$$\tilde{\theta}_j(t_2) \leq \tilde{\theta}_j(t_1);$$

(iv) (Elementwise tuning) changing γ_j directly influences the transient of $\tilde{\theta}_j$ only.

Proof. See Appendix A.2. Q.E.D

Remark 2.12. Meeting the DREM condition is easier than satisfying the PE condition, especially since it has been shown again in Aranovskiy et al. (2017) that it is possible to find $\boldsymbol{m}(t) \notin PE$ and $\phi \notin \mathcal{L}_2[0, \infty)$. Q.E.D

Remark 2.13. As can be seen in Aranovskiy et al. (2017), a poor choice of filters can hinder convergence as it is possible to have $\boldsymbol{m}(t) \in PE$ and still $\phi \in \mathcal{L}_2[0, \infty)$. However, Korotina et al. (2020) demonstrate that it is always possible to find operators H_i such that if the PE condition (2.37) is satisfied, then $\phi \notin \mathcal{L}_2[t_0, \infty)$. Q.E.D

2.7 Final Remarks

In this chapter, the Euler-Lagrange equations in its canonical form were presented and some properties of such systems were introduced. As have been pointed out in Johan et al. (2014), in the context of Euler-Lagrange systems, certain properties are often presumed, and these assumptions are sometimes extended to multibody systems without explicit demonstration. As a result, many studies omit these crucial proofs, occasionally citing proofs from other systems, such as fixed-base manipulators. This practice can compromise the rigor of stability proofs. Therefore, to maintain formal correctness, it is imperative to rigorously establish these properties for the specific system and parameterization under consideration.

Regarding robust adaptive controllers, this chapter briefly discussed two key topics for this master thesis, namely, the advantadges of formulating controllers in the Sobolev spaces and how to relax the PE condition. Regarding the former, to address the limitations of classic $\mathcal{H}_2$ and $\mathcal{H}_\infty$ controllers, which provide limited control over closed-system transient performance, the $\mathcal{H}_2$ and $\mathcal{H}_\infty$ control approaches formulated within the weighted Sobolev space, by incorporating the weighted Sobolev norm of the cost variable, enhance the transient performance of the $\mathcal{H}_2$ and $\mathcal{H}_\infty$ controllers. These findings suggest that the $\mathcal{W}_2$ and $\mathcal{W}_\infty$ frameworks could serve as more attractive alternatives to traditional robust controllers.

Regarding relaxing the PE condition, the DREM technique is presented as a possible solution. As demonstrated in Aranovskiy et al. (2017), selecting inappropriate filters can avoid convergence, as it is possible for the regressor to be in PE while $\phi(t)$ remains in the $\mathcal{L}_2$ space. However, Korotina et al. (2020) shows that suitable filters can always be found such that if the PE condition is met, then $\phi(t)$ will not belong to the $\mathcal{L}_2$ space. Therefore, satisfying the DREM condition is generally easier than the PE condition, especially since Aranovskiy et al. (2017) also demonstrate that it is possible for the regressor to not be PE while $\phi(t)$ remains outside the $\mathcal{L}_2$ space. Nevertheless, one fundamental problem still remains, that is how to ensure a suitable selection of filters such that the DREM condition is satisfied. This is still an open ended question and research efforts must be directed towards answering it.

In the next chapter some extensions to the nonlinear adaptive $\mathcal{H}_\infty$ are presented alongside the use of the DREM technique.

3

Nonlinear Adaptive $\mathcal{H}_\infty$ Optimal Control

This chapter introduces a general method for obtaining vector regressors from matrix regressors based on the notion of the Euler-Lagrange first integral. In addition, it extends the adaptive nonlinear $\mathcal{H}_\infty$ control strategy by building on Chen et al. (1997), where the adaptive $\mathcal{H}_\infty$ control was first proposed without exact parameter estimation. Here, we incorporate advancements from Aranovskiy et al. (2017), aiming at achieving exact parameter estimation, state tracking, and enabling finite-time estimation. Furthermore, the controller's stability are rigorously proved using Lyapunov theory.

3.1 The Euler-Lagrange First Integral Regressor

Within this section, we detail a systematic methodology aimed at simplifying the construction of the augmented regressor employed in the DREM method. By utilizing the Euler-Lagrange first integral method, we are able to transform a relationship originally expressed as $\boldsymbol{\tau}(t) = \boldsymbol{Y}(\boldsymbol{q}, \dot{\boldsymbol{q}}, \ddot{\boldsymbol{q}})\boldsymbol{\theta}$ into the form $\tau_{\mathcal{I}}(t) = \boldsymbol{Y}_{\mathcal{I}}(\boldsymbol{q}, \dot{\boldsymbol{q}})\boldsymbol{\theta}$, where $\tau_{\mathcal{I}} : \mathbb{R}_{\geq 0} \to \mathbb{R}$ and $\boldsymbol{Y}_{\mathcal{I}}(\boldsymbol{q}, \dot{\boldsymbol{q}}) : \mathbb{R}^n \times \mathbb{R}^n \to \mathbb{R}^{1\times p}$. This method ensures that the procedure for assembling the augmented regressor consistently involves aggregating $p-1$ filtered regressors, as outlined in equation (2.39). Let us first introduce the concept of the Euler-Lagrange first integral.

Consider the Euler-Lagrange equation

$$\frac{d}{dt}\left(\frac{\partial \mathcal{L}(\boldsymbol{q}, \dot{\boldsymbol{q}})}{\partial \dot{\boldsymbol{q}}}\right) - \frac{\partial \mathcal{L}(\boldsymbol{q}, \dot{\boldsymbol{q}})}{\partial \boldsymbol{q}} = \boldsymbol{\tau}(t), \tag{3.1}$$

where

$$\mathcal{L}(\boldsymbol{q}(t), \dot{\boldsymbol{q}}(t)) = \mathcal{K}(\boldsymbol{q}(t), \dot{\boldsymbol{q}}(t)) - \mathcal{P}(\boldsymbol{q}(t)), \tag{3.2}$$

is the Lagrangian function defined as the difference between the kinetic energy, $\mathcal{K}(\boldsymbol{q}(t), \dot{\boldsymbol{q}}(t)) : \mathbb{R}^n \times \mathbb{R}^n \to \mathbb{R}$, and the potential energy, $\mathcal{P}(\boldsymbol{q}(t)) : \mathbb{R}^n \to \mathbb{R}$. To go from (3.2) to the Euler-Lagrange first integral equation, initially, we expand the partial derivative in the first term on the left-hand side of equation (3.1), and pre-multiplied both sides by the time derivative of the generalized coordinates, leading to

$$\begin{aligned}
\dot{\boldsymbol{q}}' \left(\frac{\partial}{\partial \boldsymbol{q}} \left(\frac{\partial \mathcal{L}}{\partial \dot{\boldsymbol{q}}} \right) \dot{\boldsymbol{q}} + \frac{\partial}{\partial \dot{\boldsymbol{q}}} \left(\frac{\partial \mathcal{L}}{\partial \dot{\boldsymbol{q}}} \right) \ddot{\boldsymbol{q}} - \left(\frac{\partial \mathcal{L}}{\partial \boldsymbol{q}} \right) - \boldsymbol{\tau} \right) &= 0, \\
\dot{\boldsymbol{q}}' \left(\frac{d}{dt} \left(\frac{\partial \mathcal{L}}{\partial \dot{\boldsymbol{q}}} \right) - \left(\frac{\partial \mathcal{L}}{\partial \boldsymbol{q}} \right) - \boldsymbol{\tau} \right) &= 0, \\
\left(\dot{\boldsymbol{q}}' \frac{d}{dt} \left(\frac{\partial \mathcal{L}}{\partial \dot{\boldsymbol{q}}} \right) + \ddot{\boldsymbol{q}}' \frac{\partial \mathcal{L}}{\partial \dot{\boldsymbol{q}}} \right) - \left(\dot{\boldsymbol{q}}' \frac{\partial \mathcal{L}}{\partial \boldsymbol{q}} + \ddot{\boldsymbol{q}}' \frac{\partial \mathcal{L}}{\partial \dot{\boldsymbol{q}}} \right) - \dot{\boldsymbol{q}}' \boldsymbol{\tau} &= 0.
\end{aligned} \tag{3.3}$$

Subsequently, we simplified the expression by performing a straightforward contraction of terms, yielding

$$\frac{d}{dt} \left(\dot{\boldsymbol{q}}' \frac{\partial \mathcal{L}}{\partial \dot{\boldsymbol{q}}} - \mathcal{L} - \int_0^t \dot{\boldsymbol{q}}' \boldsymbol{\tau} ds \right) = 0. \tag{3.4}$$

The final step involves taking the integral of both sides of (3.4) and reorganizing the terms to achieve

$$\dot{\boldsymbol{q}}' \frac{\partial \mathcal{L}}{\partial \dot{\boldsymbol{q}}} - \mathcal{L} - \int_0^t \dot{\boldsymbol{q}}' \boldsymbol{\tau} ds = \mathcal{C} \left(\boldsymbol{q}(0), \dot{\boldsymbol{q}}(0) \right), \tag{3.5}$$

where $\mathcal{C} \left(\boldsymbol{q}(0), \dot{\boldsymbol{q}}(0) \right) \in \mathbb{R}$ is a constant.

The Euler-Lagrange first integral equation (3.5) is linear in the unknown parameters, allowing to write

$$\begin{aligned}
\dot{\boldsymbol{q}}' \frac{\partial \mathcal{L}(\boldsymbol{q}, \dot{\boldsymbol{q}})}{\partial \dot{\boldsymbol{q}}} - \mathcal{L}(\boldsymbol{q}, \dot{\boldsymbol{q}}) - \mathcal{C} \left(\boldsymbol{q}(0), \dot{\boldsymbol{q}}(0) \right) = \\
\frac{1}{2} \dot{\boldsymbol{q}}' \boldsymbol{M} \dot{\boldsymbol{q}} + \mathcal{P}(\boldsymbol{q}) - \mathcal{P}(\boldsymbol{q}(0)) = \tau_{\mathcal{I}} = \boldsymbol{Y}_{\mathcal{I}}(\boldsymbol{q}, \dot{\boldsymbol{q}})' \boldsymbol{\theta},
\end{aligned} \tag{3.6}$$

with $\tau_{\mathcal{I}}(t) = \int_0^t \dot{\boldsymbol{q}}' \boldsymbol{\tau} ds$ and $\boldsymbol{Y}_{\mathcal{I}}(\boldsymbol{q}, \dot{\boldsymbol{q}}) : \mathbb{R}^n \times \mathbb{R}^n \to \mathbb{R}^{p \times 1}$ and under the assumption that $\dot{\boldsymbol{q}}(0) = \boldsymbol{0}$.

The next step, in order to obtain a square regressor like (2.40), is to filter the original regressor obtained from the Euler-Lagrange first integral.

Corollary 3.1 (Swapping Lemma (Ioannou and Sun, 1996))**.** *Consider the following* $p - 1$

first-order stable linear filters:

$$\dot{\boldsymbol{Y}}_{\phi_j} = -b_j \boldsymbol{Y}_{\phi_j} + \bar{a}_j \boldsymbol{Y}_{\mathcal{I}}(\boldsymbol{q}, \dot{\boldsymbol{q}}), \tag{3.7}$$

$$\dot{\tau}_{\phi_j} = -b_j \tau_{\phi_j} + \bar{a}_j \tau_{\mathcal{I}}, \tag{3.8}$$

with $\boldsymbol{Y}_{\phi_j} : \mathbb{R}_{\geq 0} \to \mathbb{R}^{1\times p}$ *and* $\tau_{\phi_j} : \mathbb{R}_{\geq 0} \to \mathbb{R}$, *for* $j = 1, \ldots, p-1$, *and* $\boldsymbol{Y}_{\phi_j}(0) = \boldsymbol{0}$, $\tau_{\phi_j}(0) = 0$, $\bar{a}_j, b_j, c_j \in \mathbb{R}_{>0}$. *Therefore, the following relation is true*

$$\tau_{\phi_j} = \boldsymbol{Y}_{\phi_j} \boldsymbol{\theta}. \tag{3.9}$$

Proof. See Appendix A.5. Q.E.D

Once we have established the relation (3.9), we are ready to apply some regression extension in order to obtain a relation of the form (2.40). The usual approach following the DREM procedure, as idealized by Aranovskiy et al. (2017), would involve filtering the regressor obtained from the First-Integral approach and piling up the results to construct a square matrix. It is worth noting that the Fist-Integral approach allows a systematic manner to obtain linear regression equations suitable for direct application of the DREM technique.

In view of (3.9) we can write

$$\boldsymbol{\tau}_f = \boldsymbol{Y}_f \boldsymbol{\theta}, \tag{3.10}$$

where the augmented regressor is constructed by pilling up $p-1$ filtered regressors as

$$\boldsymbol{Y}_f = \begin{bmatrix} \boldsymbol{Y}_{\mathcal{I}} \\ \boldsymbol{Y}_{\phi_1} \\ \vdots \\ \boldsymbol{Y}_{\phi_{p-1}} \end{bmatrix}, \tag{3.11}$$

and the augmented output is obtained, similarly, as

$$\boldsymbol{\tau}_f = \begin{bmatrix} \boldsymbol{\tau}_{\mathcal{I}} & \boldsymbol{\tau}_{\phi_1} & \ldots & \boldsymbol{\tau}_{\phi_{p-1}} \end{bmatrix}'. \tag{3.12}$$

Multiplying the left-hand of (3.10) by $\mathrm{adj}(\boldsymbol{Y}_f)$, yields

$$\boldsymbol{\tau}_e = \mathrm{adj}(\boldsymbol{Y}_f) \boldsymbol{Y}_f \boldsymbol{\theta} = \phi \boldsymbol{\theta}, \tag{3.13}$$

where $\phi = \det(\boldsymbol{Y}_f)$ and $\boldsymbol{\tau}_e = \mathrm{adj}(\boldsymbol{Y}_f)\boldsymbol{\tau}_f$. It is worth highlighting that (3.13) is designed in a way that yields p decoupled equations.

An essential aspect of the DREM procedure is the extension of the regressor. The challenge lies in executing this extension in a manner that maintains or increases the excitation level, whether PE or IE, of the regressor. Such selection can hinder convergence, even if the initial regressor is PE, as demonstrated in Aranovskiy et al. (2017). Notably, by following the filtering steps of the DREM procedure to obtain the square regressor, very little can be inferred about the preservation of excitation properties of the initial regressor obtained through the First-Integral procedure. In the following, a Linear Regression Extension is proposed based on the Kresseilmeier Regression Extension scheme (Kreisselmeier, 1977) and the Euler-Lagrange First-Integral. Such choice is based on the well-known qualitative and quantitative results that this scheme can preserve excitation properties of the original regressor.

3.2 Memory Regressor Extension and Mixing (MREM)

One commonly used method in adaptive control for extending the dynamics while preserving excitation is the Kreisselmeier's regressor extension (Kreisselmeier, 1977). The authors in Ortega et al. (2020) and Gerasimov and Nikiforov (2022) referred to such extension, in the context of the DREM, as Memory Regressor Extension (MRE). For the sake of completeness, the recent results proving the preserving of excitation properties in the Kresseilmeier Regression Extension obtained in Aranovskiy et al. (2023) are presented in the following.

The Kresseilmeier Regression Extension can be obtained solving the following,[1]

$$\dot{\boldsymbol{Y}}_f(t) = -b\boldsymbol{Y}_f(t) + a\left(\boldsymbol{Y}_{\mathcal{I}}(t)\boldsymbol{Y}_{\mathcal{I}}(t)'\right), \tag{3.14}$$

$$\dot{\boldsymbol{T}}_f(t) = -b\boldsymbol{T}_f(t) + a\left(\boldsymbol{Y}_{\mathcal{I}}(t)\boldsymbol{\tau}_{\mathcal{I}}(t)\right), \tag{3.15}$$

where $\boldsymbol{Y}_f(0) \geq \mathbf{0}$, $\boldsymbol{T}_f(0) = \boldsymbol{T}_{f_0}$, and $a, b \in \mathbb{R} > 0$ are scalar tuning parameters which render true the relation

$$\boldsymbol{T}_f(t) = \boldsymbol{Y}_f(t)\boldsymbol{\theta}. \tag{3.16}$$

The preservation of excitation implies

$$\boldsymbol{Y}_{\mathcal{I}} \in PE \implies \boldsymbol{Y}_f > 0, \tag{3.17}$$

or in the case of the DREM context,

$$\boldsymbol{Y}_{\mathcal{I}} \in PE \implies \boldsymbol{\phi} > 0, \tag{3.18}$$

[1] For the sake of simplicity consider $\boldsymbol{Y}_{\mathcal{I}}(t) \equiv \boldsymbol{Y}_{\mathcal{I}}(\boldsymbol{q}(t), \dot{\boldsymbol{q}}(t))$ and $\boldsymbol{Y}_f(t) \equiv \boldsymbol{Y}_f(\boldsymbol{q}(t), \dot{\boldsymbol{q}}(t))$.

where $\boldsymbol{\phi} = det(\boldsymbol{Y}_f)$. Appying the mixing step to (3.16) yields

$$\mathcal{T}(t) = \phi(t)\boldsymbol{\theta}, \tag{3.19}$$

where $\mathcal{T}(t) = adj\left(\boldsymbol{Y}_f(t)\right)\boldsymbol{T}_f(t)$ and $\phi(t) = det(\boldsymbol{Y}_f)$.

The proof of (3.17) and (3.18) can be found in Ioannou and Sun (1996). In addition, the recent results from Aranovskiy et al. (2023) where a quantitative analysis of the preserving properties of the Kreseilemeirs regressor extension in the context of the DREM technique are shown in the following theorem.

Theorem 3.2 (Excitation Propagation (Aranovskiy et al., 2023))**.** *Take into consideration the bounded function $\boldsymbol{Y}_{\mathcal{I}} : \mathbb{R}_{\geq 0} \to \mathbb{R}^p$ and let $\boldsymbol{Y}_f : \mathbb{R}_{\geq 0} \to \mathbb{R}^{p\times p}$ be a solution to (3.14) for $\boldsymbol{Y}_f(t_0) = \boldsymbol{Y}_{\mathcal{I}}(t_0)\boldsymbol{Y}'_{\mathcal{I}}(t_0) \geq 0$. Let $\phi : \mathbb{R}_{\geq 0} \to \mathbb{R}$ be the determinant of $\boldsymbol{Y}_f(t)$. Then, if $\boldsymbol{Y}_{\mathcal{I}}(t)$ is (μ)-PE (see Definition 2.9), then for any positive integer $k \geq 1$ and for any $t \geq kT$, it holds*

$$\boldsymbol{Y}_f(t) \geq \mu \sum_{j=1}^{k} e^{-aj\Delta T}\boldsymbol{I}. \tag{3.20}$$

consequently,

$$\phi(t) \geq \mu^p \left(\sum_{i=1}^{k} e^{-bq\Delta T}\right)^p, \tag{3.21}$$

and

$$lim_{t\to\infty} \inf \phi(t) \geq \left(\frac{\mu}{e^{b\Delta T} - 1}\right)^p. \tag{3.22}$$

In addition, the following implication is true

$$\boldsymbol{Y}_{\mathcal{I}}(t) \in PE \Leftrightarrow \phi \in PE \tag{3.23}$$

Proof. See Appendix A.4. Q.E.D

3.3 Adaptive $\mathcal{H}_\infty$ Control

In this section we detail the development of the nonlinear adaptive $\mathcal{H}_\infty$ controller developed in Chen et al. (1997). Initially recall the dynamic model of an n-degrees of freedom Euler-Lagrange system which can be written as follows

$$\boldsymbol{M}(\boldsymbol{q})\ddot{\boldsymbol{q}}(t) + \boldsymbol{C}(\dot{\boldsymbol{q}}, \boldsymbol{q})\dot{\boldsymbol{q}}(t) + \boldsymbol{G}(\boldsymbol{q}) = \boldsymbol{\tau}(t) + \boldsymbol{\tau}_l(t), \tag{3.24}$$

where $\boldsymbol{q}(t) : \mathbb{R}_+ \to \mathbb{R}^n$ denotes the vector of generalized coordinates, $\boldsymbol{M}(\boldsymbol{q}) : \mathbb{R}^n \to \mathbb{R}^{n\times n}$ represents the inertia matrix, $\boldsymbol{C}(\dot{\boldsymbol{q}}, \boldsymbol{q}) : \mathbb{R}^n \times \mathbb{R}^n \to \mathbb{R}^{n\times n}$ corresponds to the Coriolis and centripetal force matrix, $\boldsymbol{G}(\boldsymbol{q}) : \mathbb{R}^n \to \mathbb{R}^n$ is the gravitational force vector, $\boldsymbol{\tau}(t) : \mathbb{R}_{\geq 0} \to \mathbb{R}^n$ is the vector of generalized control inputs, and $\boldsymbol{\tau}_l(t) : \mathbb{R}_{\geq 0} \to \mathbb{R}^n$ represents the external disturbances. For control design purposes, we define the state vector $\tilde{\boldsymbol{x}} = \begin{bmatrix} \dot{\tilde{\boldsymbol{q}}}' & \tilde{\boldsymbol{q}}' \end{bmatrix}'$, where $\tilde{\boldsymbol{q}} \triangleq \boldsymbol{q}(t) - \boldsymbol{q}_r(t)$, with $\boldsymbol{q}_r(t) \in \mathcal{C}^3$ being the desired reference, Then, the tracking error dynamics of the system with unknown parameters and external disturbances can be written as

$$\dot{\tilde{\boldsymbol{x}}}=\boldsymbol{A}(\boldsymbol{q}(t),\dot{\boldsymbol{q}}(t))\tilde{\boldsymbol{x}}+\boldsymbol{B}_0(\dot{\boldsymbol{q}}_r(t),\ddot{\boldsymbol{q}}_r(t),\boldsymbol{q}(t),\dot{\boldsymbol{q}}(t))+\boldsymbol{B}\boldsymbol{M}^{-1}\left(\boldsymbol{\tau}+\boldsymbol{\tau}_l\right), \tag{3.25}$$

with

$$\begin{aligned} \boldsymbol{A}(\boldsymbol{q}(t),\dot{\boldsymbol{q}}(t)) &= \begin{bmatrix} -\boldsymbol{M}^{-1}\boldsymbol{C} & \boldsymbol{0} \\ \boldsymbol{I} & \boldsymbol{0} \end{bmatrix}, \\ \boldsymbol{B}_0(\dot{\boldsymbol{q}}_r(t),\ddot{\boldsymbol{q}}_r(t),\boldsymbol{q}(t),\dot{\boldsymbol{q}}(t)) &= \begin{bmatrix} -\ddot{\boldsymbol{q}}_r(t) - \boldsymbol{M}^{-1}\left(\boldsymbol{G} + \boldsymbol{C}\dot{\boldsymbol{q}}_r\right) \\ \boldsymbol{0} \end{bmatrix}, \\ \boldsymbol{B} &= \begin{bmatrix} \boldsymbol{I} \\ \boldsymbol{0} \end{bmatrix}. \end{aligned}$$

Consider the state-space transformation (Johansson, 1990)

$$\boldsymbol{z} = \begin{bmatrix} \boldsymbol{z}_1 \\ \boldsymbol{z}_2 \end{bmatrix} = \boldsymbol{T}_0\tilde{\boldsymbol{x}} = \begin{bmatrix} \boldsymbol{T}_1 \\ \boldsymbol{T}_2 \end{bmatrix} \begin{bmatrix} \dot{\tilde{\boldsymbol{q}}} \\ \tilde{\boldsymbol{q}} \end{bmatrix} = \begin{bmatrix} \boldsymbol{T}_{11} & \boldsymbol{T}_{12} \\ \boldsymbol{0} & \boldsymbol{I} \end{bmatrix} \begin{bmatrix} \dot{\tilde{\boldsymbol{q}}} \\ \tilde{\boldsymbol{q}} \end{bmatrix}, \tag{3.26}$$

where $\boldsymbol{T}_{11}, \boldsymbol{T}_{12} \in \mathbb{R}^{n\times n}$ are constant matrices to be determined. In what follows, $\boldsymbol{T}_{11}$ is assumed to be a diagonal matrix such that $\boldsymbol{T}_{11} = t_{11}\boldsymbol{I}$, for some $t_{11} > 0$. Taking into account *Property 5* (see Chapter 2), one can write

$$\dot{\boldsymbol{z}}=\begin{bmatrix} -\boldsymbol{M}^{-1}\boldsymbol{C} & \boldsymbol{0} \\ \boldsymbol{T}_{11}^{-1} & -\boldsymbol{T}_{11}^{-1}\boldsymbol{T}_{12} \end{bmatrix}\boldsymbol{z}+\boldsymbol{B}\boldsymbol{T}_{11}\boldsymbol{M}^{-1}\left(-\boldsymbol{Y}\boldsymbol{\theta}+\boldsymbol{\tau}+\boldsymbol{\tau}_l\right), \tag{3.27}$$

with $\boldsymbol{B} = [\boldsymbol{I}\ \boldsymbol{0}]'$ and $\boldsymbol{Y}\boldsymbol{\theta} = \boldsymbol{M}(\boldsymbol{q})\left(\ddot{\boldsymbol{q}}_r(t) - \boldsymbol{T}_{11}^{-1}\boldsymbol{T}_{12}\dot{\tilde{\boldsymbol{q}}}\right) + \boldsymbol{C}(\dot{\boldsymbol{q}}, \boldsymbol{q})\left(\dot{\boldsymbol{q}}_r(t) - \boldsymbol{T}_{11}^{-1}\boldsymbol{T}_{12}\tilde{\boldsymbol{q}}\right) + \boldsymbol{G}(\boldsymbol{q})$. Applying the state space transformation (3.26) into (3.27) results in the following dynamic equation for $\tilde{\boldsymbol{x}}$:

$$\dot{\tilde{\boldsymbol{x}}} = \boldsymbol{f}(\tilde{\boldsymbol{x}}, t)\tilde{\boldsymbol{x}} + \boldsymbol{g}(\tilde{\boldsymbol{x}}, t)\boldsymbol{u} + \boldsymbol{g}(\tilde{\boldsymbol{x}}, t)\boldsymbol{d}, \tag{3.28}$$

where

$$\boldsymbol{f}(\tilde{\boldsymbol{x}},t) \triangleq \boldsymbol{T}_0^{-1}\begin{bmatrix} -\boldsymbol{M}^{-1}\boldsymbol{C} & \boldsymbol{0} \\ \boldsymbol{T}_{11}^{-1} & -\boldsymbol{T}_{11}^{-1}\boldsymbol{T}_{12} \end{bmatrix}\boldsymbol{T}_0, \tag{3.29}$$

$$\boldsymbol{g}(\tilde{\boldsymbol{x}},t) \triangleq \boldsymbol{T}_0^{-1}\boldsymbol{B}\boldsymbol{M}^{-1}, \tag{3.30}$$

$$\boldsymbol{d} \triangleq \boldsymbol{T}_{11}\boldsymbol{\tau}_l, \tag{3.31}$$

$$\boldsymbol{u} \triangleq \boldsymbol{T}_{11}\left(-\boldsymbol{Y}\boldsymbol{\theta} + \boldsymbol{\tau}\right). \tag{3.32}$$

The nonlinear $\mathcal{H}_\infty$ control problem is formulated as a quadratic optimization problem where the cost functional is expressed as

$$\mathcal{J}(\boldsymbol{u},\boldsymbol{d}) = \int_{t_0}^{\infty} \mathcal{L}(\tilde{\boldsymbol{x}},\boldsymbol{u},\boldsymbol{d})ds = \int_{t_0}^{\infty}\left(\frac{1}{2}\tilde{\boldsymbol{x}}'\boldsymbol{Q}\tilde{\boldsymbol{x}} + \frac{1}{2}\boldsymbol{u}'\boldsymbol{R}\boldsymbol{u} - \frac{\rho^2}{2}\boldsymbol{d}'\boldsymbol{d}\right)dt. \tag{3.33}$$

Given the performance index (3.33), we seek for an optimal control $\boldsymbol{u}^*$ that minimizes $J(\tilde{\boldsymbol{x}},\boldsymbol{u})$ for the worst-case disturbance $\boldsymbol{d}^*$. The optimal control, $\boldsymbol{u}^*$, guides the system from any initial state to an arbitrary desired state, minimizing the weighted sum of the energy associated with the control effort and states with the matrix $\boldsymbol{R}' = \boldsymbol{R} > 0 \in \mathbb{R}^{n\times n}$ and matrix $\boldsymbol{Q}' = \boldsymbol{Q} > 0 \in \mathbb{R}^{2n\times 2n}$. The weights in $\boldsymbol{Q}$ and $\boldsymbol{R}$ can be adjusted to achieve desired performance.

When considering the cost functional for the case when $\boldsymbol{d} \neq 0$, it is not sufficient to minimize the Hamiltonian with respect to the control effort. Instead, minimizing (3.33) involves solving the so-called Hamilton-Jacobi-Bellman-Isaacs (HJBI) equation which can be done finding a settle point of the Hamiltonian with respect to both the control effort and the worst-case disturbance. The HJBI equation is shown in the following:

$$\frac{\partial V(\tilde{\boldsymbol{x}},t)}{\partial t} + \min_{\boldsymbol{u}(t)}\max_{\boldsymbol{d}(t)}\left\{\mathbb{H}\left(\tilde{\boldsymbol{x}},\boldsymbol{u},\boldsymbol{d},\frac{\partial V(\tilde{\boldsymbol{x}},t)}{\partial\tilde{\boldsymbol{x}}}\right)\right\} = 0. \tag{3.34}$$

The Hamiltonian is computed as

$$\mathbb{H}\left(\tilde{\boldsymbol{x}},\boldsymbol{u},\boldsymbol{d},\frac{\partial V(\tilde{\boldsymbol{x}},t)}{\partial\tilde{\boldsymbol{x}}}\right) = \mathcal{L}(\tilde{\boldsymbol{x}},\boldsymbol{u},\boldsymbol{d}) + \frac{\partial V(\tilde{\boldsymbol{x}},t)}{\partial\tilde{\boldsymbol{x}}}'\dot{\tilde{\boldsymbol{x}}}. \tag{3.35}$$

In addition, consider the candidate Lyapunov function

$$V(\tilde{\boldsymbol{x}},t) \triangleq \frac{1}{2}\tilde{\boldsymbol{x}}'\boldsymbol{T}_0'\begin{bmatrix} \boldsymbol{M}(\boldsymbol{q}) & \boldsymbol{0} \\ * & \boldsymbol{K} \end{bmatrix}\boldsymbol{T}_0\tilde{\boldsymbol{x}}, \tag{3.36}$$

which satisfies

$$\lambda_1||\tilde{\boldsymbol{x}}||^2 \leq V(\tilde{\boldsymbol{x}},t) \leq \lambda_2||\tilde{\boldsymbol{x}}||^2, \tag{3.37}$$

where $\lambda_1 = \lambda_{min}(\boldsymbol{H})$, in which $\boldsymbol{K} > 0$, $\boldsymbol{H} \triangleq \boldsymbol{T}_0'\text{blkdiag}(\boldsymbol{M}, \boldsymbol{K})\boldsymbol{T}_0$. Also, $\lambda_2 = \lambda_{max}(\boldsymbol{H})$, where $\lambda_{min}(\cdot)$ and $\lambda_{max}(\cdot)$ stand for the smallest and highest eigenvalue of $(\cdot)$, respectively.

Taking the partial derivative of (3.36) with respect to $\tilde{\boldsymbol{x}}$ yields

$$\frac{\partial V(\tilde{\boldsymbol{x}},t)'}{\partial \tilde{\boldsymbol{x}}}\dot{\tilde{\boldsymbol{x}}} = \tilde{\boldsymbol{x}}\boldsymbol{T}_0' \begin{bmatrix} \boldsymbol{M} & \boldsymbol{0} \\ \boldsymbol{0} & \boldsymbol{K} \end{bmatrix} \boldsymbol{T}_0\dot{\tilde{\boldsymbol{x}}} + \frac{1}{2}\sum_{i=1}^{2n}\tilde{\boldsymbol{x}}'\boldsymbol{T}_0' \begin{bmatrix} \frac{\partial \boldsymbol{M}}{\partial \tilde{x}_i}\dot{\tilde{\boldsymbol{x}}}_i & \boldsymbol{0} \\ \boldsymbol{0} & \boldsymbol{0} \end{bmatrix} \boldsymbol{T}_0\tilde{\boldsymbol{x}},$$
$$= \tilde{\boldsymbol{x}}'\boldsymbol{T}_0' \begin{bmatrix} -\boldsymbol{C} & \boldsymbol{0} \\ \boldsymbol{K}\boldsymbol{T}_{11}^{-1} & -\boldsymbol{K}\boldsymbol{T}_{11}^{-1}\boldsymbol{T}_{12} \end{bmatrix} \boldsymbol{T}_0\tilde{\boldsymbol{x}} + \frac{1}{2}\sum_{i=1}^{2n}\tilde{\boldsymbol{x}}'\boldsymbol{T}_0' \begin{bmatrix} \frac{\partial \boldsymbol{M}}{\partial \tilde{x}_i}\dot{\tilde{\boldsymbol{x}}}_i & \boldsymbol{0} \\ \boldsymbol{0} & \boldsymbol{0} \end{bmatrix} \boldsymbol{T}_0\tilde{\boldsymbol{x}} + \tilde{\boldsymbol{x}}'\boldsymbol{T}_0'\boldsymbol{B}(\boldsymbol{u}+\boldsymbol{d}).$$

Using *Property 4* (see Chapter 2) renders

$$\frac{\partial V_{\tilde{x}}(\tilde{\boldsymbol{x}},t)'}{\partial \tilde{\boldsymbol{x}}}\dot{\tilde{\boldsymbol{x}}} = \frac{1}{2}\tilde{\boldsymbol{x}}' \begin{bmatrix} \boldsymbol{0} & \boldsymbol{K} \\ \boldsymbol{K} & \boldsymbol{0} \end{bmatrix} \tilde{\boldsymbol{x}} + \frac{1}{2}\tilde{\boldsymbol{x}}'\boldsymbol{T}_0' \begin{bmatrix} \sum_{i=1}^{2n}\frac{\partial \boldsymbol{M}}{\partial \tilde{x}_i}\dot{\tilde{\boldsymbol{x}}}_i - \dot{\boldsymbol{M}} & \boldsymbol{0} \\ \boldsymbol{0} & \boldsymbol{0} \end{bmatrix} \boldsymbol{T}_0\tilde{\boldsymbol{x}} + \tilde{\boldsymbol{x}}'\boldsymbol{T}_0'\boldsymbol{B}(\boldsymbol{u}+\boldsymbol{d}). \quad (3.38)$$

Taking the partial derivative with respect to $\boldsymbol{u}(t)$ in order to minimize the Hamiltonian (3.35) yields,

$$\frac{\partial \mathbb{H}}{\partial \boldsymbol{u}}\left(\tilde{\boldsymbol{x}}, \boldsymbol{u}, \boldsymbol{d}, \frac{\partial V(\tilde{\boldsymbol{x}},t)}{\partial \tilde{\boldsymbol{x}}}\right) = \boldsymbol{R}\boldsymbol{u}^* + \boldsymbol{B}'\boldsymbol{T}_0\tilde{\boldsymbol{x}} = 0. \quad (3.39)$$

Consequently, the optimal control effort is given by

$$\boldsymbol{u}^* = -\boldsymbol{R}^{-1}\boldsymbol{B}'\boldsymbol{T}_0\tilde{\boldsymbol{x}}. \quad (3.40)$$

Taking the second partial derivative of the Hamiltonian with respect to $\boldsymbol{u}$, it is possible to infer that

$$\frac{\partial^2 \mathbb{H}}{\partial \boldsymbol{u}^2}\left(\tilde{\boldsymbol{x}}, \boldsymbol{u}, \boldsymbol{d}, \frac{\partial V(\tilde{\boldsymbol{x}},t)}{\partial \tilde{\boldsymbol{x}}}\right) = \boldsymbol{R} > 0. \quad (3.41)$$

Thus, it is sufficient to confirm that $\boldsymbol{u}^*(t)$ in (3.40) attains a local minimum of the Hamiltonian.

Remark 3.3. It can be appreciated that if $\boldsymbol{d} = 0$, meaning that we are solving the nonlinear $\mathcal{H}_2$ control problem instead, (3.35) can be written as

$$\mathbb{H}\left(\tilde{\boldsymbol{x}}, \boldsymbol{u}, \frac{\partial V(\tilde{\boldsymbol{x}},t)}{\partial \tilde{\boldsymbol{x}}}\right) = \boldsymbol{h}(\tilde{\boldsymbol{x}},t) + \boldsymbol{k}(\tilde{\boldsymbol{x}},t)'\boldsymbol{u}(t) + \frac{1}{2}\boldsymbol{u}'(t)\boldsymbol{R}\boldsymbol{u}, \quad (3.42)$$

with[2]

$$\boldsymbol{h}(\tilde{\boldsymbol{x}},t) = \frac{1}{2}\tilde{\boldsymbol{x}}' \begin{bmatrix} \mathbf{0}\,\boldsymbol{K} \\ \boldsymbol{K}\,\mathbf{0} \end{bmatrix} \tilde{\boldsymbol{x}} + \frac{1}{2}\tilde{\boldsymbol{x}}'\boldsymbol{T}_0' \begin{bmatrix} \sum_{i=1}^{2n} \frac{\partial \boldsymbol{M}}{\partial \tilde{\boldsymbol{x}}_i}\dot{\tilde{\boldsymbol{x}}}_i - \dot{\boldsymbol{M}} & \mathbf{0} \\ \mathbf{0} & \mathbf{0} \end{bmatrix} \boldsymbol{T}_0\tilde{\boldsymbol{x}} + \frac{1}{2}\tilde{\boldsymbol{x}}'\boldsymbol{Q}\tilde{\boldsymbol{x}}, \tag{3.43}$$

$$\boldsymbol{k}(\tilde{\boldsymbol{x}},t) = \boldsymbol{B}'\boldsymbol{T}_0\tilde{\boldsymbol{x}}. \tag{3.44}$$

Then, (3.39) and (3.41) are necessary and sufficient conditions to ensure that (3.40) attains a global minimum of the Hamiltonian (3.35) (Kirk, 2004). Q.E.D

Taking the partial derivative of (3.35) with respect to $\boldsymbol{d}(t)$ allows to find the worst-case disturbance $\boldsymbol{d}^*(t)$, as follows

$$\frac{\partial \mathbb{H}}{\partial \boldsymbol{d}}\left(\tilde{\boldsymbol{x}}, \boldsymbol{u}, \boldsymbol{d}, \frac{\partial V(\tilde{\boldsymbol{x}},t)}{\partial \tilde{\boldsymbol{x}}}\right) = -\rho^2\boldsymbol{d}^* + \boldsymbol{B}'\boldsymbol{T}_0\tilde{\boldsymbol{x}} = 0, \tag{3.45}$$

which implies that the worst-case disturbance is given by

$$\boldsymbol{d}^*(t) = \frac{1}{\rho^2}\boldsymbol{B}'\boldsymbol{T}_0\tilde{\boldsymbol{x}}. \tag{3.46}$$

Similar reasoning used for showing that (3.40) attains a minimum of the Hamiltonian is employed to show the worst-case disturbance conversely attains a maximum.

Before solving the resulting HJ partial differential equation (PDE), first the partial derivative of (3.36) with respect to time is computed as

$$\frac{\partial V_{\tilde{\boldsymbol{x}}}(\tilde{\boldsymbol{x}},t)}{\partial t} = \frac{1}{2}\tilde{\boldsymbol{x}}'\boldsymbol{T}_0' \begin{bmatrix} \frac{\partial \boldsymbol{M}}{\partial t} & \mathbf{0} \\ \mathbf{0} & \mathbf{0} \end{bmatrix} \boldsymbol{T}_0\tilde{\boldsymbol{x}}. \tag{3.47}$$

In what follows, substituting (3.40), (3.46) and (3.47) into (3.34) yields the Hamilton-Jacobi equation

$$\frac{1}{2}\tilde{\boldsymbol{x}}' \begin{bmatrix} \mathbf{0}\,\boldsymbol{K} \\ \boldsymbol{K}\,\mathbf{0} \end{bmatrix} \tilde{\boldsymbol{x}} + \frac{1}{2}\tilde{\boldsymbol{x}}'\boldsymbol{Q}\tilde{\boldsymbol{x}} + \frac{1}{2\rho}\tilde{\boldsymbol{x}}'\boldsymbol{T}_0'\boldsymbol{B}\boldsymbol{B}'\boldsymbol{T}_0\tilde{\boldsymbol{x}} - \frac{1}{2}\tilde{\boldsymbol{x}}'\boldsymbol{T}_0'\boldsymbol{B}\boldsymbol{R}^{-1}\boldsymbol{B}'\boldsymbol{T}_0\tilde{\boldsymbol{x}} = 0. \tag{3.48}$$

The solution of the Hamilton-Jacobi equation (3.48) is obtained by solving the following algebraic Riccati equation

$$\begin{bmatrix} \mathbf{0}\,\boldsymbol{K} \\ \boldsymbol{K}\,\mathbf{0} \end{bmatrix} + \boldsymbol{Q} - \boldsymbol{T}_0'\boldsymbol{B}\left(\boldsymbol{R}^{-1} - \frac{1}{\rho^2}\boldsymbol{I}\right)\boldsymbol{B}'\boldsymbol{T}_0 = 0. \tag{3.49}$$

Finally, it is possible to state the following corollary regarding the nonlinear adaptive $\mathcal{H}_\infty$ control.

[2] It is noteworthy that although $\boldsymbol{h}(\tilde{\boldsymbol{x}},t)$ has a dependence on $\dot{\tilde{\boldsymbol{x}}}(t)$ and, therefore, could potentially depend on $\boldsymbol{u}(t)$, such dependence vanishes due $\frac{\partial \boldsymbol{M}(\boldsymbol{q})}{\partial \dot{\tilde{\boldsymbol{q}}}_i} = \mathbf{0}$ for all $i = 1, ..., n$.

Corollary 3.4 (Nonlinear Adaptive $\mathcal{H}_\infty$ Control Adapted from Chen et al. (1997)). *Consider the nonlinear system described by* (3.28)*. Let* $\boldsymbol{R} \in \mathbb{R}^{n\times n}$ *and* $\boldsymbol{Q} \in \mathbb{R}^{2n\times 2n}$ *be given symmetric positive definite matrices. Suppose* $\rho^2\boldsymbol{I} > \boldsymbol{R}$ *and both* $\boldsymbol{T}_0$ *and* $\boldsymbol{K}$*, with* $\boldsymbol{K} = \boldsymbol{K}' > 0$ *and* $\boldsymbol{K} \in \mathbb{R}^{n\times n}$*, satisfy the algebraic Riccati equation* (3.49)*. Then, the robust nonlinear adaptive* $\mathcal{H}_\infty$ *control law*

$$\dot{\hat{\boldsymbol{\theta}}}(t) = -\boldsymbol{K}_\theta^{-1}\boldsymbol{Y}'\boldsymbol{T}_{11}\boldsymbol{B}'\boldsymbol{T}_0\tilde{\boldsymbol{x}}(t), \tag{3.50}$$

$$\boldsymbol{\tau}(t) = \boldsymbol{Y}\hat{\boldsymbol{\theta}}(t) + \boldsymbol{T}_{11}^{-1}\boldsymbol{u}^*(t), \tag{3.51}$$

$$\boldsymbol{\tau}_l(t) = \boldsymbol{T}_{11}^{-1}\boldsymbol{d}^*(t), \tag{3.52}$$

with $\boldsymbol{u}^* = -\boldsymbol{R}^{-1}\boldsymbol{B}'\boldsymbol{T}_0\tilde{\boldsymbol{x}}$*,* $\boldsymbol{d}^* = \frac{1}{2\rho^2}\boldsymbol{B}'\boldsymbol{T}_0\tilde{\boldsymbol{x}}$*, and the symmetric and positive definite matrix* $\boldsymbol{K}_\theta \in \mathbb{R}^{p\times p}$*, is a solution to the nonlinear* $\mathcal{H}_\infty$ *optimal control problem*

$$\mathcal{J}^* = \min_{\boldsymbol{u}\in\mathcal{L}_2}\max_{\boldsymbol{d}\in\mathcal{L}_2}\int_{t_0}^{t}\left(||\tilde{\boldsymbol{x}}||_{\boldsymbol{Q}}^2 + ||\boldsymbol{u}||_{\boldsymbol{R}}^2 - \rho^2||\boldsymbol{d}||^2\right)d\tau, \tag{3.53}$$

in which $\rho \in \mathbb{R}$ *is the a priori provided* $\mathcal{H}_\infty$ *attenuation level and, therefore, ensures*

(i) $\dot{\tilde{\boldsymbol{q}}}(t)$, $\tilde{\boldsymbol{q}}(t)$ *remain bounded for* $t \geq t_0$.

(ii) $\dot{\tilde{\boldsymbol{q}}}(t) \to 0$*, and* $\tilde{\boldsymbol{q}}(t) \to 0$ *as* $t \to \infty$.

Proof. See Appendix A.3. Q.E.D

3.4 Adaptive $\mathcal{H}_\infty$ Control via DREM/MREM

Now consider the following modification to the adaptive law (3.50):

$$\dot{\hat{\boldsymbol{\theta}}} = -\boldsymbol{K}_\theta^{-1}\left(\boldsymbol{Y}'\boldsymbol{T}_{11}\boldsymbol{B}'\boldsymbol{T}_0\tilde{\boldsymbol{x}} + \boldsymbol{f}_\theta\right). \tag{3.54}$$

Note that (3.54) is a composite estimation law that depends on both the system state, $\tilde{\boldsymbol{x}}$, and the DREM component vector, $\boldsymbol{f}_\theta$, whose elements are given by

$$f_{\theta_i} = \gamma_i\phi\left(\phi\hat{\theta}_i - \tau_{e_i}\right), \tag{3.55}$$

where $\gamma_i > 0$ is the i-th component of the positive definite diagonal matrix $\boldsymbol{\Gamma} \in \mathbb{R}^{p\times p}$, with $\boldsymbol{\Gamma} \triangleq \mathrm{diag}(\gamma_1, \gamma_2, \cdots, \gamma_p)$. Given that the unknown parameters are constant, the closed-loop dynamics of the parameter error can be described by

$$\dot{\tilde{\boldsymbol{\theta}}} = -\boldsymbol{K}_\theta^{-1}\left(\boldsymbol{Y}'\boldsymbol{T}_{11}\boldsymbol{B}'\boldsymbol{T}_0\tilde{\boldsymbol{x}} + \bar{\boldsymbol{f}}_\theta\right), \tag{3.56}$$

with

$$\bar{\boldsymbol{f}}_\theta = \boldsymbol{\Gamma}\phi^2\tilde{\boldsymbol{\theta}}. \tag{3.57}$$

To derive (3.57), we have substituted (3.13) into (3.55). It is noteworthy that $\boldsymbol{f}_\theta = \bar{\boldsymbol{f}}_\theta$; however, $\boldsymbol{f}_\theta$ is implementable, whereas $\bar{\boldsymbol{f}}_\theta$ is not. The latter is used only for stability analysis purposes.

The main contribution of this section is summarized in the subsequently presented Theorem 3.5. To facilitate the proof of this theorem, the following factorizations are considered:

$$\boldsymbol{Q} = \begin{bmatrix} \boldsymbol{Q}_{11} & \boldsymbol{Q}_{12} \\ * & \boldsymbol{Q}_{22} \end{bmatrix} = \begin{bmatrix} \boldsymbol{Q}_1'\boldsymbol{Q}_1 & \boldsymbol{Q}_{12} \\ * & \boldsymbol{Q}_2'\boldsymbol{Q}_2 \end{bmatrix}, \tag{3.58}$$

and

$$\boldsymbol{R}_1'\boldsymbol{R}_1 = \left(\boldsymbol{R}^{-1} - \frac{1}{\rho^2}\boldsymbol{I}\right)^{-1}. \tag{3.59}$$

Then, taking into account (3.58) and (3.59), we compute

$$\boldsymbol{T}_{11} = \boldsymbol{R}_1'\boldsymbol{Q}_1, \qquad \boldsymbol{T}_{12} = \boldsymbol{R}_1'\boldsymbol{Q}_2, \tag{3.60}$$

to tune the nonlinear $\mathcal{H}_\infty$, yielding

$$\boldsymbol{K} = \frac{1}{2}\left(\boldsymbol{Q}_1'\boldsymbol{Q}_2 + \boldsymbol{Q}_2'\boldsymbol{Q}_1\right) - \frac{1}{2}\left(\boldsymbol{Q}_{12}' + \boldsymbol{Q}_{12}\right) > 0. \tag{3.61}$$

Considering the factorizations (3.58) and (3.59), one can show via direct calculation that (3.60) and (3.61) compose a solution of the Riccati equation (3.49).

Theorem 3.5 (DREM/MREM Nonlinear Adaptive $\mathcal{H}_\infty$ Control)**.** *Let $\boldsymbol{R} = r^2\boldsymbol{I} > 0$ and*

$$\boldsymbol{Q} = \begin{bmatrix} a_1^2\boldsymbol{I}_{n\times n} & \boldsymbol{0} \\ * & a_2^2\boldsymbol{I}_{n\times n} \end{bmatrix} > 0, \tag{3.62}$$

with given parameters $r, a \in \mathbb{R}_+$. Consider a desired disturbance attenuation level, ρ, such that $\rho^2\boldsymbol{I} > \boldsymbol{R}$. and both $\boldsymbol{T}_0$ and $\boldsymbol{K}$, with $\boldsymbol{K} = \boldsymbol{K}' > 0$ and $\boldsymbol{K} \in \mathbb{R}^{n\times n}$, satisfy the algebraic Riccati equation (3.49). Then, the adaptive robust nonlinear $\mathcal{H}_\infty$ optimal control law and *worst case disturbance*

$$\dot{\hat{\boldsymbol{\theta}}}(t) = -\frac{1}{a_1}\boldsymbol{Y}'\begin{bmatrix} a_1\boldsymbol{I} & a_2\boldsymbol{I}\end{bmatrix}\tilde{\boldsymbol{x}} - \frac{1}{t_{11}^2}\boldsymbol{f}_\theta, \tag{3.63}$$

$$\boldsymbol{\tau}(t) = -\frac{1}{a_1 r^2}\begin{bmatrix} a_1\boldsymbol{I} & a_2\boldsymbol{I}\end{bmatrix}\tilde{\boldsymbol{x}} + \boldsymbol{Y}\hat{\boldsymbol{\theta}}, \tag{3.64}$$

$$\boldsymbol{\tau}_l^*(t) = \frac{1}{a_1\rho^2}\begin{bmatrix} a_1\boldsymbol{I} & a_2\boldsymbol{I}\end{bmatrix}\tilde{\boldsymbol{x}}, \tag{3.65}$$

with $t_{11} = \frac{r\rho a_1}{\sqrt{\rho^2 - r^2}}$ *and* $\boldsymbol{f}_\theta = \boldsymbol{\Gamma}\phi\left(\phi\hat{\boldsymbol{\theta}} - \boldsymbol{\tau}_e\right)$*, is a solution to the nonlinear* $\mathcal{H}_\infty$ *optimal control problem*

$$\mathcal{J}^* = \min_{\boldsymbol{u}\in\mathcal{L}_2}\max_{\boldsymbol{d}\in\mathcal{L}_2}\int_{t_0}^{\infty}\left(||\tilde{\boldsymbol{x}}||_{\boldsymbol{Q}}^2 + ||\boldsymbol{u}||_{\boldsymbol{R}}^2 - \rho^2||\boldsymbol{d}||^2\right)d\tau. \tag{3.66}$$

in which $\rho \in \mathbb{R}$ *is the a priori provided* $\mathcal{H}_\infty$ *attenuation level and, therefore, ensures*

(i) $\dot{\tilde{\boldsymbol{q}}}(t)$*,* $\tilde{\boldsymbol{q}}(t)$*, and* $\tilde{\boldsymbol{\theta}}(t)$ *remain bounded for* $t \geq t_0$*.*

(ii) $\dot{\tilde{\boldsymbol{q}}}(t) \to 0$*, and* $\tilde{\boldsymbol{q}}(t) \to 0$ *as* $t \to \infty$*.*

(iii) Moreover, since

$$\boldsymbol{\Theta} \triangleq \boldsymbol{Q} + \begin{bmatrix} a_1^2\boldsymbol{I} & a_1a_2\boldsymbol{I} \\ * & a_2^2\boldsymbol{I}\end{bmatrix} > 0, \tag{3.67}$$

it holds that

$$\phi^2 \geq \frac{1}{2}\left(\frac{\lambda_{min}(\boldsymbol{\Theta})}{\lambda_{min}(\boldsymbol{\Gamma})}\right), \quad \forall t \in [t_1, t_2], \tag{3.68}$$

with $t_1 \geq t_0$*,* $t_2 = t_1 + \Delta T$[3]*,* $\phi = det(\boldsymbol{Y}_f)$*, and*

$$\Delta T = -\frac{1}{\kappa}\ln\left(\frac{1}{N}\right) \geq 0, \quad \kappa = \left(\frac{\lambda_{min}(\boldsymbol{\Theta})}{2\lambda_2}\right), \quad \forall N \geq 1, \tag{3.69}$$

in which N *measures how much the Lyapunov function has decayed , that is* $V(\boldsymbol{\mathcal{X}}, t_2) = \frac{1}{N}V(\boldsymbol{\mathcal{X}}(t_1), t_1)$*. Then, exponential stability is guaranteed for the closed-loop system (3.24) with the control law (3.63)-(3.64), ensuring that both* $\tilde{\boldsymbol{x}}$ *and* $\tilde{\boldsymbol{\theta}}$ *converges with decay rate* κ*.*

Proof. From $\boldsymbol{R} = r^2\boldsymbol{I}$, we have that (3.59) becomes

$$\boldsymbol{R}_1'\boldsymbol{R}_1 = \frac{r^2\rho^2}{\rho^2 - r^2}\boldsymbol{I} \implies \boldsymbol{R}_1 = \frac{r\rho}{\sqrt{\rho^2 - r^2}}\boldsymbol{I}. \tag{3.70}$$

[3]The reader may appreciate the fact that $ln(x) \leq 0,\ \forall\, x \in [0, 1]$, which ensures $\Delta T \geq 0,\ \forall\, N \geq 1$.

From (3.60), (3.62) and (3.70), we have that

$$\boldsymbol{T}_{11} = t_{11}\boldsymbol{I} = \left(\frac{r\rho a_1}{\sqrt{\rho^2 - r^2}}\right)\boldsymbol{I}, \quad \boldsymbol{T}_{12} = \left(\frac{r\rho a_2}{\sqrt{\rho^2 - r^2}}\right)\boldsymbol{I}. \tag{3.71}$$

Also, from the definitions of $\boldsymbol{B}$ and $\boldsymbol{T}_0$, we obtain

$$\boldsymbol{B}'\boldsymbol{T}_0 = \frac{\rho r}{\sqrt{\rho^2 - r^2}}\begin{bmatrix} a_1\boldsymbol{I} & a_2\boldsymbol{I} \end{bmatrix}. \tag{3.72}$$

Replacing (3.71) and (3.72) into (3.51), (3.52) and (3.54), and choosing $\boldsymbol{K}_\theta = t_{11}^2\boldsymbol{I}$, render the adaptive robust nonlinear $\mathcal{H}_\infty$ control law (3.63)-(3.65). Next, for the sake of convenience, let us rewrite (3.28) in terms of $\boldsymbol{\tau}$ and $\boldsymbol{\tau}_l$ as follows

$$\dot{\tilde{\boldsymbol{x}}} = \boldsymbol{T}_0^{-1}\begin{bmatrix} -\boldsymbol{M}^{-1}\boldsymbol{C} & \boldsymbol{0} \\ \boldsymbol{T}_{11}^{-1} & -\boldsymbol{T}_{11}^{-1}\boldsymbol{T}_{12} \end{bmatrix}\boldsymbol{T}_0\tilde{\boldsymbol{x}} + \boldsymbol{T}_0^{-1}\boldsymbol{B}\boldsymbol{M}^{-1}\boldsymbol{T}_{11}\left(-\boldsymbol{Y}\boldsymbol{\theta} + \boldsymbol{\tau} + \boldsymbol{\tau}_l\right), \tag{3.73}$$

and consider the candidate Lyapunov function

$$V(\mathcal{X}, t) = V_{\tilde{\boldsymbol{x}}}(\tilde{\boldsymbol{x}}, t) + V_{\tilde{\boldsymbol{\theta}}}(\tilde{\boldsymbol{\theta}}), \tag{3.74}$$

with the augmented state vector $\boldsymbol{\mathcal{X}} = [\tilde{\boldsymbol{x}}' \; \tilde{\boldsymbol{\theta}}']'$, such that

$$V_{\tilde{\boldsymbol{x}}}(\tilde{\boldsymbol{x}}, t) \triangleq \frac{1}{2}\tilde{\boldsymbol{x}}'\boldsymbol{T}_0'\begin{bmatrix} \boldsymbol{M}(\boldsymbol{q}) & \boldsymbol{0} \\ * & \boldsymbol{K} \end{bmatrix}\boldsymbol{T}_0\tilde{\boldsymbol{x}}, \tag{3.75}$$

$$V_{\tilde{\boldsymbol{\theta}}}(\tilde{\boldsymbol{\theta}}) \triangleq \frac{1}{2}\tilde{\boldsymbol{\theta}}'\boldsymbol{K}_\theta\tilde{\boldsymbol{\theta}}, \tag{3.76}$$

which satisfies

$$\lambda_1||\boldsymbol{\mathcal{X}}||^2 \leq V(\boldsymbol{\mathcal{X}}, t) \leq \lambda_2||\boldsymbol{\mathcal{X}}||^2, \tag{3.77}$$

where $\lambda_1 = \frac{1}{2}\min\{\lambda_h, \lambda_{min}(\boldsymbol{K}_\theta)\}$, with $\lambda_h \triangleq \lambda_{min}(\boldsymbol{H})$ in which $\boldsymbol{H} \triangleq \boldsymbol{T}_0'\text{blkdiag}(\boldsymbol{M}, \boldsymbol{K})\boldsymbol{T}_0$. Also, $\lambda_2 = \frac{1}{2}\max\{\lambda_H, \lambda_{max}(\boldsymbol{K}_\theta)\}$, $\lambda_H = \lambda_{max}(\boldsymbol{H})$, where $\lambda_{min}(\cdot)$ and $\lambda_{max}(\cdot)$ stand for the smallest and highest eigenvalue of $(\cdot)$, respectively. Then, the time derivative of (3.74) is

$$\dot{V}(\mathcal{X}, t) = \frac{\partial V_{\tilde{\boldsymbol{x}}}(\tilde{\boldsymbol{x}}, t)}{\partial t} + \left(\frac{\partial V_{\tilde{\boldsymbol{x}}}(\tilde{\boldsymbol{x}}, t)}{\partial \tilde{\boldsymbol{x}}}\right)'\dot{\tilde{\boldsymbol{x}}} + \tilde{\boldsymbol{\theta}}'\boldsymbol{K}_\theta\dot{\tilde{\boldsymbol{\theta}}}. \tag{3.78}$$

Taking the partial derivative of (3.75) with respect to $\tilde{\boldsymbol{x}}$ and multiplying it by (3.73) yields

$$\frac{\partial V_{\tilde{x}}(\tilde{\boldsymbol{x}},t)'}{\partial \tilde{\boldsymbol{x}}}\dot{\tilde{\boldsymbol{x}}}=\tilde{\boldsymbol{x}}\boldsymbol{T}_0'\begin{bmatrix}\boldsymbol{M} & \boldsymbol{0}\\ \boldsymbol{0} & \boldsymbol{K}\end{bmatrix}\boldsymbol{T}_0\dot{\tilde{\boldsymbol{x}}}+\frac{1}{2}\sum_{i=1}^{2n}\tilde{\boldsymbol{x}}'\boldsymbol{T}_0'\begin{bmatrix}\frac{\partial \boldsymbol{M}}{\partial \tilde{x}_i}\dot{\tilde{\boldsymbol{x}}}_i & \boldsymbol{0}\\ \boldsymbol{0} & \boldsymbol{0}\end{bmatrix}\boldsymbol{T}_0\tilde{\boldsymbol{x}}$$

$$=\tilde{\boldsymbol{x}}'\boldsymbol{T}_0'\begin{bmatrix}-\boldsymbol{C} & \boldsymbol{0}\\ \boldsymbol{K}\boldsymbol{T}_{11}^{-1} & -\boldsymbol{K}\boldsymbol{T}_{11}^{-1}\boldsymbol{T}_{12}\end{bmatrix}\boldsymbol{T}_0\tilde{\boldsymbol{x}}+\frac{1}{2}\sum_{i=1}^{2n}\tilde{\boldsymbol{x}}'\boldsymbol{T}_0'\begin{bmatrix}\frac{\partial \boldsymbol{M}}{\partial \tilde{x}_i}\dot{\tilde{\boldsymbol{x}}}_i & \boldsymbol{0}\\ \boldsymbol{0} & \boldsymbol{0}\end{bmatrix}\boldsymbol{T}_0\tilde{\boldsymbol{x}}+\tilde{\boldsymbol{x}}'\boldsymbol{T}_0'\boldsymbol{B}\boldsymbol{T}_{11}\left(-\boldsymbol{Y}\boldsymbol{\theta}+\boldsymbol{\tau}+$$

Using *Property 4* (see Chapter 2) renders

$$\frac{\partial V_{\tilde{x}}(\tilde{\boldsymbol{x}},t)'}{\partial \tilde{\boldsymbol{x}}}\dot{\tilde{\boldsymbol{x}}}=\tilde{\boldsymbol{x}}'\begin{bmatrix}\boldsymbol{0} \boldsymbol{0}\\ \boldsymbol{K} \boldsymbol{0}\end{bmatrix}\tilde{\boldsymbol{x}}+\frac{1}{2}\tilde{\boldsymbol{x}}'\boldsymbol{T}_0'\begin{bmatrix}\sum_{i=1}^{2n}\frac{\partial \boldsymbol{M}}{\partial \tilde{x}_i}\dot{\tilde{\boldsymbol{x}}}_i-\dot{\boldsymbol{M}} \boldsymbol{0}\\ \boldsymbol{0} & \boldsymbol{0}\end{bmatrix}\boldsymbol{T}_0\tilde{\boldsymbol{x}}+\tilde{\boldsymbol{x}}'\boldsymbol{T}_0'\boldsymbol{B}\boldsymbol{T}_{11}\left(-\boldsymbol{Y}\boldsymbol{\theta}+\boldsymbol{\tau}+\boldsymbol{\tau}_l\right). \tag{3.79}$$

In the following, the partial derivative of (3.75) with respect to time is computed as

$$\frac{\partial V_{\tilde{x}}(\tilde{\boldsymbol{x}},t)}{\partial t}=\frac{1}{2}\tilde{\boldsymbol{x}}'\boldsymbol{T}_0'\begin{bmatrix}\frac{\partial \boldsymbol{M}}{\partial t} & \boldsymbol{0}\\ \boldsymbol{0} & \boldsymbol{0}\end{bmatrix}\boldsymbol{T}_0\tilde{\boldsymbol{x}}. \tag{3.80}$$

Since $\boldsymbol{M}(\boldsymbol{q})=\boldsymbol{M}(\tilde{\boldsymbol{q}}+\boldsymbol{q}_r(t))=\boldsymbol{M}(\tilde{\boldsymbol{x}},t)$ then $\dot{\boldsymbol{M}}(\tilde{\boldsymbol{x}},t)=\frac{\partial \boldsymbol{M}}{\partial t}+\frac{\partial \boldsymbol{M}}{\partial \tilde{\boldsymbol{x}}}\dot{\tilde{\boldsymbol{x}}}$. Considering this and replacing (3.56) and (3.79)-(3.80) into (3.78) yields

$$\dot{V}(\mathcal{X},t)=\tilde{\boldsymbol{x}}'\begin{bmatrix}\boldsymbol{0} & \boldsymbol{0}\\ \boldsymbol{K} & \boldsymbol{0}\end{bmatrix}\tilde{\boldsymbol{x}}+\tilde{\boldsymbol{x}}'\boldsymbol{T}_0'\boldsymbol{B}\boldsymbol{T}_{11}\left(-\boldsymbol{Y}\boldsymbol{\theta}+\boldsymbol{\tau}+\boldsymbol{\tau}_l\right)-\tilde{\boldsymbol{\theta}}'\boldsymbol{Y}'\boldsymbol{T}_{11}\boldsymbol{B}'\boldsymbol{T}_0\tilde{\boldsymbol{x}}-\tilde{\boldsymbol{\theta}}'\bar{\boldsymbol{f}}_\theta. \tag{3.81}$$

Note that we can write (3.81) as

$$\dot{V}(\mathcal{X},t)=\frac{1}{2}\tilde{\boldsymbol{x}}'\begin{bmatrix}\boldsymbol{0} & \boldsymbol{K}\\ \boldsymbol{K} & \boldsymbol{0}\end{bmatrix}\tilde{\boldsymbol{x}}+\tilde{\boldsymbol{x}}'\boldsymbol{T}_0'\boldsymbol{B}\boldsymbol{T}_{11}\left(-\boldsymbol{Y}\boldsymbol{\theta}+\boldsymbol{\tau}+\boldsymbol{\tau}_l\right)-\tilde{\boldsymbol{\theta}}'\boldsymbol{Y}'\boldsymbol{T}_{11}\boldsymbol{B}'\boldsymbol{T}_0\tilde{\boldsymbol{x}}-\tilde{\boldsymbol{\theta}}'\bar{\boldsymbol{f}}_\theta. \tag{3.82}$$

Using (3.49) and (3.59), yields

$$\begin{aligned}\dot{V}(\mathcal{X},t)=&\frac{1}{2}\tilde{\boldsymbol{x}}'\left(-\boldsymbol{Q}+\boldsymbol{T}_0'\boldsymbol{B}\left(\boldsymbol{R}_1'\boldsymbol{R}_1\right)^{-1}\boldsymbol{B}'\boldsymbol{T}_0\right)\tilde{\boldsymbol{x}}-\tilde{\boldsymbol{\theta}}'\bar{\boldsymbol{f}}_\theta\\&+\tilde{\boldsymbol{x}}'\boldsymbol{T}_0'\boldsymbol{B}\boldsymbol{T}_{11}\left(-\boldsymbol{Y}\boldsymbol{\theta}+\boldsymbol{\tau}+\boldsymbol{\tau}_l\right)-\tilde{\boldsymbol{\theta}}'\boldsymbol{Y}'\boldsymbol{T}_{11}\boldsymbol{B}'\boldsymbol{T}_0\tilde{\boldsymbol{x}}.\end{aligned} \tag{3.83}$$

Substituting (3.63)-(3.65), (3.71), and (3.72) into (3.83), and recalling $\phi(t)=det(\boldsymbol{Y}_f)$, one can achieve

$$\dot{V}(\mathcal{X},t)=-\frac{1}{2}\tilde{\boldsymbol{x}}'\left(\boldsymbol{Q}+\begin{bmatrix}a_1^2\boldsymbol{I} & a_1a_2\boldsymbol{I}\\ * & a_1^2\boldsymbol{I}\end{bmatrix}\right)\tilde{\boldsymbol{x}}-\tilde{\boldsymbol{\theta}}'\bar{\boldsymbol{f}}_\theta=-\frac{1}{2}\tilde{\boldsymbol{x}}'\boldsymbol{\Theta}\tilde{\boldsymbol{x}}-\phi^2\tilde{\boldsymbol{\theta}}'\boldsymbol{\Gamma}\tilde{\boldsymbol{\theta}}. \tag{3.84}$$

Then, we can conclude (i), (ii) and (iii) as follows:

(i) From (3.75) we conclude that $V(\mathcal{X},t)$ is positive definite, and from (3.84), that

$\dot{V}(\mathcal{X},t) \leq 0$ for all $t \geq t_0$, which in turn implies that $\tilde{\boldsymbol{x}}(t) \in \mathcal{L}_\infty$ and $\tilde{\boldsymbol{\theta}}(t) \in \mathcal{L}_\infty$;

(ii) Accordingly to Barbalat's Lemma, since $V(\boldsymbol{\mathcal{X}},t)$ is bounded as seen in (3.77), $\dot{V}(\mathcal{X},t) \to 0$, if it is uniformly continuous (Slotine et al., 1991). Proving uniform continuity of $\dot{V}(\mathcal{X},t)$ can be achieved by showing that $\ddot{V}(\mathcal{X},t)$ is bounded. In view of (3.84), by demonstrating that $\dot{V}(\mathcal{X},t) \to 0$ as $t \to \infty$ is sufficient to infer that $\dot{\tilde{\boldsymbol{q}}} \to 0$ and $\tilde{\boldsymbol{q}} \to 0$ as $t \to \infty$. Since (3.84) has only two terms, in the following we show that $\ddot{V}(\mathcal{X},t)$ is bounded by taking the time derivative of these terms. First, consider,

$$\frac{d}{dt}\left(-\frac{1}{2}\tilde{\boldsymbol{x}}'\boldsymbol{\Theta}\tilde{\boldsymbol{x}}\right) = -\tilde{\boldsymbol{x}}'\boldsymbol{\Theta}\dot{\tilde{\boldsymbol{x}}}. \tag{3.85}$$

The first term in (3.84) will be bounded if $\dot{\tilde{\boldsymbol{x}}}(t)$ is bounded, which is defined as

$$\begin{aligned}\dot{\tilde{\boldsymbol{x}}} = \boldsymbol{T}_0^{-1}&\begin{bmatrix}-\boldsymbol{M}^{-1}(\boldsymbol{q})\boldsymbol{C}(\boldsymbol{q},\dot{\boldsymbol{q}}) & \boldsymbol{0}\\ \boldsymbol{T}_{11}^{-1} & -\boldsymbol{T}_{11}^{-1}\boldsymbol{T}_{12}\end{bmatrix}\boldsymbol{T}_0\tilde{\boldsymbol{x}}\\ &- \boldsymbol{T}_0^{-1}\boldsymbol{B}\boldsymbol{M}^{-1}(\boldsymbol{q})\left(\boldsymbol{R}^{-1} - \frac{1}{\rho^2}\boldsymbol{I}\right)\boldsymbol{B}'\boldsymbol{T}_0\tilde{\boldsymbol{x}} + \boldsymbol{T}_0^{-1}\boldsymbol{B}\boldsymbol{M}^{-1}(\boldsymbol{q})\boldsymbol{Y}(\boldsymbol{q},\dot{\boldsymbol{q}},\boldsymbol{q}_r,\dot{\boldsymbol{q}}_r,\ddot{\boldsymbol{q}}_r)\tilde{\boldsymbol{\theta}}.\end{aligned} \tag{3.86}$$

Therefore, since we have shown in (i) that $\tilde{\boldsymbol{\theta}}(t) \in \mathcal{L}_\infty$, $\tilde{\boldsymbol{x}}(t) \in \mathcal{L}_\infty$, and the desired configuration values $\ddot{\boldsymbol{q}}_r(t), \dot{\boldsymbol{q}}_r(t), \boldsymbol{q}_r(t)$ are bounded by assumption, it is sufficient to conclude that $\dot{\tilde{\boldsymbol{x}}}$ is bounded as well, which concludes the proof.

The derivative of the second term in (3.84) is computed as follows

$$\frac{d}{dt}\left(-\phi^2\tilde{\boldsymbol{\theta}}'\boldsymbol{\Gamma}\tilde{\boldsymbol{\theta}}\right) = -2\phi\dot{\phi}\tilde{\boldsymbol{\theta}}'\boldsymbol{\Gamma}\tilde{\boldsymbol{\theta}} + 2\phi^2\tilde{\boldsymbol{\theta}}'\boldsymbol{\Gamma}\boldsymbol{K}_\theta^{-1}\boldsymbol{Y}'(\boldsymbol{q},\dot{\boldsymbol{q}},\boldsymbol{q}_r,\dot{\boldsymbol{q}}_r,\ddot{\boldsymbol{q}}_r)\boldsymbol{T}_{11}\boldsymbol{B}'\boldsymbol{T}_0\tilde{\boldsymbol{x}} + 2\phi^2\tilde{\boldsymbol{\theta}}'\boldsymbol{\Gamma}\boldsymbol{K}_\theta^{-1}\boldsymbol{\Gamma}\tilde{\boldsymbol{\theta}} \tag{3.87}$$

where (3.56) has been used. As it has already been shown that $\tilde{\boldsymbol{\theta}}(t) \in \mathcal{L}_\infty$ and $\tilde{\boldsymbol{x}}(t) \in \mathcal{L}_\infty$, to prove that the derivative of the second term is bounded, it remains to show that $\dot{\phi}$ and ϕ are also bounded. Recall that the determinant of any matrix can be obtained by means of the Laplace expansion (Horn and Johnson, 2012). Through the Laplace expansion it can be verified that ϕ is a sum of products of the elements of $\boldsymbol{Y}_f$. Thus, ϕ will be bounded if the elements in $\boldsymbol{Y}_f$ are bounded. Considering that $\dot{\boldsymbol{Y}}_f$ is obtained through the Kresselmeier's Regressor Extension using a stable linear filter with input being $\boldsymbol{Y}_\mathcal{I}\boldsymbol{Y}_\mathcal{I}'$, and that the Euler-Lagrange First Integral regressor depends only on $\dot{\boldsymbol{q}}$ and $\boldsymbol{q}$, i.e $\boldsymbol{Y}_\mathcal{I}(\dot{\boldsymbol{q}},\boldsymbol{q})$, which have already been shown to be bounded, then one can infer that $\dot{\boldsymbol{Y}}_f$ and $\boldsymbol{Y}_f$ are also bounded and therefore so is ϕ. The boundedness of $\dot{\phi}$ can be proved in a straightforward manner by employing Jacobi's formula (Magnus and Neudecker, 2019). Hence, the boundedness of $\dot{\boldsymbol{Y}}_f$ and $\boldsymbol{Y}_f$

implies the boundedness of $\dot{\phi}$, as it can be computed using $\dot{\phi} = Trace\left(adj\left(\mathbf{Y}_f\right)\dot{\mathbf{Y}}_f\right)$. In conclusion, since $\ddot{V}(\boldsymbol{\mathcal{X}},t)$ has been shown to be bounded, then, according to Barbalat's Lemma, $\dot{V}(\boldsymbol{\mathcal{X}},t) \to 0$ as $t \to \infty$. Consequently, from (3.84), this ensures that $\tilde{\boldsymbol{x}}(t) \to 0$ as $t \to \infty$.

Remark 3.6. Regardless of (3.84) containing elements of $\tilde{\boldsymbol{\theta}}$, this does not imply that $\tilde{\boldsymbol{\theta}} \to 0$ since it is not possible to always guarantee that $\phi \neq 0$, $\forall t \geq t_0$. Nevertheless, (ii) has demonstrated that it is possible to ensure trajectory tracking even in cases where parameter estimation is not occurring. Q.E.D

(iii) Replacing (3.57) into (3.84) and given inequalities (3.67)-(3.68), yields

$$\begin{aligned}\dot{V}(\mathcal{X},t) &\leq -\frac{1}{2}\sum_{i=1}^{2n}\lambda_{min}\left(\mathbf{\Theta}\right)(\tilde{x}_i)^2 - \sum_{j=1}^{p}\lambda_{min}\left(\mathbf{\Gamma}\right)\phi^2(\tilde{\theta}_j)^2,\\ &\leq -\sum_{i=1}^{2n}\left(\frac{\lambda_{min}\left(\mathbf{\Theta}\right)}{2}\right)(\tilde{x}_i)^2 - \sum_{j=1}^{p}\left(\frac{\lambda_{min}\left(\mathbf{\Theta}\right)}{2}\right)(\tilde{\theta}_j)^2, \quad \forall\, t \in [t_1, t_2],\end{aligned}$$

which implies $\dot{V}(\mathcal{X},t) \leq -\sum_{k=1}^{2n+p}\left(\frac{\lambda_{min}(\mathbf{\Theta})}{2}\right)(\mathcal{X}_k)^2 = -\left(\frac{\lambda_{min}(\mathbf{\Theta})}{2}\right)||\boldsymbol{\mathcal{X}}||_2^2$, where $\mathcal{X}_k$ is the k-th element of the augmented state vector $\boldsymbol{\mathcal{X}} \in \mathbb{R}^{2n+p}$. Using (3.77), we obtain

$$\begin{aligned}\dot{V}(\mathcal{X},t) &\leq -\left(\frac{\lambda_{min}\left(\mathbf{\Theta}\right)}{2}\right)\frac{1}{\lambda_2}\left(\lambda_2||\boldsymbol{\mathcal{X}}||^2\right), \\ &= -\left(\frac{\lambda_{min}\left(\mathbf{\Theta}\right)}{2\lambda_2}\right)V(\boldsymbol{\mathcal{X}},t) \leq -\kappa V(\boldsymbol{\mathcal{X}},t), \quad \forall\, t \in [t_1, t_2],\end{aligned} \tag{3.88}$$

with κ given in (3.69). According to the Comparison Lemma (Khalil, 1996), the solution of (3.88) is given by

$$V(\boldsymbol{\mathcal{X}},t) \leq e^{-\kappa(t-t_1)}V(\boldsymbol{\mathcal{X}}(t_1),t_1), \quad \forall\, t \in [t_1, t_2], \tag{3.89}$$

which completes the proof of exponential convergence of the system (3.28) in closed-loop with the control law (3.63)-(3.65) and, consequently, for the system (3.24).

Remark 3.7. In view of the discussion presented in Section 2.2, it is possible to ensure globally uniform exponential stability only if there are no singularities in the inertia matrix. Q.E.D

It is straightforward to note that at $t_2 = t_1 + \Delta T$, by substituting (3.69) into (3.89), results in

$$V(\boldsymbol{\mathcal{X}},t_2) \leq \frac{1}{N}V(\boldsymbol{\mathcal{X}}(t_1),t_1), \tag{3.90}$$

which indicates how much the Lyapunov function has decayed.

In addition, it is noteworthy that [4]

$$\dot{V}(\boldsymbol{\mathcal{X}},t) = \dot{V}(\tilde{\boldsymbol{x}},t)\Big|_{\tau} + \tilde{\boldsymbol{\theta}}'\boldsymbol{K}_{\tilde{\theta}}\dot{\tilde{\boldsymbol{\theta}}}. \tag{3.91}$$

Furthermore, it can be verified that

$$\dot{V}(\tilde{\boldsymbol{x}},t)\Big|_{\tau} = \dot{V}(\tilde{\boldsymbol{x}},t)\Big|_{\tau^*} + \tilde{\boldsymbol{x}}'\boldsymbol{T}_0\boldsymbol{B}'\boldsymbol{Y}\tilde{\boldsymbol{\theta}}. \tag{3.92}$$

By direct substitution of (3.50) and (3.92) in (3.91), produces

$$\dot{V}(\boldsymbol{\mathcal{X}},t) = \dot{V}(\tilde{\boldsymbol{x}},t)\Big|_{\tau^*} - \phi^2\tilde{\boldsymbol{\theta}}\boldsymbol{\Gamma}\tilde{\boldsymbol{\theta}} = -\mathcal{L}\Big|_{\tau^*} - \phi^2\tilde{\boldsymbol{\theta}}\boldsymbol{\Gamma}\tilde{\boldsymbol{\theta}} \leq 0. \tag{3.93}$$

where (A.49) has been used. By integrating both sides, renders,

$$V(\boldsymbol{\mathcal{X}},\infty) - V(\boldsymbol{\mathcal{X}},t_0) = -\int_{t_0}^{\infty}\left(\phi^2\tilde{\boldsymbol{\theta}}\boldsymbol{\Gamma}\tilde{\boldsymbol{\theta}}\right)ds - \int_{t_0}^{\infty}\left(\frac{1}{2}\tilde{\boldsymbol{x}}'\boldsymbol{Q}\tilde{\boldsymbol{x}} + \frac{1}{2}\boldsymbol{u}'\boldsymbol{R}\boldsymbol{u}\right)ds + \int_{t_0}^{\infty}\rho^2\boldsymbol{d}'\boldsymbol{d}ds$$

Remark 3.8. Indeed notice that $h(\tilde{\boldsymbol{\theta}}) \triangleq \left(\phi^2\tilde{\boldsymbol{\theta}}\boldsymbol{\Gamma}\tilde{\boldsymbol{\theta}}\right) \in \mathcal{L}_2[t_0,\infty]$ since if the DREM conditions hold, i.e. $\phi \notin \mathcal{L}_2[t_0,\infty]$, then $\tilde{\boldsymbol{\theta}} \to 0$ as $t \to \infty$, which ensures that $h(\tilde{\boldsymbol{\theta}}) \in \mathcal{L}_2[t_0,\infty]$. Furthermore, if $\phi \in \mathcal{L}_2[t_0,\infty]$, then $\tilde{\boldsymbol{\theta}}\boldsymbol{\Gamma}\tilde{\boldsymbol{\theta}} > 0$, and still $h(\tilde{\boldsymbol{\theta}}) \in \mathcal{L}_2[t_0,\infty]$ since $\phi \to 0$ as $t \to \infty$. Q.E.D

Since $V(\boldsymbol{\mathcal{X}},\infty) \geq 0$, then

$$\int_{t_0}^{\infty}\left(\frac{1}{2}\tilde{\boldsymbol{x}}'\boldsymbol{Q}\tilde{\boldsymbol{x}} + \frac{1}{2}\boldsymbol{u}'\boldsymbol{R}\boldsymbol{u} + \phi^2\tilde{\boldsymbol{\theta}}\boldsymbol{\Gamma}\tilde{\boldsymbol{\theta}}\right)ds \leq V(\boldsymbol{\mathcal{X}},t_0) + \rho^2\int_{t_0}^{\infty}\boldsymbol{d}'\boldsymbol{d}ds,$$
$$||\boldsymbol{z}(t)||_{\mathcal{L}_2}^2 \leq V(\boldsymbol{\mathcal{X}},t_0) + \rho^2||\boldsymbol{d}(t)||_{\mathcal{L}_2}^2. \tag{3.94}$$

and therefore we guarantee the $\mathcal{H}_\infty$ criteria, completing the proof.

Q.E.D

3.5 Adaptive $\mathcal{H}_\infty$ Control via DREM/MREM in Finite-time

Now, based on Wang et al. (2019), consider the following modification to the adaptive law (3.50):

$$\dot{\hat{\boldsymbol{\theta}}} = -\boldsymbol{K}_\theta^{-1}\left(\boldsymbol{Y}'\boldsymbol{T}_{11}\boldsymbol{B}'\boldsymbol{T}_0\tilde{\boldsymbol{x}} + \boldsymbol{f}_\theta\right). \tag{3.95}$$

[4] $f(x)\Big|_x^*$ is the function $f(x)$ evaluated at x^*

Note that (3.95) is a composite estimation law that depends on both the system state, $\tilde{\boldsymbol{x}}$, and the vector, $\boldsymbol{f}_\theta$, whose elements are given by

$$f_{\theta_i} = \gamma_i \left\lfloor \phi \left(\phi \hat{\theta}_i - \tau_{e_i} \right) \right\rceil^{\alpha_i}, \tag{3.96}$$

where $\lfloor . \rceil^{\alpha_i} = |.|^{\alpha_i} sign(.)$, $\alpha_i \in (0.5, 1), \forall i \in [1, \cdots, p]$, and $\gamma_i > 0$ is the i-th component of the positive definite diagonal matrix $\boldsymbol{\Gamma} \in \mathbb{R}^{p \times p}$, with $\boldsymbol{\Gamma} \triangleq \text{diag}(\gamma_1, \gamma_2, \cdots, \gamma_p)$. Given that the unknown parameters are constant, the closed-loop dynamics of the parameter error can be described as

$$\dot{\tilde{\boldsymbol{\theta}}} = -\boldsymbol{K}_\theta^{-1} \left(\boldsymbol{Y}' \boldsymbol{T}_{11} \boldsymbol{B}' \boldsymbol{T}_0 \tilde{\boldsymbol{x}} + \bar{\boldsymbol{f}}_\theta \right), \tag{3.97}$$

with

$$\bar{f}_{\theta_i} = \gamma_i \phi^{2\alpha_i} |\tilde{\theta}_i|^{\alpha_i} sign(\tilde{\theta}_i). \tag{3.98}$$

To derive (3.98), we have substituted (3.13) into (3.96) and used the fact that $sign(\phi^2 \tilde{\theta}_i) = sign(\tilde{\theta}_i)$ for $\phi \neq 0$. Conversely, when $\phi = 0$, then $\bar{f}_{\theta_i} = 0$. As discussed in the previous section, $\boldsymbol{f}_\theta = \bar{\boldsymbol{f}}_\theta$; however, $\boldsymbol{f}_\theta$ is implementable, whereas $\bar{\boldsymbol{f}}_\theta$ is not. The latter is used only for stability analysis purposes.

The main contribution of this section is presented in Theorem 3.9. To facilitate the proof of this theorem, the same factorizations (3.58), (3.59), (3.60) and (3.61) have been considered.

Theorem 3.9 (Finite-Time DREM/MREM Nonlinear Adaptive $\mathcal{H}_\infty$ Control)**.** *Let* $\boldsymbol{R} = r^2 \boldsymbol{I} > 0$ *and*

$$\boldsymbol{Q} = \begin{bmatrix} a_1^2 \boldsymbol{I}_{n \times n} & \boldsymbol{0} \\ * & a_2^2 \boldsymbol{I}_{n \times n} \end{bmatrix} > 0, \tag{3.99}$$

with given parameters $r, a \in \mathbb{R}_+$*. Consider a desired disturbance attenuation level,* ρ*, such that* $\rho^2 \boldsymbol{I} > \boldsymbol{R}$*, and* $\boldsymbol{T}_0$ *satisfy the algebraic Riccati equation*

$$\boldsymbol{Q} - \boldsymbol{T}_0' \boldsymbol{B} \left(\boldsymbol{R}^{-1} - \frac{1}{\rho^2} \boldsymbol{I} \right) \boldsymbol{B}' \boldsymbol{T}_0 = 0. \tag{3.100}$$

The following robust nonlinear adaptive $\mathcal{H}_\infty$ *control law*

$$\dot{\hat{\boldsymbol{\theta}}}(t) = -\frac{1}{a_1} \boldsymbol{Y}' \boldsymbol{z} - \frac{1}{t_{11}^2} \boldsymbol{f}_\theta, \tag{3.101}$$

$$\boldsymbol{\tau}(t) = -\frac{1}{a_1 r^2} \boldsymbol{z} + \boldsymbol{Y} \hat{\boldsymbol{\theta}} - \boldsymbol{f}_z, \tag{3.102}$$

$$\boldsymbol{\tau}_l(t) = \frac{1}{a_1 \rho^2} \boldsymbol{z}, \tag{3.103}$$

with

$$\boldsymbol{z} = \begin{bmatrix} a_1\boldsymbol{I} & a_2\boldsymbol{I} \end{bmatrix} \tilde{\boldsymbol{x}}, \tag{3.104}$$

$$\boldsymbol{f_\theta} = \boldsymbol{\Gamma} \left\lfloor \phi \left(\phi\hat{\boldsymbol{\theta}} - \boldsymbol{\tau}_e \right) \right\rceil^{\boldsymbol{\alpha}}, \tag{3.105}$$

$$\boldsymbol{f_z} = \frac{1}{a_1 r^2} \lfloor \boldsymbol{z} \rceil^{\boldsymbol{\alpha_z}}, \tag{3.106}$$

and $t_{11} = \frac{r\rho a_1}{\sqrt{\rho^2 - r^2}}$, *is a solution to the nonlinear $\mathcal{H}_\infty$ optimal control problem*

$$\mathcal{J}^* = \min_{\boldsymbol{u}\in\mathcal{L}_2} \max_{\boldsymbol{d}\in\mathcal{L}_2} \int_{t_0}^{t} \left(||\tilde{\boldsymbol{x}}||^2_{\boldsymbol{Q}} + ||\boldsymbol{u}||^2_{\boldsymbol{R}} - \rho^2 ||\boldsymbol{d}||^2 \right) d\tau, \tag{3.107}$$

and the following holds

(i) $\boldsymbol{z}(t)$, $\dot{\tilde{\boldsymbol{q}}}(t)$, $\tilde{\boldsymbol{q}}(t)$, *and* $\tilde{\boldsymbol{\theta}}(t)$ *remain bounded for* $t \geq t_0$*;*

(ii) $\boldsymbol{z}(t) \to 0$, $\dot{\tilde{\boldsymbol{q}}}(t) \to 0$, *and* $\tilde{\boldsymbol{q}}(t) \to 0$ *as* $t \to \infty$*;*

(iii) If for some $t_1 \geq t_0$, *it holds that*

$$\phi^2 \geq \left(\frac{\rho^2}{(\rho^2 - r^2)\, \lambda_{min}(\boldsymbol{\Gamma})} \right)^{\frac{1}{\alpha}}, \forall t \in [t_1, t_2], \tag{3.108}$$

with $\lambda_{min}(\boldsymbol{\Gamma})$ *denoting the minimum eigenvalue of matrix* $\boldsymbol{\Gamma}$ *from* (3.96), $\phi = det(\boldsymbol{Y}_f)$, $\alpha_i = \alpha_{\tilde{\boldsymbol{x}}_j} = \alpha$, $\forall i \in [1, \cdots, p], j \in [1, \cdots, 2n]$ *with* $\alpha \in (0.5, 1)$, *and* $t_2 = t_1 + \Delta T$.

Then, the closed-loop system (3.28) *along with the control law* (3.101)-(3.103) *guarantees asymptotically tracking of the states and exact estimation of the unknown parameters in finite time, ensuring*

$$\tilde{\boldsymbol{\theta}} = \boldsymbol{0}, \quad \text{and} \quad \boldsymbol{z} = \boldsymbol{0}, \quad \forall t \geq t_1 + \Delta T, \tag{3.109}$$

with

$$\Delta T = \frac{2}{\eta(1-\alpha)} V^{\frac{1-\alpha}{2}}(t_1), \quad \eta = \frac{\rho^2}{(\rho^2 - r^2)\, \lambda_2^{\frac{2}{\alpha+1}}}. \tag{3.110}$$

Proof. From $\boldsymbol{R} = r^2\boldsymbol{I}$, we have that

$$\boldsymbol{R}_1'\boldsymbol{R}_1 = \frac{r^2\rho^2}{\rho^2 - r^2}\boldsymbol{I} \implies \boldsymbol{R}_1 = \frac{r\rho}{\sqrt{\rho^2 - r^2}}\boldsymbol{I}. \tag{3.111}$$

From (3.99) and (3.111), we have that

$$\boldsymbol{T}_{11} = t_{11}\boldsymbol{I} = \left(\frac{r\rho a_1}{\sqrt{\rho^2 - r^2}} \right) \boldsymbol{I}, \quad \boldsymbol{T}_{12} = \left(\frac{r\rho a_2}{\sqrt{\rho^2 - r^2}} \right) \boldsymbol{I} \tag{3.112}$$

Also, from the definitions of $\boldsymbol{B}$ and $\boldsymbol{T}_0$, in (3.27) and (3.26), respectively, we have that

$$\boldsymbol{B}'\boldsymbol{T}_0 = \frac{\rho r}{\sqrt{\rho^2 - r^2}} \begin{bmatrix} a_1\boldsymbol{I} & a_2\boldsymbol{I} \end{bmatrix}. \tag{3.113}$$

Replacing (3.112) and (3.113) into (3.51), (3.52) and (3.95), and choosing $\boldsymbol{K}_\theta = t_{11}^2\boldsymbol{I}$, render the robust nonlinear adaptive $\mathcal{H}_\infty$ control law (3.101)-(3.103). Next, for the sake of convenience, let us rewrite (3.28) in terms of $\boldsymbol{\tau}$ and $\boldsymbol{\tau}_l$ as

$$\dot{\tilde{\boldsymbol{x}}} = \boldsymbol{T}_0^{-1} \begin{bmatrix} -\boldsymbol{M}^{-1}\boldsymbol{C} & \boldsymbol{0} \\ \boldsymbol{T}_{11}^{-1} & -\boldsymbol{T}_{11}^{-1}\boldsymbol{T}_{12} \end{bmatrix} \boldsymbol{T}_0\tilde{\boldsymbol{x}} + \boldsymbol{T}_0^{-1}\boldsymbol{B}\boldsymbol{M}^{-1}\boldsymbol{T}_{11}\left(-\boldsymbol{Y}\boldsymbol{\theta} + \boldsymbol{\tau} + \boldsymbol{\tau}_l\right), \tag{3.114}$$

and consider the candidate Lyapunov function

$$V(\boldsymbol{\mathcal{X}}, t) = V_{\tilde{\boldsymbol{x}}}(\tilde{\boldsymbol{x}}, t) + V_{\tilde{\boldsymbol{\theta}}}(\tilde{\boldsymbol{\theta}}), \tag{3.115}$$

with the augmented state vector

$$\boldsymbol{\mathcal{X}} \triangleq \left[\left(\begin{bmatrix} a_1\boldsymbol{I} & a_2\boldsymbol{I} \end{bmatrix}\tilde{\boldsymbol{x}}\right)' \quad \tilde{\boldsymbol{\theta}}'\right]' = \begin{bmatrix} \boldsymbol{z}' & \tilde{\boldsymbol{\theta}}' \end{bmatrix}', \tag{3.116}$$

such that

$$V_z(\boldsymbol{z}, t) \triangleq \frac{1}{2}\tilde{\boldsymbol{x}}'\boldsymbol{T}_0'\boldsymbol{B}\boldsymbol{M}(\boldsymbol{q})\boldsymbol{B}'\boldsymbol{T}_0\tilde{\boldsymbol{x}} = \frac{1}{2}\left(\frac{\rho^2 r^2}{\rho^2 - r^2}\right)\boldsymbol{z}'\boldsymbol{M}(\boldsymbol{q})\boldsymbol{z}, \tag{3.117}$$

$$V_{\tilde{\boldsymbol{\theta}}}(\tilde{\boldsymbol{\theta}}) \triangleq \frac{1}{2}\tilde{\boldsymbol{\theta}}'\boldsymbol{K}_\theta\tilde{\boldsymbol{\theta}}, \tag{3.118}$$

which satisfies

$$\lambda_1||\boldsymbol{\mathcal{X}}||^2 \leq V(\boldsymbol{\mathcal{X}}, t) \leq \lambda_2||\boldsymbol{\mathcal{X}}||^2, \tag{3.119}$$

where $\lambda_1 = \frac{1}{2}\min\{\lambda_h, \lambda_{min}(\boldsymbol{K}_\theta)\}$, with $\lambda_h \triangleq \lambda_{min}(\boldsymbol{H})$ in which $\boldsymbol{H} \triangleq \boldsymbol{T}_0'\text{blkdiag}(\boldsymbol{M}, \boldsymbol{K})\boldsymbol{T}_0$. Also, $\lambda_2 = \frac{1}{2}\max\{\lambda_H, \lambda_{max}(\boldsymbol{K}_\theta)\}$, $\lambda_H = \lambda_{max}(\boldsymbol{H})$, where $\lambda_{min}(\cdot)$ and $\lambda_{max}(\cdot)$ stand for the smallest and highest eigenvalue of $(\cdot)$, respectively.

Then, the time derivative of (3.115) is

$$\dot{V}(\boldsymbol{\mathcal{X}}, t) = \frac{\partial V_z(\boldsymbol{z}, t)}{\partial t} + \left(\frac{\partial V_z(\boldsymbol{z}, t)}{\partial \boldsymbol{z}}\right)'\dot{\boldsymbol{z}} + \tilde{\boldsymbol{\theta}}'\boldsymbol{K}_\theta\dot{\tilde{\boldsymbol{\theta}}}, \tag{3.120}$$

$$= \frac{\partial V_z(\tilde{\boldsymbol{x}}, t)}{\partial t} + \left(\frac{\partial V_z(\tilde{\boldsymbol{x}}, t)}{\partial \tilde{\boldsymbol{x}}}\right)'\dot{\tilde{\boldsymbol{x}}} + \tilde{\boldsymbol{\theta}}'\boldsymbol{K}_\theta\dot{\tilde{\boldsymbol{\theta}}}. \tag{3.121}$$

Taking the partial derivative of (3.117) with respect to $\tilde{\boldsymbol{x}}$ and multiplying by (3.73) yields

$$\begin{aligned}\frac{\partial V_{\tilde{x}}(\tilde{\boldsymbol{x}},t)}{\partial \tilde{\boldsymbol{x}}}' \dot{\tilde{\boldsymbol{x}}} &= \tilde{\boldsymbol{x}}\boldsymbol{T}_0'\boldsymbol{B}\boldsymbol{M}\boldsymbol{B}'\boldsymbol{T}_0\dot{\tilde{\boldsymbol{x}}} + \frac{1}{2}\sum_{i=1}^{2n}\tilde{\boldsymbol{x}}'\boldsymbol{T}_0'\boldsymbol{B}\frac{\partial \boldsymbol{M}}{\partial \tilde{\boldsymbol{x}}_i}\dot{\tilde{\boldsymbol{x}}}_i\boldsymbol{B}'\boldsymbol{T}_0\tilde{\boldsymbol{x}}, \\ &= -\tilde{\boldsymbol{x}}'\boldsymbol{T}_0'\boldsymbol{B}\boldsymbol{C}\boldsymbol{B}'\boldsymbol{T}_0\tilde{\boldsymbol{x}} + \frac{1}{2}\sum_{i=1}^{2n}\tilde{\boldsymbol{x}}'\boldsymbol{T}_0'\boldsymbol{B}\frac{\partial \boldsymbol{M}}{\partial \tilde{\boldsymbol{x}}_i}\dot{\tilde{\boldsymbol{x}}}_i\boldsymbol{B}'\boldsymbol{T}_0\tilde{\boldsymbol{x}} + \tilde{\boldsymbol{x}}'\boldsymbol{T}_0'\boldsymbol{B}\boldsymbol{T}_{11}\left(-\boldsymbol{Y}\boldsymbol{\theta} + \boldsymbol{\tau} + \boldsymbol{\tau}_l\right).\end{aligned} \tag{3.122}$$

Using *Property 4* (see Chapter 2), renders

$$\frac{\partial V_{\tilde{x}}(\tilde{\boldsymbol{x}},t)}{\partial \tilde{\boldsymbol{x}}}' \dot{\tilde{\boldsymbol{x}}} = \frac{1}{2}\tilde{\boldsymbol{x}}'\boldsymbol{T}_0'\boldsymbol{B}\left(\sum_{i=1}^{2n}\frac{\partial \boldsymbol{M}}{\partial \tilde{\boldsymbol{x}}_i}\dot{\tilde{\boldsymbol{x}}}_i - \dot{\boldsymbol{M}}\right)\boldsymbol{B}'\boldsymbol{T}_0\tilde{\boldsymbol{x}} + \tilde{\boldsymbol{x}}'\boldsymbol{T}_0'\boldsymbol{B}\boldsymbol{T}_{11}\left(-\boldsymbol{Y}\boldsymbol{\theta} + \boldsymbol{\tau} + \boldsymbol{\tau}_l\right). \tag{3.123}$$

In the following, the partial derivative of (3.117) with respect to time is computed as

$$\frac{\partial V_{\tilde{x}}(\tilde{\boldsymbol{x}},t)}{\partial t} = \frac{1}{2}\tilde{\boldsymbol{x}}'\boldsymbol{T}_0'\boldsymbol{B}\frac{\partial \boldsymbol{M}}{\partial t}\boldsymbol{B}'\boldsymbol{T}_0\tilde{\boldsymbol{x}}. \tag{3.124}$$

Since $\boldsymbol{M}(\boldsymbol{q}) = \boldsymbol{M}(\tilde{\boldsymbol{q}} + \boldsymbol{q}_r(t)) = \boldsymbol{M}(\tilde{\boldsymbol{x}},t)$, then $\dot{\boldsymbol{M}}(\tilde{\boldsymbol{x}},t) = \frac{\partial M}{\partial t} + \frac{\partial M}{\partial \tilde{x}}\dot{\tilde{\boldsymbol{x}}}$. Considering this and substituting (3.97) and (3.123)-(3.124) into (3.120), yields

$$\dot{V}(\boldsymbol{\mathcal{X}},t) = \tilde{\boldsymbol{x}}'\boldsymbol{T}_0'\boldsymbol{B}\boldsymbol{T}_{11}\left(-\boldsymbol{Y}\boldsymbol{\theta} + \boldsymbol{\tau} + \boldsymbol{\tau}_l\right) + \tilde{\boldsymbol{\theta}}'\boldsymbol{K}_\theta\dot{\tilde{\boldsymbol{\theta}}}. \tag{3.125}$$

Note that for the worst case disturbance in the system and using (3.101)-(3.102) we can write

$$\dot{V}(\boldsymbol{\mathcal{X}},t) = -\boldsymbol{z}'\boldsymbol{z} - \frac{\rho^2}{\rho^2 - r^2}\boldsymbol{z}'\lfloor\boldsymbol{z}\rceil^{\alpha_z} - \tilde{\boldsymbol{\theta}}'\bar{\boldsymbol{f}}_\theta. \tag{3.126}$$

Considering (3.104) and (3.113) yields

$$\dot{V}(\boldsymbol{\mathcal{X}},t) \leq -\frac{\rho^2}{\rho^2 - r^2}\boldsymbol{z}'\lfloor\boldsymbol{z}\rceil^{\alpha_z} - \tilde{\boldsymbol{\theta}}'\bar{\boldsymbol{f}}_\theta. \tag{3.127}$$

From (3.127), one has

$$\dot{V}(\boldsymbol{\mathcal{X}},t) \leq -\left(\frac{\rho^2}{\rho^2 - r^2}\right)\sum_{i=1}^{n}|z_i|^{\alpha_{z_i}+1} - \sum_{j=1}^{p}\gamma_j\phi^{2\alpha_j}|\tilde{\theta}_j|^{\alpha_j+1}, \tag{3.128}$$

where z_i and $\tilde{\theta}_j$ are respectively the i-th and j-th elements of $\boldsymbol{z}(t)$ and $\tilde{\boldsymbol{\theta}}(t)$, and the relation $z_i sign(z_i) = |z_i|$ has been used.

Then, we can conclude (i),(ii) and (iii) as follows:

(i) From (3.115) $V(\boldsymbol{z},t)$ is positive definite, and from (3.127) $\dot{V}(\boldsymbol{z},t) \leq 0$ for all $t \geq t_0$, which in turn implies that $\boldsymbol{z}(t) \in \mathcal{L}_\infty$ and $\tilde{\boldsymbol{\theta}}(t) \in \mathcal{L}_\infty$. Note that expanding (3.104) it is possible to write the variable $\boldsymbol{z}(t)$ as the input of a stable linear filter,

$$\dot{\tilde{\boldsymbol{q}}}(t) = -\frac{a_2}{a_1}\tilde{\boldsymbol{q}}(t) + \frac{1}{a_1}\boldsymbol{z}(t) \implies \boldsymbol{Q}(s) = \left(\frac{\left(\frac{1}{a_1}\right)}{\frac{a_2}{a_1}+s}\right)\boldsymbol{Z}(s), \tag{3.129}$$

which implies that since $\boldsymbol{z}(t) \in \mathcal{L}_\infty$ so are $\dot{\tilde{\boldsymbol{q}}}(t), \tilde{\boldsymbol{q}}(t) \in \mathcal{L}_\infty$.

(ii) Accordingly to Barbalat's Lemma, since $V(\boldsymbol{\mathcal{X}}, t)$ is bounded as in (3.119), $\dot{V}(\mathcal{X}, t) \to 0$, if it is uniformly continuous (Slotine et al., 1991). Proving uniform continuity of $\dot{V}(\boldsymbol{\mathcal{X}}, t)$ can be achieved by showing that $\ddot{V}(\mathcal{X}, t)$ is bounded. In view of (3.126), by demonstrating that $\dot{V}(\boldsymbol{\mathcal{X}}, t) \to 0$ as $t \to \infty$ is sufficient to infer that $\boldsymbol{z} \to 0$, and as consequence, $\dot{\tilde{\boldsymbol{q}}}, \tilde{\boldsymbol{q}} \to 0$ as $t \to \infty$. Since (3.126) has only three terms, in the following, we show that $\ddot{V}(\boldsymbol{\mathcal{X}}, t)$ is bounded by taking the time derivative of these terms. First, consider

$$\frac{d}{dt}\left(-\boldsymbol{z}'\boldsymbol{z}\right) = -2\boldsymbol{z}'\dot{\boldsymbol{z}}. \tag{3.130}$$

The first term will be bounded if $\dot{\boldsymbol{z}}$ is bounded. Substituting (3.102) into the time derivative of (3.129) yields

$$\begin{aligned}\dot{\boldsymbol{z}} = &-\left(a_1\boldsymbol{M}(\boldsymbol{q})^{-1}\boldsymbol{C}(\dot{\boldsymbol{q}}, \boldsymbol{q}) - a_2\boldsymbol{I}\right)\dot{\tilde{\boldsymbol{q}}} - a_1\boldsymbol{M}(\boldsymbol{q})^{-1}\boldsymbol{Y}(\boldsymbol{q}(t), \dot{\boldsymbol{q}}(t), \boldsymbol{q}_r(t), \dot{\boldsymbol{q}}_r(t))\tilde{\boldsymbol{\theta}} \\ &- \frac{1}{r^2}\boldsymbol{M}(\boldsymbol{q})^{-1}\left(\boldsymbol{z} + \lfloor \boldsymbol{z} \rceil^{\alpha_{\boldsymbol{z}}}\right).\end{aligned} \tag{3.131}$$

Therefore, since we have shown in (i) that $\tilde{\boldsymbol{\theta}}(t) \in \mathcal{L}_\infty$, $\boldsymbol{z}(t) \in \mathcal{L}_\infty$, $\dot{\tilde{\boldsymbol{q}}}(t), \tilde{\boldsymbol{q}}(t) \in \mathcal{L}_\infty$, and $\dot{\boldsymbol{q}}_r(t), \boldsymbol{q}_r(t)$ are bounded by assumption, to demonstrate the boundedness of $\dot{\boldsymbol{z}}(t)$ it is sufficent to show that $\dot{\boldsymbol{q}}(t)$ and $\boldsymbol{q}(t)$ are bounded. However, since $\dot{\tilde{\boldsymbol{q}}}(t) = \dot{\boldsymbol{q}}(t) - \dot{\boldsymbol{q}}_r(t)$ and $\tilde{\boldsymbol{q}}(t) = \boldsymbol{q}(t) - \boldsymbol{q}_r(t)$, then it is clear that $\dot{\boldsymbol{q}}(t)$ and $\boldsymbol{q}(t)$ are bounded as well, which concludes the proof of the boundedness of $\dot{\boldsymbol{z}}(t)$.

In what follows, the time derivative of the second term of (3.126) is expanded as

$$\frac{d}{dt}\left(-\frac{\rho^2}{\rho^2 - r^2}\sum_{i=1}^{n}|z_i|^{1+\alpha_{\boldsymbol{z}_i}}\right) = -\frac{\rho^2}{\rho^2 - r^2}\left(1 + \alpha_{\boldsymbol{z}_i}\right)|z_i|^{\alpha_{\boldsymbol{z}_i}} sign(z_i)\dot{z}_i, \tag{3.132}$$

where the relation $\frac{d}{dt}\left(|z_i|\right) = sign(z_i)\dot{z}_i$ has been used. Since we have already shown that $\dot{\boldsymbol{z}}(t)$ is bounded, then the derivative of the second term of (3.126) is also bounded.

Finally, the time derivative of the third term in (3.126) is computed as follows

$$\frac{d}{dt}\left(-\gamma_j\phi^{2\alpha_j}|\tilde{\theta}_j|^{1+\alpha_j}\right) = -\gamma_j 2\alpha_j\phi^{2\alpha_j - 1}|\tilde{\theta}_j|^{1+\alpha_j}\dot{\phi} - \gamma_j\phi^{2\alpha_j}\left(1+\alpha_j\right)|\tilde{\theta}_j|^{\alpha_j} sign(\tilde{\theta}_j)\dot{\tilde{\theta}}_j. \tag{3.133}$$

As it has already been shown that $\tilde{\boldsymbol{\theta}} \in \mathcal{L}_\infty$, to prove that the derivative of the third term is bounded, it remains to show that $\dot{\phi}$ and ϕ are also bounded. Furthermore, note that since $\alpha_j \in (0.5, 1)$, then $2\alpha_j - 1 > 0$, and consequently, $\phi^{2\alpha_j - 1} = 0$ if and only if $\phi = 0$. In addition, recall that the determinant of any matrix can be obtained by means of the Laplace expansion (Horn and Johnson, 2012). Through the Laplace expansion, it can be verified that ϕ is a sum of products of the elements of $\boldsymbol{Y}_f$. Thus, ϕ will be bounded if $\boldsymbol{Y}_f$ is bounded. Considering that $\dot{\boldsymbol{Y}}_f$ is obtained through the Kresselmeier's Regressor Extension using a stable linear filter with input being $\boldsymbol{Y}_I \boldsymbol{Y}_I'$, and that the Euler-Lagrange First Integral regressor depends only on $\dot{\boldsymbol{q}}$ and $\boldsymbol{q}$, i.e $\boldsymbol{Y}_I(\dot{\boldsymbol{q}}, \boldsymbol{q})$, which have already been shown to be bounded, then one can infer that $\dot{\boldsymbol{Y}}_f$ and $\boldsymbol{Y}_f$ are also bounded, and therefore so is ϕ. The boundedness of $\dot{\phi}$ can be proved in a straightforward manner by employing Jacobi's formula (Magnus and Neudecker, 2019). Hence, the boundedness of $\dot{\boldsymbol{Y}}_f$ and $\boldsymbol{Y}_f$ implies the boundedness of $\dot{\phi}$, as it can be computed using $\dot{\phi} = Trace\left(adj\left(\boldsymbol{Y}_f\right)\dot{\boldsymbol{Y}}_f\right)$. It is noteworthy that boundedness of ϕ also implies boundedness of $\dot{\tilde{\boldsymbol{\theta}}}(t)$, as can be verified from (3.97).

In conclusion, since $\ddot{V}(\boldsymbol{\mathcal{X}}, t)$ has been shown to be bounded, then, according to Barbalat's Lemma, $\dot{V}(\boldsymbol{\mathcal{X}}, t) \to 0$ as $t \to \infty$. Consequently, from (3.126) and (3.129), this ensures that $\boldsymbol{z} \to 0$ and $\dot{\tilde{\boldsymbol{q}}}, \tilde{\boldsymbol{q}} \to 0$ as $t \to \infty$.

Remark 3.10. It is noteworthy that regardless of (3.126) containing elements of $\tilde{\boldsymbol{\theta}}$, this does not imply that $\tilde{\boldsymbol{\theta}} \to 0$ since it is not possible to always guarantee that $\phi \neq 0,\ \forall t \geq t_0$. Nevertheless, (ii) has demonstrated that it is possible to ensure trajectory tracking even in cases where parameter estimation is not occurring. Q.E.D

(iii) Considering the fact that $\alpha_{\boldsymbol{z}_i} = \alpha_j = \alpha \in (0.5, 1)$, for all $i = 1, ..., p$ and $j = 1, ..., 2n$. From (3.128), one obtains

$$\dot{V}(\boldsymbol{\mathcal{X}}, t) \leq -\left(\frac{\rho^2}{\rho^2 - r^2}\right)\sum_{j=1}^{n}|z_j^2|^{\frac{\alpha+1}{2}} - \lambda_{min}\left(\boldsymbol{\Gamma}\right)\phi^{2\alpha}\sum_{i=1}^{p}|\tilde{\theta}_i^2|^{\frac{\alpha+1}{2}}. \tag{3.134}$$

Next, taking into account that (3.68) holds for any $t_1 \geq t_0$ and $t_2 = t_1 + \Delta T$, yields

$$\begin{aligned}\dot{V}(\boldsymbol{\mathcal{X}}, t) &\leq -\left(\frac{\rho^2}{\rho^2 - r^2}\right)\sum_{j=1}^{n}\left(z_j^2\right)^{\frac{\alpha+1}{2}} - \left(\frac{\rho^2}{\rho^2 - r^2}\right)\sum_{i=1}^{p}\left(\tilde{\theta}_i^2\right)^{\frac{\alpha+1}{2}}, \\ &\leq -\left(\frac{\rho^2}{\rho^2 - r^2}\right)\sum_{k=1}^{n+p}\left(\mathcal{X}_k^2\right)^{\frac{\alpha+1}{2}}, \end{aligned} \tag{3.135}$$

where $\mathcal{X}_k$ is the k-th element of the augmented state vector $\boldsymbol{\mathcal{X}} \in \mathbb{R}^{n+p}$.

Applying Lemma A.1 from Arteaga (2023), we obtain

$$\left(\sum_{k=1}^{n+p} \mathcal{X}_k^2\right)^{\frac{\alpha+1}{2}} \leq \sum_{k=1}^{n+p} \left(\mathcal{X}_k^2\right)^{\frac{\alpha+1}{2}},$$

which allows to write (3.135) as

$$\begin{aligned} \dot{V}(\boldsymbol{\mathcal{X}}, t) &\leq -\left(\frac{\rho^2}{\rho^2 - r^2}\right)\left(||\boldsymbol{\mathcal{X}}||^2\right)^{\frac{\alpha+1}{2}}, \\ &= -\frac{\left(\frac{\rho^2}{\rho^2-r^2}\right)}{\lambda_2^{\frac{2}{\alpha+1}}}\left(\lambda_2||\boldsymbol{\mathcal{X}}||^2\right)^{\frac{\alpha+1}{2}}. \end{aligned} \tag{3.136}$$

From (3.119) and (3.110),

$$\dot{V}(\mathcal{X}, t) \leq -\eta V^{\frac{\alpha+1}{2}}, \forall t \in [t_1, t_2]. \tag{3.137}$$

According to the Comparison Lemma (Khalil, 1996), the solution of (3.137) is given by

$$V(\boldsymbol{\mathcal{X}}, t) \leq \left(-\eta\frac{1-\alpha}{2}(t - t_1) + V^{\frac{1-\alpha}{2}}(t_1)\right)^{\frac{2}{1-\alpha}}, \forall t \in [t_1, t_2]. \tag{3.138}$$

Therefore, at $t = t_2 = t_1 + \Delta T$,

$$V(\boldsymbol{\mathcal{X}}, t_2) \leq \left(-\eta\frac{1-\alpha}{2}(\Delta T) + V^{\frac{1-\alpha}{2}}(t_1)\right)^{\frac{2}{1-\alpha}}. \tag{3.139}$$

Replacing ΔT for (3.110), yields,

$$V(\boldsymbol{\mathcal{X}}, t_2) \leq 0. \tag{3.140}$$

Since $V(\boldsymbol{\mathcal{X}}, t) \geq 0 \forall t \geq t_0$, at $t = t_2$ we have $V(\boldsymbol{\mathcal{X}}, t_2) = 0$. From (3.74), one can observe that this is only possible when $\tilde{\boldsymbol{\theta}}(t) = \boldsymbol{z}(t) = \mathbf{0}$. Thus, concluding the proof.

Q.E.D

3.6 Final Remarks

In conclusion, this chapter introduced a general method for converting matrix regressors into vector regressors using the Euler-Lagrange first integral. This transformation allowed the direct application of DREM-based techniques. However, it remains uncertain whether this method enhances or diminishes excitation, requiring further analysis in this regard. This uncertainty also suggests potential future research directions, particularly in increasing the excitation level of a signal, akin to the work in Arteaga (2024). In addition, the MREM technique was presented as a common method in adaptive control for extending the dynamics while preserving excitation. This technique is based on the overlooked work Kreisselmeier (1977) and provides an alternative to the drawnback brought by the DREM technique in which it is stated that a poor choice of filters can hinder convergence even when the original regressor is PE. Although the MREM makes the tuning process easier as only two filter-tuning parameters are required, to the best of the author knowledge, it is unclear if one of the key advantadges of the DREM, that is if the regressor is not PE, it is still possible to satisfy the DREM condition, which is also true for the MREM case. The nonlinear adaptive $\mathcal{H}_\infty$ controller based on the DREM technique has been introduced. Two estimation laws based on the DREM technique were employed, with one being the classic DREM gradient estimator and the other which includes a modification in order to achieve finite-time estimation. The $\mathcal{H}_\infty$ controllers were modified accordingly and stability proofs based on Lyapunov theory were presented. In the next chapter, the nonlinear adaptive $\mathcal{W}_\infty$ optimal control is proposed.

4

Nonlinear Adaptive $\mathcal{W}_\infty$ Optimal Control

This chapter extends the nonlinear $\mathcal{W}_\infty$ optimal control proposed in Cardoso et al. (2021a) to its adaptive version. This extension leverages the DREM technique, which enhances the controller's ability to adjust to varying system dynamics online. Initially, this chapter presents a concise derivation of the nonlinear $\mathcal{W}_\infty$ optimal control, highlighting its foundational principles and mathematical formulation. Later, the novel adaptive nonlinear $\mathcal{W}_\infty$ control is presented and rigorous proofs based on Lyapunov stability theory are conducted.

4.1 Nonlinear $\mathcal{W}_\infty$ Control

In this section we recall the nonlinear $\mathcal{W}_\infty$ controller developed in Cardoso et al. (2021b). Firstly, consider again the equations of motion describing the dynamics of a fully actuated systems

$$\boldsymbol{M}(\boldsymbol{q})\ddot{\boldsymbol{q}}(t) + \boldsymbol{C}(\dot{\boldsymbol{q}}, \boldsymbol{q})\dot{\boldsymbol{q}}(t) + \boldsymbol{G}(\boldsymbol{q}) = \boldsymbol{\tau}(t) + \boldsymbol{\tau}_l(t), \tag{4.1}$$

where $\boldsymbol{q}(t) : \mathbb{R}_+ \to \mathbb{R}^n$ denotes the vector of generalized coordinates, $\boldsymbol{M}(\boldsymbol{q}) : \mathbb{R}^n \to \mathbb{R}^{n\times n}$ represents the inertia matrix, $\boldsymbol{C}(\dot{\boldsymbol{q}}, \boldsymbol{q}) : \mathbb{R}^n \times \mathbb{R}^n \to \mathbb{R}^{n\times n}$ corresponds to the Coriolis and centripetal force matrix, $\boldsymbol{G}(\boldsymbol{q}) : \mathbb{R}^n \to \mathbb{R}^n$ is the gravitational force vector, $\boldsymbol{\tau}(t) : \mathbb{R}_{\geq 0} \to \mathbb{R}^n$ is the vector of generalized control inputs, and $\boldsymbol{\tau}_l(t) : \mathbb{R}_{\geq 0} \to \mathbb{R}^n$ represents the external disturbances.

Therefore, by defining the state vector

$$\tilde{\boldsymbol{x}} = \begin{bmatrix} \dot{\tilde{\boldsymbol{q}}} \\ \tilde{\boldsymbol{q}} \end{bmatrix} = \begin{bmatrix} \dot{\boldsymbol{q}} - \dot{\boldsymbol{q}}_r \\ \boldsymbol{q} - \boldsymbol{q}_r \end{bmatrix}, \tag{4.2}$$

where $\boldsymbol{q}_r \in \mathcal{C}^2$ denotes the reference trajectory for the vector of generalized coordinates, the dynamics of the tracking error is given as

$$\dot{\tilde{\boldsymbol{x}}} = \boldsymbol{f}(\boldsymbol{q}, \dot{\boldsymbol{q}})\tilde{\boldsymbol{x}} + \boldsymbol{g}(\boldsymbol{q})\left(-\boldsymbol{Y}(\boldsymbol{q}, \dot{\boldsymbol{q}}, \boldsymbol{q}_r, \dot{\boldsymbol{q}}_r, \ddot{\boldsymbol{q}}_r)\boldsymbol{\theta} + \boldsymbol{\tau}\right) + \boldsymbol{g}(\boldsymbol{q})\boldsymbol{\tau}_l, \tag{4.3}$$

with $\boldsymbol{Y}(\boldsymbol{q}, \dot{\boldsymbol{q}}, \boldsymbol{q}_r, \dot{\boldsymbol{q}}_r, \ddot{\boldsymbol{q}}_r)\boldsymbol{\theta} = \boldsymbol{M}(\boldsymbol{q}, \boldsymbol{\theta})\ddot{\boldsymbol{q}}_r(t) + \boldsymbol{C}(\boldsymbol{q}, \dot{\boldsymbol{q}}, \boldsymbol{\theta})\dot{\boldsymbol{q}}_r(t) + \boldsymbol{G}(\boldsymbol{q}, \boldsymbol{\theta})$, and

$$\boldsymbol{f}(\boldsymbol{q}, \dot{\boldsymbol{q}}) = \begin{bmatrix} -\boldsymbol{M}^{-1}(\boldsymbol{q})\boldsymbol{C}(\dot{\boldsymbol{q}}, \boldsymbol{q}) & \boldsymbol{0} \\ \boldsymbol{I} & \boldsymbol{0} \end{bmatrix}, \quad \boldsymbol{g}(\boldsymbol{q}) = \begin{bmatrix} \boldsymbol{M}^{-1}(\boldsymbol{q}) \\ \boldsymbol{0} \end{bmatrix}. \tag{4.4}$$

In the following, the adaptive nonlinear control problem is formulated considering the tracking error dynamics (4.3), such that the generalized control forces minimize the performance index

$$\mathcal{J} = ||\boldsymbol{z}(t)||^2_{\mathcal{W}_{2,2,\boldsymbol{\Psi}}} - \rho^2||\boldsymbol{\tau}_l(t)||^2_{\mathcal{L}_2}, \tag{4.5}$$

for the worst case of all possible disturbances $\boldsymbol{\tau}_l(t) \in \mathcal{L}_2$, in which $\boldsymbol{\Psi} = (\boldsymbol{\Psi}_0, \boldsymbol{\Psi}_1, \boldsymbol{\Psi}_2)$ are positive definite tuning matrices, $\gamma \in \mathbb{R}_{\geq 0}$ is the $\mathcal{W}_\infty$ attenuating level, and $||\boldsymbol{z}(t)||_{\mathcal{W}_{m,p,\sigma}} = \left(\sum_{\alpha=0}^{m} ||\frac{d^\alpha \boldsymbol{z}(t)}{dt^\alpha}||^p_{\mathcal{L}_p,\sigma_\alpha}\right)^{\frac{1}{p}}$ is a weighted Sobolev norm of $\boldsymbol{z}(t)$, where $||\boldsymbol{z}(t)||^p_{\mathcal{L}_p,\sigma_\alpha}$ stands for the weighted $\mathcal{L}_p$ norm of $\boldsymbol{z}(t)$, for any function $\boldsymbol{z} : \mathbb{R}_{\geq 0} \to \mathbb{R}^n$, $n \in \mathbb{N}$. In this work, we consider the particular case when $\boldsymbol{z}(t) = \tilde{\boldsymbol{q}}(t)$.

Considering the performance index (4.5), the optimal $\mathcal{W}_\infty$ control problem is posed as

$$\min_{\boldsymbol{\tau} \in \mathbb{R}^n} \max_{\boldsymbol{\tau}_l \in \mathcal{L}_2} \frac{1}{2}\mathcal{J}, \tag{4.6}$$

which is here formulated via dynamic programming using differential game theory (Kirk, 2004), from where the Hamilton-Jacobi-Bellman-Isaacs equation is given by

$$\frac{\partial V}{\partial t} + \min_{\boldsymbol{\tau} \in \mathbb{R}^n} \max_{\boldsymbol{\tau}_l \in \mathcal{L}_2} \left\{ \mathbb{H}(V, \tilde{\boldsymbol{x}}, \boldsymbol{\tau}, \boldsymbol{\tau}_l, t) \right\} = 0, \tag{4.7}$$

where $V(\tilde{\boldsymbol{x}}, t) : \mathbb{R}^{2n} \times \mathbb{R}_{\geq 0} \to \mathbb{R}$, with the Hamiltonian

$$\mathbb{H}(\tilde{\boldsymbol{x}}, \boldsymbol{\tau}, \boldsymbol{\tau}_l, \ddot{\tilde{\boldsymbol{q}}}, t) = \frac{\partial V'}{\partial \tilde{\boldsymbol{x}}}\dot{\tilde{\boldsymbol{x}}} + \frac{1}{2}\tilde{\boldsymbol{x}}'\boldsymbol{Q}\tilde{\boldsymbol{x}} + \frac{1}{2}\ddot{\tilde{\boldsymbol{q}}}'\boldsymbol{\Psi}_3\ddot{\tilde{\boldsymbol{q}}} - \frac{1}{2}\rho^2\boldsymbol{\tau}_l'\boldsymbol{\tau}_l, \tag{4.8}$$

and boundary condition $V(\boldsymbol{0}, t) = 0$, in which $\boldsymbol{Q} \triangleq \text{blkdiag}(\boldsymbol{\Psi}_1, \boldsymbol{\Psi}_0)$. From (4.3), we have that

$$\ddot{\tilde{\boldsymbol{q}}} = -\boldsymbol{M}^{-1}\boldsymbol{C}\dot{\tilde{\boldsymbol{q}}} + \boldsymbol{M}^{-1}\left(-\boldsymbol{Y}\boldsymbol{\theta} + \boldsymbol{\tau} + \boldsymbol{\tau}_l\right). \tag{4.9}$$

Then, using (4.9) to expand (4.8), yields

$$\begin{aligned}\mathbb{H}(\tilde{\boldsymbol{x}}, \boldsymbol{\tau}, \boldsymbol{\tau}_l, t) = \frac{\partial V}{\partial \tilde{\boldsymbol{x}}}'\dot{\tilde{\boldsymbol{x}}} + \frac{1}{2}\tilde{\boldsymbol{x}}'\boldsymbol{Q}\tilde{\boldsymbol{x}} + \frac{1}{2}\dot{\tilde{\boldsymbol{q}}}'\boldsymbol{C}'\boldsymbol{\Lambda}\boldsymbol{C}\dot{\tilde{\boldsymbol{q}}} + \dot{\tilde{\boldsymbol{q}}}'\boldsymbol{C}'\boldsymbol{\Lambda}\boldsymbol{Y}\boldsymbol{\theta} - \dot{\tilde{\boldsymbol{q}}}'\boldsymbol{C}'\boldsymbol{\Lambda}\boldsymbol{\tau} \\ - \dot{\tilde{\boldsymbol{q}}}'\boldsymbol{C}'\boldsymbol{\Lambda}\boldsymbol{\tau}_l + \frac{1}{2}\boldsymbol{\theta}'\boldsymbol{Y}'\boldsymbol{\Lambda}\boldsymbol{Y}\boldsymbol{\theta} - \boldsymbol{\theta}'\boldsymbol{Y}'\boldsymbol{\Lambda}\boldsymbol{\tau} - \boldsymbol{\theta}'\boldsymbol{Y}'\boldsymbol{\Lambda}\boldsymbol{\tau}_l + \frac{1}{2}\boldsymbol{\tau}'\boldsymbol{\Lambda}\boldsymbol{\tau} \\ - \boldsymbol{\tau}'\boldsymbol{\Lambda}\boldsymbol{\tau}_l + \frac{1}{2}\boldsymbol{\tau}_l'\boldsymbol{\Lambda}\boldsymbol{\tau}_l - \frac{1}{2}\rho^2\boldsymbol{\tau}_l'\boldsymbol{\tau}_l,\end{aligned} \tag{4.10}$$

with $\boldsymbol{\Lambda} = \boldsymbol{M}^{-1}\boldsymbol{\Psi}_3\boldsymbol{M}^{-1}$.

To obtain the optimal control law, $\boldsymbol{\tau}^*(t)$, and the worst case disturbance, $\boldsymbol{\tau}_l^*(t)$, the partial derivatives of (4.10) with respect to these variables are computed as

$$\frac{\partial \mathbb{H}}{\partial \boldsymbol{\tau}} = \boldsymbol{\Lambda}\boldsymbol{\tau}^* + \boldsymbol{g}'\frac{\partial V}{\partial \tilde{\boldsymbol{x}}} - \boldsymbol{\Lambda}\boldsymbol{C}\dot{\tilde{\boldsymbol{q}}} - \boldsymbol{\Lambda}\boldsymbol{Y}\boldsymbol{\theta} + \boldsymbol{\Lambda}\boldsymbol{\tau}_l^* = 0, \tag{4.11}$$

$$\frac{\partial \mathbb{H}}{\partial \boldsymbol{\tau}_l} = \boldsymbol{g}'\frac{\partial V}{\partial \tilde{\boldsymbol{x}}} - \boldsymbol{\Lambda}\boldsymbol{C}\dot{\tilde{\boldsymbol{q}}} - \boldsymbol{\Lambda}\boldsymbol{Y}\boldsymbol{\theta} + \boldsymbol{\Lambda}\boldsymbol{\tau}^* + \boldsymbol{\Lambda}\boldsymbol{\tau}_l^* - \rho^2\boldsymbol{\tau}_l^* = 0. \tag{4.12}$$

Then, by manipulating (4.11) and (4.12), we obtain

$$\boldsymbol{\tau}^* = -\boldsymbol{\Lambda}^{-1}(\boldsymbol{q})\boldsymbol{g}(\boldsymbol{q})'\frac{\partial V}{\partial \tilde{\boldsymbol{x}}} + \boldsymbol{C}(\dot{\boldsymbol{q}}, \boldsymbol{q})\dot{\tilde{\boldsymbol{q}}} + \boldsymbol{Y}(\boldsymbol{q}, \dot{\boldsymbol{q}}, \boldsymbol{q}_r, \dot{\boldsymbol{q}}_r, \ddot{\boldsymbol{q}}_r)\boldsymbol{\theta}, \tag{4.13}$$

$$\boldsymbol{\tau}_l^* = 0. \tag{4.14}$$

In addition, through the second derivatives

$$\frac{\partial^2 \mathbb{H}}{\partial \boldsymbol{\tau}^2} = \boldsymbol{\Lambda}(\boldsymbol{q}) = \boldsymbol{M}(\boldsymbol{q})^{-1}\boldsymbol{\Psi}_3\boldsymbol{M}(\boldsymbol{q})^{-1} > 0, \tag{4.15}$$

$$\frac{\partial^2 \mathbb{H}}{\partial \boldsymbol{\tau}_l^2} = \Lambda - \rho^2\boldsymbol{I} < 0, \tag{4.16}$$

it can be demonstrated that $\boldsymbol{\tau}^*$ and $\boldsymbol{\tau}_l^*$ are a min-max solution of (4.6).

Replacing (4.13) and (4.14) into (4.3), the closed-loop state-space dynamics results in

$$\dot{\tilde{\boldsymbol{x}}} = \begin{bmatrix} \boldsymbol{0} & \boldsymbol{0} \\ \boldsymbol{I} & \boldsymbol{0} \end{bmatrix}\tilde{\boldsymbol{x}} - \begin{bmatrix} \boldsymbol{\Psi}_2^{-1} & \boldsymbol{0} \\ \boldsymbol{0} & \boldsymbol{0} \end{bmatrix}\frac{\partial V}{\partial \tilde{\boldsymbol{x}}}. \tag{4.17}$$

Also, by substituting (4.13), (4.14) and (4.17) into (4.10), we obtain the optimized Hamiltonian $\mathbb{H}(V, \tilde{\boldsymbol{x}}, \boldsymbol{\tau}^*, \boldsymbol{\tau}_l^*, t)$, which leads to the Hamilton-Jacobi partial differential equation

$$\frac{\partial V}{\partial t} + \mathbb{H}(V, \tilde{\boldsymbol{x}}, \boldsymbol{\tau}^*, \boldsymbol{\tau}_l^*, t) = 0. \tag{4.18}$$

Thus, the control problem results in obtaining a solution $V(\tilde{\boldsymbol{x}}, t)$ to (4.18). A particular solution to the Hamilton-Jacobi equation (4.18) is presented in the following theorem.

Theorem 4.1 (Nonlinear $\mathcal{W}_\infty$ Control - Adapted from Cardoso et al. (2021a)). *Consider a system described by (4.3) and let $\boldsymbol{P} = \boldsymbol{P}' > 0$ be the solution of the following Riccati equation*

$$\boldsymbol{PA} + \boldsymbol{A}'\boldsymbol{P} - \boldsymbol{PRP} + \boldsymbol{Q} = 0, \tag{4.19}$$

where $\boldsymbol{A} \triangleq \begin{bmatrix} \mathbf{0} & \mathbf{0} \\ \boldsymbol{I} & \mathbf{0} \end{bmatrix}$, $\boldsymbol{R} \triangleq \begin{bmatrix} \boldsymbol{\Psi}_2^{-1} & \mathbf{0} \\ \mathbf{0} & \mathbf{0} \end{bmatrix}$, $\boldsymbol{Q} \triangleq blkdiag(\boldsymbol{\Psi}_1, \boldsymbol{\Psi}_0)$. *Then, the following robust nonlinear $\mathcal{W}_\infty$ optimal control law*

$$\boldsymbol{\tau}^*(t) = -\boldsymbol{\Lambda}^{-1}(\boldsymbol{q})\boldsymbol{g}(\boldsymbol{q})'\boldsymbol{P}\tilde{\boldsymbol{x}} + \boldsymbol{C}(\dot{\boldsymbol{q}}, \boldsymbol{q})\dot{\tilde{\boldsymbol{q}}} + \boldsymbol{Y}(\boldsymbol{q}, \dot{\boldsymbol{q}}, \boldsymbol{q}_r, \dot{\boldsymbol{q}}_r, \ddot{\boldsymbol{q}}_r)\boldsymbol{\theta}, \tag{4.20}$$

with $\boldsymbol{\Lambda}(\boldsymbol{q}) = \boldsymbol{M}(\boldsymbol{q})^{-1}\boldsymbol{\Psi}_3\boldsymbol{M}(\boldsymbol{q})^{-1}$, $\boldsymbol{g}(\boldsymbol{q}) = [\boldsymbol{M}(\boldsymbol{q})^{-1'} \;\; \mathbf{0}']'$, *and*

$$\boldsymbol{Y}(\boldsymbol{q}, \dot{\boldsymbol{q}}, \boldsymbol{q}_r, \dot{\boldsymbol{q}}_r, \ddot{\boldsymbol{q}}_r)\boldsymbol{\theta} = \boldsymbol{M}(\boldsymbol{q})\ddot{\boldsymbol{q}}_r(t) + \boldsymbol{C}(\boldsymbol{q}, \dot{\boldsymbol{q}})\dot{\boldsymbol{q}}_r(t) + \boldsymbol{G}(\boldsymbol{q}). \tag{4.21}$$

is a solution to the following nonlinear $\mathcal{W}_\infty$ optimal control problem:

$$\mathcal{J}^* = \min_{\boldsymbol{\tau} \in \mathbb{R}^n} \max_{\boldsymbol{\tau}_l \in \mathcal{L}_2} \left(\frac{1}{2} ||\tilde{\boldsymbol{q}}(t)||^2_{\mathcal{W}_{2,2,\boldsymbol{\Psi}}} - \frac{\rho^2}{2} ||\boldsymbol{\tau}_l(t)||^2_{\mathcal{L}_2} \right), \tag{4.22}$$

$$= \min_{\boldsymbol{\tau} \in \mathbb{R}^n} \max_{\boldsymbol{\tau}_l \in \mathcal{L}_2} \int_{t_0}^{t} \left(\frac{1}{2} ||\tilde{\boldsymbol{q}}||^2_{\boldsymbol{\Psi}_0} + \frac{1}{2} ||\dot{\tilde{\boldsymbol{q}}}||^2_{\boldsymbol{\Psi}_1} + \frac{1}{2} ||\ddot{\tilde{\boldsymbol{q}}}||^2_{\boldsymbol{\Psi}_2} - \frac{\rho^2}{2} ||\boldsymbol{\tau}_l||^2 \right) d\tau. \tag{4.23}$$

In addition, the control law (4.20) ensures assymptotic stability for the system (4.3).

Proof. See Appendix A.6. Q.E.D

4.2 Adaptive $\mathcal{W}_\infty$ Control via DREM/MREM

In this section we introduce the novel nonlinear adaptive $\mathcal{W}_\infty$ control. First, consider the gradient DREM/MREM adaptive law

$$\dot{\hat{\boldsymbol{\theta}}} = -\boldsymbol{\Gamma}\phi \left(\phi\hat{\boldsymbol{\theta}} - \boldsymbol{\tau}_e \right), \tag{4.24}$$

where $\gamma_i > 0$ is the i-th component of the positive definite diagonal matrix $\boldsymbol{\Gamma} \in \mathbb{R}^{p \times p}$, with $\boldsymbol{\Gamma} \triangleq \text{diag}(\gamma_1, \gamma_2, \cdots, \gamma_p)$. Given that the unknown parameters are constant, the closed-loop dynamics of the parameter error can be described by

$$\dot{\tilde{\boldsymbol{\theta}}} = -\boldsymbol{\Gamma}\phi^2\tilde{\boldsymbol{\theta}}. \tag{4.25}$$

The main contribution of this chapter is presented in the following Theorem 4.2.

Theorem 4.2 (DREM/MREM Nonlinear Adaptive $\mathcal{W}_\infty$ Control)**.** *Let $V(\tilde{\boldsymbol{x}}, t)$ be the parameterized scalar function*

$$V(\tilde{\boldsymbol{x}}, t) = \frac{1}{2}\tilde{\boldsymbol{x}}'\boldsymbol{P}\tilde{\boldsymbol{x}}, \tag{4.26}$$

such that $\boldsymbol{P} = \boldsymbol{P}' > 0$ is computed from the solution of the following Riccati equation

$$\boldsymbol{PA} + \boldsymbol{A}'\boldsymbol{P} - \boldsymbol{PRP} + \boldsymbol{Q} = 0, \tag{4.27}$$

where

$$\boldsymbol{A} \triangleq \begin{bmatrix} \boldsymbol{0} & \boldsymbol{0} \\ \boldsymbol{I} & \boldsymbol{0} \end{bmatrix}, \ \boldsymbol{R} \triangleq \begin{bmatrix} \boldsymbol{\Psi}_2^{-1} & \boldsymbol{0} \\ \boldsymbol{0} & \boldsymbol{0} \end{bmatrix} \quad \boldsymbol{Q} \triangleq blkdiag(\boldsymbol{\Psi}_1, \boldsymbol{\Psi}_0) \ .$$

Choose $\xi_0, \xi_1, \xi_2 \in \mathbb{R}_{\geq 0}$, such that $\xi_0 < 1$,

$$b(\tilde{\boldsymbol{x}}, t) = \frac{1}{1-\xi_0}\left(\xi_0 \boldsymbol{a}_{max} + \xi_0 \|\boldsymbol{\Phi}\| \|\tilde{\boldsymbol{x}}\| + \overline{M}\xi_1 \|\dot{\boldsymbol{q}}(t)\|^2 + \overline{M}\xi_2\right), \tag{4.28}$$

$$\hat{\boldsymbol{M}}(\boldsymbol{q}(t), \hat{\boldsymbol{\theta}}) = \frac{2}{\overline{\boldsymbol{M}} + \underline{\boldsymbol{M}}}\boldsymbol{I}, \tag{4.29}$$

$$\boldsymbol{\Phi} \triangleq \begin{bmatrix} \boldsymbol{\Psi}_2^{-1} & \boldsymbol{0} \end{bmatrix} \boldsymbol{P}, \tag{4.30}$$

$$\|\ddot{\boldsymbol{q}}_r\| \leq \boldsymbol{a}_{max} < \infty \tag{4.31}$$

with

$$\|\boldsymbol{E}\| \triangleq \|\boldsymbol{M}^{-1}\tilde{\boldsymbol{M}}\| = \|\boldsymbol{M}^{-1}\hat{\boldsymbol{M}} - \boldsymbol{I}\| \leq \frac{\overline{M} - \underline{M}}{\overline{M} + \underline{M}} \leq \xi_0 < 1, \tag{4.32}$$

where $\hat{\boldsymbol{M}}$ is the estimated inertia matrix and the following holds $0 < \underline{M} \leq ||\boldsymbol{M}^{-1}(\boldsymbol{q})|| \leq \overline{M} < \infty$, and $b : \mathbb{R}^{2n} \times \mathbb{R}_{\geq 0} \to \mathbb{R}_{\geq 0}$. Next, consider that

$$\phi^2 \geq \lambda_{min}(\boldsymbol{\Theta}), \quad \forall t \in [t_1, t_2]. \tag{4.33}$$

with

$$\boldsymbol{\Theta} \triangleq \begin{bmatrix} \boldsymbol{0} & \boldsymbol{I} \\ \boldsymbol{0} & \boldsymbol{0} \end{bmatrix} \boldsymbol{P} + \begin{bmatrix} \boldsymbol{\Psi}_1 & \boldsymbol{0} \\ \boldsymbol{0} & \boldsymbol{\Psi}_0 \end{bmatrix} > 0. \tag{4.34}$$

Then, the following modified robust nonlinear $\mathcal{W}_\infty$ control law, the update law, and worst *case disturbance*

$$\boldsymbol{\tau}(t) = -\hat{\boldsymbol{\Lambda}}^{-1}(\boldsymbol{q})\hat{\boldsymbol{g}}(\boldsymbol{q})'\boldsymbol{P}\tilde{\boldsymbol{x}} + \hat{\boldsymbol{C}}(\dot{\boldsymbol{q}},\boldsymbol{q})\dot{\tilde{\boldsymbol{q}}} + \boldsymbol{Y}(\boldsymbol{q},\dot{\boldsymbol{q}},\boldsymbol{q}_r,\dot{\boldsymbol{q}}_r,\ddot{\boldsymbol{q}}_r)\hat{\boldsymbol{\theta}} + \hat{\boldsymbol{M}}\boldsymbol{v}, \tag{4.35}$$

$$\dot{\hat{\boldsymbol{\theta}}}(t) = -\boldsymbol{\Gamma}\phi\left(\phi\hat{\boldsymbol{\theta}} - \boldsymbol{\tau}_e\right), \tag{4.36}$$

$$\boldsymbol{\tau}_l^*(t) = 0, \tag{4.37}$$

with

$$\boldsymbol{v} = \begin{cases} -b(\tilde{\boldsymbol{x}},t)\boldsymbol{B}'\boldsymbol{P}\tilde{\boldsymbol{x}}\|\boldsymbol{B}'\boldsymbol{P}\tilde{\boldsymbol{x}}\|^{-1}; & ||\boldsymbol{B}'\boldsymbol{P}\tilde{\boldsymbol{x}}|| > \frac{\epsilon}{1+\phi^2(t)}, \\ -b(\tilde{\boldsymbol{x}},t)\left(\frac{1+\phi^2(t)}{\epsilon}\right)\boldsymbol{B}'\boldsymbol{P}\tilde{\boldsymbol{x}}; & \|\boldsymbol{B}'\boldsymbol{P}\tilde{\boldsymbol{x}}\| \le \frac{\epsilon}{1+\phi^2(t)}, \end{cases} \tag{4.38}$$

where $\hat{\boldsymbol{\Lambda}}(\boldsymbol{q}) = \hat{\boldsymbol{M}}^{-1}\boldsymbol{\Psi}_2\hat{\boldsymbol{M}}^{-1}$, $\hat{\boldsymbol{g}}(\boldsymbol{q}) = [\hat{\boldsymbol{M}}^{-1} \quad \boldsymbol{0}']'$, $\boldsymbol{B} = [\boldsymbol{I} \quad \boldsymbol{0}]'$, $\epsilon > 0$, *provide that all trajectories of the system* (4.3) *in closed loop with the control law* (4.35) *are uniformly ultimately bounded (u.u.b.) with ultimate bound given by*

$$\|\boldsymbol{\mathcal{X}}\| > \left(\frac{\epsilon b(\tilde{\boldsymbol{x}},t)}{4\lambda_{min}(\boldsymbol{\Theta})(1+\phi^2(t))}\right)^{\frac{1}{2}} := \delta, \tag{4.39}$$

where $\boldsymbol{\mathcal{X}} = [\tilde{\boldsymbol{x}}' \; \tilde{\boldsymbol{\theta}}']'$.

Proof. The proof is conducted inspired by the results in (Raffo, 2011, Chp.5). Initially, substituting (4.35)-(4.37) in(4.3) yields

$$\dot{\tilde{\boldsymbol{x}}} = \begin{bmatrix} \boldsymbol{0} & \boldsymbol{0} \\ \boldsymbol{I} & \boldsymbol{0} \end{bmatrix}\tilde{\boldsymbol{x}} + \begin{bmatrix} \boldsymbol{I} \\ \boldsymbol{0} \end{bmatrix}\left(\boldsymbol{M}^{-1}\boldsymbol{Y}\tilde{\boldsymbol{\theta}} + \boldsymbol{M}^{-1}\begin{bmatrix}\tilde{\boldsymbol{C}} & \boldsymbol{0}\end{bmatrix}\tilde{\boldsymbol{x}} - \boldsymbol{M}^{-1}\begin{bmatrix}\hat{\boldsymbol{M}}\boldsymbol{\Psi}_{\boldsymbol{2}}^{-1} & \boldsymbol{0}\end{bmatrix}\boldsymbol{P}\tilde{\boldsymbol{x}} + \boldsymbol{M}^{-1}\hat{\boldsymbol{M}}\boldsymbol{v}\right) \tag{4.40}$$

where $\tilde{(.)} = \hat{(.)} - (.)$ and $\boldsymbol{v}$ is an additional control law responsible to ensure stability. In addition, note that we can write

$$\boldsymbol{E} = \boldsymbol{M}^{-1}\tilde{\boldsymbol{M}}(\boldsymbol{q}) = \boldsymbol{M}^{-1}(\boldsymbol{q})\hat{\boldsymbol{M}}(\boldsymbol{q}) - \boldsymbol{I},$$

which allows to write (4.40) as

$$\begin{aligned} \dot{\tilde{\boldsymbol{x}}} &= \begin{bmatrix} \boldsymbol{0} & \boldsymbol{0} \\ \boldsymbol{I} & \boldsymbol{0} \end{bmatrix}\tilde{\boldsymbol{x}} - \begin{bmatrix} \boldsymbol{\Psi}_2^{-1} & \boldsymbol{0} \\ \boldsymbol{0} & \boldsymbol{0} \end{bmatrix}\boldsymbol{P}\tilde{\boldsymbol{x}} + \begin{bmatrix} \boldsymbol{I} \\ \boldsymbol{0} \end{bmatrix}\left(\boldsymbol{E}\left(\ddot{\boldsymbol{q}}_r - \begin{bmatrix}\boldsymbol{\Psi}_2^{-1} & \boldsymbol{0}\end{bmatrix}\boldsymbol{P}\tilde{\boldsymbol{x}}\right) + \boldsymbol{M}^{-1}\left(\tilde{\boldsymbol{C}}\dot{\boldsymbol{q}} + \tilde{\boldsymbol{G}}\right) + \boldsymbol{E}\boldsymbol{v} + \boldsymbol{v}\right), \\ &= \left(\begin{bmatrix} \boldsymbol{0} & \boldsymbol{0} \\ \boldsymbol{I} & \boldsymbol{0} \end{bmatrix} - \begin{bmatrix} \boldsymbol{\Psi}_2^{-1} & \boldsymbol{0} \\ \boldsymbol{0} & \boldsymbol{0} \end{bmatrix}\boldsymbol{P}\right)\tilde{\boldsymbol{x}} + \boldsymbol{B}(\boldsymbol{\eta} + \boldsymbol{v}), \end{aligned} \tag{4.41}$$

where the fact $\boldsymbol{Y}\tilde{\boldsymbol{\theta}} = \boldsymbol{Y}\hat{\boldsymbol{\theta}} - \boldsymbol{Y}\boldsymbol{\theta} = \tilde{\boldsymbol{M}}\ddot{\boldsymbol{q}}_r + \tilde{\boldsymbol{C}}\dot{\boldsymbol{q}}_r + \tilde{\boldsymbol{G}}$ has been used, and the nonlinear function

$$\boldsymbol{\eta}(\boldsymbol{q},\dot{\boldsymbol{q}},\tilde{\boldsymbol{\theta}},\boldsymbol{v},t) \triangleq \boldsymbol{E}\boldsymbol{v} + \boldsymbol{E}\left(\ddot{\boldsymbol{q}}_r - \begin{bmatrix}\boldsymbol{\Psi}_2^{-1} & \boldsymbol{0}\end{bmatrix}\boldsymbol{P}\tilde{\boldsymbol{x}}\right) + \boldsymbol{M}^{-1}\left(\tilde{\boldsymbol{C}}\dot{\boldsymbol{q}} + \tilde{\boldsymbol{G}}\right), \tag{4.42}$$

is defined as the uncertainty of the system.

Assumption 4.3. Assume that there exists a bound $b(\tilde{\boldsymbol{x}},t) \geq 0$ on the uncertainty $\boldsymbol{\eta}$ such that

$$||\boldsymbol{\eta}|| \leq b(\tilde{\boldsymbol{x}},t), \tag{4.43}$$

$$\|\boldsymbol{v}\| \leq b(\tilde{\boldsymbol{x}},t). \tag{4.44}$$

Q.E.D

Assumption 4.4. Through the Cauchy-Schwartz inequality and the properties of the Coriolis matrix and gravitational forces vector (see Chapter 2), we have

$$\|\tilde{\boldsymbol{C}}\dot{\boldsymbol{q}} + \tilde{\boldsymbol{G}}\| \leq \|\tilde{\boldsymbol{C}}\dot{\boldsymbol{q}}\| + \|\tilde{\boldsymbol{G}}\| \leq \xi_1\|\dot{\boldsymbol{q}}\|^2 + \xi_2. \tag{4.45}$$

Q.E.D

Next, notice that using the Cauchy-Schwartz inequality, we can write

$$\begin{aligned}
\|\boldsymbol{\eta}\| &= \|\boldsymbol{E}\boldsymbol{v} + \boldsymbol{E}\left(\ddot{\boldsymbol{q}}_r - \begin{bmatrix}\boldsymbol{\Psi}_2^{-1} & \boldsymbol{0}\end{bmatrix}\boldsymbol{P}\tilde{\boldsymbol{x}}\right) + \boldsymbol{M}^{-1}\left(\tilde{\boldsymbol{C}}\dot{\boldsymbol{q}} + \tilde{\boldsymbol{G}}\right)\|,\\
&\leq \|\boldsymbol{E}\boldsymbol{v}\| + \|\boldsymbol{E}\left(\ddot{\boldsymbol{q}}_r - \begin{bmatrix}\boldsymbol{\Psi}_2^{-1} & \boldsymbol{0}\end{bmatrix}\boldsymbol{P}\tilde{\boldsymbol{x}}\right)\| + \|\boldsymbol{M}^{-1}\left(\tilde{\boldsymbol{C}}\dot{\boldsymbol{q}} + \tilde{\boldsymbol{G}}\right)\|,\\
&\leq \xi_0 b(\tilde{\boldsymbol{x}},t) + \xi_0\boldsymbol{a}_{max} + \xi_0\left\|\begin{bmatrix}\boldsymbol{\Psi}_2^{-1} & \boldsymbol{0}\end{bmatrix}\boldsymbol{P}\right\|\|\tilde{\boldsymbol{x}}\| + \overline{M}\|\tilde{\boldsymbol{C}}\dot{\boldsymbol{q}} + \tilde{\boldsymbol{G}}\|,\\
&\leq \xi_0 b(\tilde{\boldsymbol{x}},t) + \xi_0\boldsymbol{a}_{max} + \xi_0\|\boldsymbol{\Phi}\|\|\tilde{\boldsymbol{x}}\| + \overline{M}\xi_1\|\dot{\boldsymbol{q}}(t)\|^2 + \overline{M}\xi_2 =: b(\tilde{\boldsymbol{x}},t),
\end{aligned} \tag{4.46}$$

where (4.30), (4.32), (4.44) and (4.45) have been used. Since $\xi_0 < 1$, then by isolating $b(\tilde{\boldsymbol{x}},t)$ yields

$$b(\tilde{\boldsymbol{x}},t) = \frac{1}{1-\xi_0}\left(\xi_0\boldsymbol{a}_{max} + \xi_0\|\boldsymbol{\Phi}\|\|\tilde{\boldsymbol{x}}\| + \overline{M}\xi_1\|\dot{\boldsymbol{q}}(t)\|^2 + \overline{M}\xi_2\right). \tag{4.47}$$

Now, consider the augmented candidate Lyapunov function with (4.26)

$$V(\boldsymbol{\mathcal{X}}) = \frac{1}{2}\tilde{\boldsymbol{x}}'\boldsymbol{P}\tilde{\boldsymbol{x}} + \frac{1}{2}\tilde{\boldsymbol{\theta}}'\boldsymbol{\Gamma}^{-1}\tilde{\boldsymbol{\theta}}, \tag{4.48}$$

in which $\boldsymbol{\mathcal{X}} = [\tilde{\boldsymbol{x}}'\ \tilde{\boldsymbol{\theta}}']'$. Then, computing its time derivative, taking into account (4.41), yields

$$\dot{V}(\boldsymbol{\mathcal{X}}) = \tilde{\boldsymbol{x}}'\left(\boldsymbol{P}\begin{bmatrix}\boldsymbol{0} & \boldsymbol{0}\\ \boldsymbol{I} & \boldsymbol{0}\end{bmatrix} - \boldsymbol{P}\begin{bmatrix}\boldsymbol{\Psi}_2^{-1} & \boldsymbol{0}\\ \boldsymbol{0} & \boldsymbol{0}\end{bmatrix}\boldsymbol{P}\right)\tilde{\boldsymbol{x}} + \tilde{\boldsymbol{x}}'\boldsymbol{P}\boldsymbol{B}\left(\boldsymbol{\eta}+\boldsymbol{v}\right) + \tilde{\boldsymbol{\theta}}'\boldsymbol{\Gamma}^{-1}\dot{\tilde{\boldsymbol{\theta}}}. \tag{4.49}$$

From the Riccati equation (4.27), using (4.25) and (4.34), results in

$$\begin{aligned}\dot{V}(\mathcal{X}) &= -\tilde{\boldsymbol{x}}'\boldsymbol{\Theta}\tilde{\boldsymbol{x}} + \tilde{\boldsymbol{x}}'\boldsymbol{PB}\left(\boldsymbol{\eta}+\boldsymbol{v}\right) - \phi^2(t)\tilde{\boldsymbol{\theta}}'\tilde{\boldsymbol{\theta}},\\ &\leq -\lambda_{min}\left(\boldsymbol{\Theta}\right)\tilde{\boldsymbol{x}}'\tilde{\boldsymbol{x}} + \tilde{\boldsymbol{x}}'\boldsymbol{PB}\left(\boldsymbol{\eta}+\boldsymbol{v}\right) - \phi^2(t)\tilde{\boldsymbol{\theta}}'\tilde{\boldsymbol{\theta}}, \end{aligned} \tag{4.50}$$

If (4.33) holds, then

$$\dot{V}(\boldsymbol{\mathcal{X}}) \leq -\lambda_{min}\left(\boldsymbol{\Theta}\right)\boldsymbol{\mathcal{X}}'\boldsymbol{\mathcal{X}} + \tilde{\boldsymbol{x}}'\boldsymbol{PB}\left(\boldsymbol{\eta}+\boldsymbol{v}\right). \tag{4.51}$$

Next, we design $\boldsymbol{v}$ in order to ensure that (4.51) is negative semi-definite. In what follows, considering the auxiliary control law as in (4.38), we consider the case when $\|\tilde{\boldsymbol{x}}'\boldsymbol{PB}\| > \frac{\epsilon}{1+\phi^2(t)}$, leading to

$$\begin{aligned}\dot{V}(\boldsymbol{\mathcal{X}}) &\leq -\lambda_{min}\left(\boldsymbol{\Theta}\right)\boldsymbol{\mathcal{X}}'\boldsymbol{\mathcal{X}} + \tilde{\boldsymbol{x}}'\boldsymbol{PB}\boldsymbol{\eta} - b(\tilde{\boldsymbol{x}},t)\|\tilde{\boldsymbol{x}}'\boldsymbol{PB}\|,\\ &\leq -\lambda_{min}\left(\boldsymbol{\Theta}\right)\boldsymbol{\mathcal{X}}'\boldsymbol{\mathcal{X}} + \|\tilde{\boldsymbol{x}}'\boldsymbol{PB}\|\|\boldsymbol{\eta}\| - b(\tilde{\boldsymbol{x}},t)\|\tilde{\boldsymbol{x}}'\boldsymbol{PB}\|, \qquad (4.52)\\ &\leq -\lambda_{min}\left(\boldsymbol{\Theta}\right)\boldsymbol{\mathcal{X}}'\boldsymbol{\mathcal{X}} < 0, \qquad (4.53)\end{aligned}$$

where the Cauchy-Schwartz inequality and (4.43) have been used. Conversely, for the case when $\|\tilde{\boldsymbol{x}}'\boldsymbol{PB}\| \leq \frac{\epsilon}{1+\phi^2(t)}$,

$$\begin{aligned}\dot{V}(\mathcal{X}) &\leq -\lambda_{min}\left(\boldsymbol{\Theta}\right)\boldsymbol{\mathcal{X}}'\boldsymbol{\mathcal{X}} + \tilde{\boldsymbol{x}}'\boldsymbol{PB}\boldsymbol{\eta} - b(\tilde{\boldsymbol{x}},t)\left(\frac{1+\phi^2(t)}{\epsilon}\right)\|\tilde{\boldsymbol{x}}'\boldsymbol{PB}\|^2,\\ &\leq -\lambda_{min}\left(\boldsymbol{\Theta}\right)\boldsymbol{\mathcal{X}}'\boldsymbol{\mathcal{X}} + \|\tilde{\boldsymbol{x}}'\boldsymbol{PB}\|b(\tilde{\boldsymbol{x}},t) - b(\tilde{\boldsymbol{x}},t)\left(\frac{1+\phi^2(t)}{\epsilon}\right)\|\tilde{\boldsymbol{x}}'\boldsymbol{PB}\|^2,\\ &:= -\lambda_{min}\left(\boldsymbol{\Theta}\right)\boldsymbol{\mathcal{X}}'\boldsymbol{\mathcal{X}} + \mathbb{W}(\boldsymbol{w},t), \qquad (4.54)\end{aligned}$$

where

$$\mathbb{W}(\boldsymbol{w},t) \triangleq b(\tilde{\boldsymbol{x}},t)\boldsymbol{w} - b(\tilde{\boldsymbol{x}},t)\left(\frac{1+\phi^2(t)}{\epsilon}\right)\boldsymbol{w}^2, \tag{4.55}$$

with $\boldsymbol{w} \triangleq \|\tilde{\boldsymbol{x}}'\boldsymbol{PB}\|$. Notice that taking the partial derivative of $\mathbb{W}$ with respect to $\boldsymbol{w}$ and setting it equal to zero allow us to obtain the maximum value of the function, that is

$$\frac{\partial\mathbb{W}}{\partial\boldsymbol{w}} = b(\tilde{\boldsymbol{x}},t) - 2b(\tilde{\boldsymbol{x}},t)\left(\frac{1+\phi^2(t)}{\epsilon}\right)\boldsymbol{w}^* = 0 \implies \boldsymbol{w}^* = \frac{\epsilon}{2\left(1+\phi^2(t)\right)}. \tag{4.56}$$

Replacing (4.56) in (4.55), yields

$$\mathbb{W}(\boldsymbol{w},t) \leq \mathbb{W}(\boldsymbol{w}^*,t) = \frac{\epsilon b(\tilde{\boldsymbol{x}},t)}{4\left(1+\phi^2(t)\right)}. \tag{4.57}$$

Then, substituting (4.57) into (4.54), results in

$$\dot{V}(\tilde{\boldsymbol{x}}) \leq -\lambda_{min}(\boldsymbol{\Theta})\,\boldsymbol{\mathcal{X}}'\boldsymbol{\mathcal{X}} + \frac{\epsilon b(\tilde{\boldsymbol{x}}, t)}{4\left(1+\phi^2(t)\right)} < 0, \tag{4.58}$$

if and only if

$$\begin{aligned} \lambda_{min}(\boldsymbol{\Theta})\,\boldsymbol{\mathcal{X}}'\boldsymbol{\mathcal{X}} &> \frac{\epsilon b(\tilde{\boldsymbol{x}}, t)}{4\left(1+\phi^2(t)\right)}, \\ \implies \|\boldsymbol{\mathcal{X}}\| &> \left(\frac{\epsilon b(\tilde{\boldsymbol{x}}, t)}{4\lambda_{min}(\boldsymbol{\Theta})\left(1+\phi^2(t)\right)}\right)^{\frac{1}{2}} := \delta, \end{aligned} \tag{4.59}$$

which represents the ultimate bound (4.39) and thus completes the proof. Since $\dot{V}(\boldsymbol{\mathcal{X}})$ is negative outside the ball $\boldsymbol{B}_\delta$, all trajectories will eventually enter the level set $\boldsymbol{\Omega}_\delta$, the smallest level set of $V(\boldsymbol{\mathcal{X}})$ containing $\boldsymbol{B}_\delta$. The system is thus u.u.b. with respect to $\boldsymbol{B}_r$, the smallest ball containing $\boldsymbol{\Omega}_\delta$.

Q.E.D

Figure 4.1 illustrates these results.

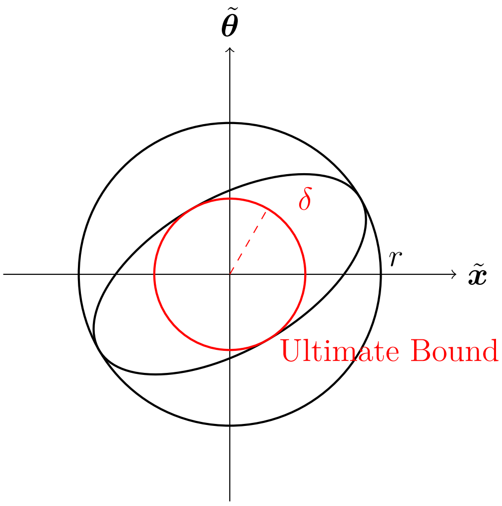

Figure 4.1: Uniform ultimate boundedness set.

4.3 Final Remarks

In conclusion, this chapter proposed the nonlinear adaptive $\mathcal{W}_\infty$ controller based on the DREM technique. The controller's stability was verified using Lyapunov stability theory resulting in uniform ultimate boundedness of the solution of $\boldsymbol{\mathcal{X}}$. These results constitute an important step towards the subsequent development of the adaptive nonlinear $\mathcal{W}_\infty$ control framework.

In the next chapter simulations results are presented in order to support the theoretical developments of the previous chapters.

5

Numerical Results

In this chapter, we present numerical results with the CRS-A465 robot manipulator to evaluate the performance of the control strategies developed in this master thesis. Specifically, we assess the nonlinear adaptive $\mathcal{H}_\infty$ controller based on the DREM technique, using both the gradient estimator and the one that ensures finite-time parameter estimation, developed in Chapter 3. Additionally, we evaluate the novel adaptive $\mathcal{W}_\infty$ controller proposed in Chapter 4, based on the DREM technique. The performance of all controllers is analyzed under conditions that either satisfy or not the exact parameter estimation requirements. We demonstrate an effectively trajectory tracking of the system states even in scenarios where exact parameter estimation conditions is violated.

5.1 The CRS-A465 Robot Manipulator

The numerical experiment is based on a simplified version of the CRS-A465 robot model (**?**). The robot A465 is a serial-link manipulator manufactured by the Canadian company CRS Robotics, which is depicted in Figure 5.1. In this simplified model, we focus on joints 2, 3 and 5, which have been relabeled as 1, 2 and 3, respectively, while the remaining degrees of freedom are kept fixed, following the methodology outlined in Arteaga (2023). The dynamics of this system are governed by the following Euler-Lagrange equations

$$\boldsymbol{M}(\boldsymbol{q})\ddot{\boldsymbol{q}}(t) + \boldsymbol{C}(\dot{\boldsymbol{q}}, \boldsymbol{q})\dot{\boldsymbol{q}}(t) + \boldsymbol{G}(\boldsymbol{q}) = \boldsymbol{\tau},$$

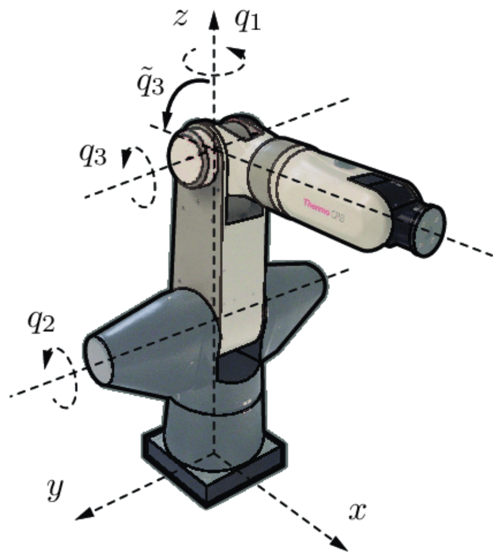

Figure 5.1: The CRS-A465 robot manipulator.

with the inertia matrix, the Coriolis and centripetal forces matrix, and the gravity vector computed as

$$\boldsymbol{M}(\boldsymbol{q}) = \begin{bmatrix} \theta_1 + 2\theta_2 s_2 + 2c_3\theta_3 + 2\theta_4 s_{23} & \theta_2 s_2 + 2\theta_3 c_3 + \theta_4 s_{23} + \theta_5 & \theta_3 c_3 + \theta_4 s_{23} + \theta_6 \\ \theta_2 s_2 + 2\theta_3 c_3 + \theta_4 s_{23} + \theta_5 & 2\theta_3 c_3 + \theta_5 & \theta_3 c_3 + \theta_6 \\ \theta_3 c_3 + \theta_4 s_{23} + \theta_6 & \theta_3 c_3 + \theta_6 & \theta_6 \end{bmatrix},$$

$$\boldsymbol{C}(\dot{\boldsymbol{q}}, \boldsymbol{q}) = \begin{bmatrix} \theta_2 c_2 \dot{q}2 - \theta_3 s_3 \dot{q}3 + \theta_4 c_{23} \dot{q}23 & \theta_2 c_2 \dot{q}12 - \theta_3 s_3 \dot{q}3 + \theta_4 c_{23} \dot{q}123 & -\theta_3 s_3 \dot{q}123 + \theta_4 c_{23} \dot{q}123 \\ -\theta_2 c_2 \dot{q}1 - \theta_3 s_3 \dot{q}3 - \theta_4 c_{23} \dot{q}1 & -\theta_3 s_3 \dot{q}3 & -\theta_3 s_3 \dot{q}123 \\ \theta_3 s_3 \dot{q}12 - \theta_4 c_{23} \dot{q}1 & \theta_3 s_3 \dot{q}12 & 0 \end{bmatrix},$$

$$\boldsymbol{G}(\boldsymbol{q}) = \begin{bmatrix} \theta_7 c_1 + \theta_8 s_{12} + \theta_9 s_{123} \\ \theta_8 s_{12} + \theta_9 s_{123} \\ \theta_9 s_{123} \end{bmatrix},$$

where $s_2 = \sin(q_2)$, $s_3 = \sin(q_3)$, $s_{12} = \sin(q_1+q_2)$, $s_{23} = \sin(q_2+q_3)$, $s_{123} = \sin(q_1+q_2+q_3)$, $c_1 = \cos(q_1)$, $c_2 = \cos(q_2)$, $c_3 = \cos(q_3)$, $c_{23} = \cos(q_2 + q_3)$, $\dot{q}_{12} = \dot{q}_1 + \dot{q}_2$, $\dot{q}_{23} = \dot{q}_2 + \dot{q}_3$, and $\dot{q}_{123} = \dot{q}_1 + \dot{q}_2 + \dot{q}_3$. The parameters are $\theta_1 = 6.3922\,\text{kg m}^2$, $\theta_2 = 1.4338\,\text{kg m}^2$, $\theta_3 = 0.0706\,\text{kg m}^2$, $\theta_4 = 0.0653\,\text{kg m}^2$, $\theta_5 = 2.4552\,\text{kg m}^2$, $\theta_6 = 0.2868\,\text{kg m}^2$, $\theta_7 = 113.6538\,\text{N m}$, $\theta_8 = 46.1168\,\text{N m}$, $\theta_9 = 2.0993\,\text{N m}$.

Remark 5.1. The properties in Chapter 2 for the CRS-A465 robot manipulator holds (Kelly et al., 2005; Spong et al., 2020). Q.E.D

5.2 Experiments - MREM based Nonlinear Adaptive $\mathcal{H}_\infty$

In this numerical experiment, the robot manipulator started at the initial condition $\boldsymbol{q}(0) = [0\ 0\ 90]'(\text{deg})$ and $\dot{\boldsymbol{q}}(0) = \mathbf{0}$, with $\hat{\boldsymbol{\theta}}(0) = \mathbf{0}$. The system was requested to track the desired non PE trajectory $\boldsymbol{q}_r(t) = [90\ \ -90\ 0](\text{deg})$, with $\dot{\boldsymbol{q}}_r(t) = \ddot{\boldsymbol{q}}_r(t) = \mathbf{0}$. The filter parameters in (3.14) are set as $a = 0.22$ and $b = 0.05$. The nonlinear adaptive $\mathcal{H}_\infty$ controller based on the DREM technique, using the gradient estimator developed in Chapter 3, is evaluated in two scenarions. In the first scenario, the conditions (3.68) are satisfied, allowing for both exact parameter estimation and trajectory tracking. In the second scenario, these conditions are not met, which allow only to guarantee the boundedness of the parameter estimation errors. Besides, trajectory tracking could still be satisfactorily achieved.

5.2.1 Case 1: Determinant Condition Satisfaction

The nonlinear adaptive $\mathcal{H}_\infty$ controller was implemented considering (3.63) along with (3.64), and synthesized with the tuning parameters $\boldsymbol{Q} = \boldsymbol{I}$, $\boldsymbol{R} = (0.8)\boldsymbol{I}$, $\rho = 0.9$, with the estimator gain $\boldsymbol{\Gamma} = 5\boldsymbol{I}$. The results of the numerical experiment are presented in Figures 5.2-5.5. Considering this tuning parameters, as mentioned before, condition (3.68) is satisfied during a sufficient long time interval, ensuring exact parameter estimation as shown in Figure 5.6.

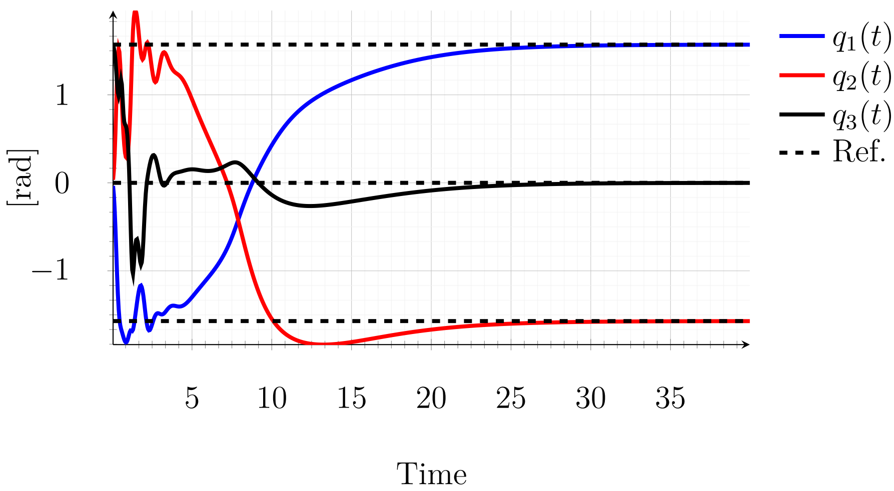

Figure 5.2: Case 1: MREM Nonlinear Adaptive $\mathcal{H}_\infty$ - Generalized coordinates.

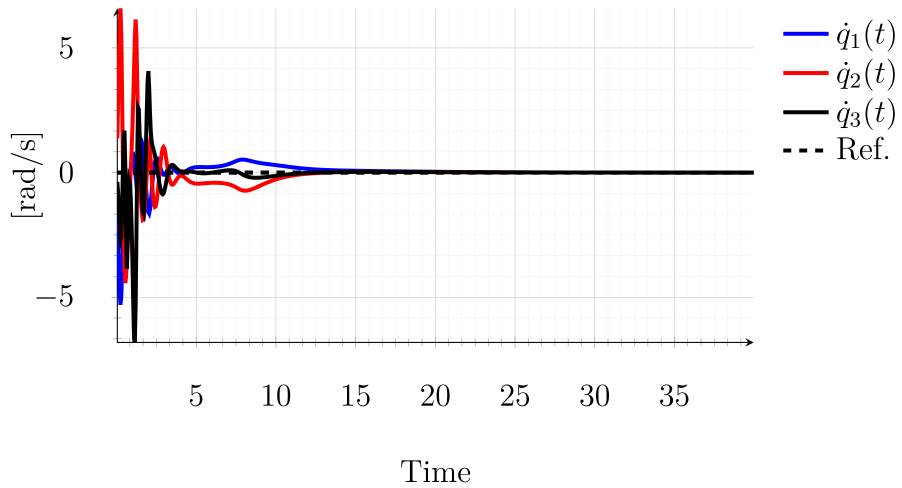

Figure 5.3: Case 1: MREM Nonlinear Adaptive $\mathcal{H}_\infty$ - Generalized velocities.

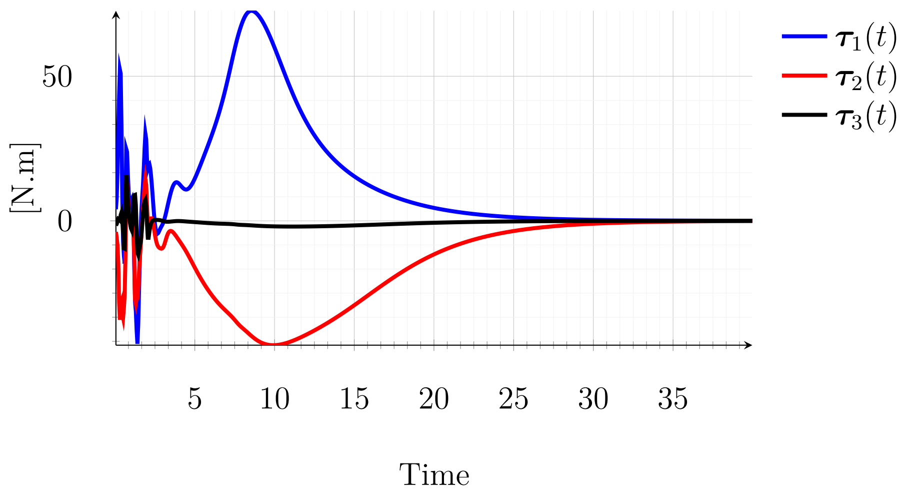

Figure 5.4: Case 1: MREM Nonlinear Adaptive $\mathcal{H}_\infty$ - Control inputs.

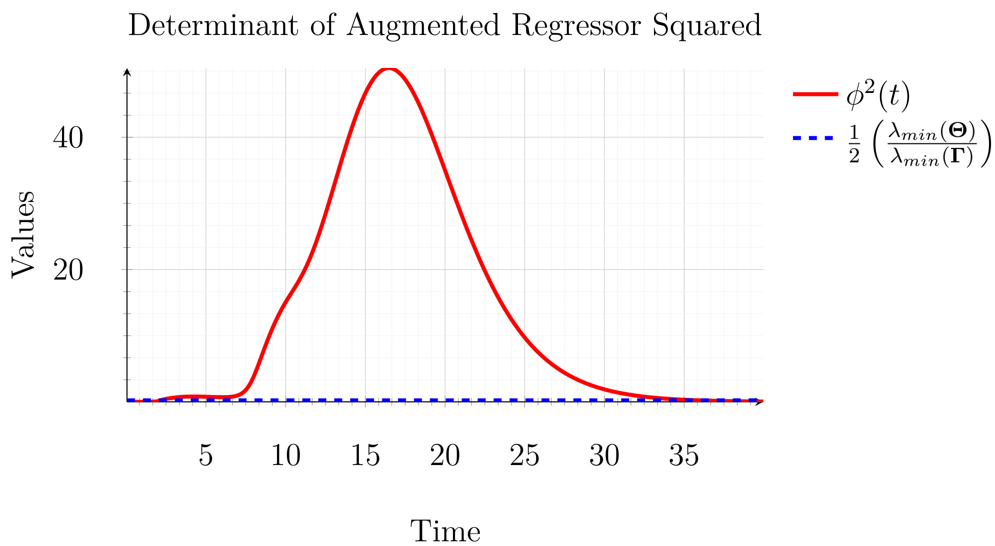

Figure 5.5: Case 1: MREM Nonlinear Adaptive $\mathcal{H}_\infty$ - Determinant condition.

In Figure 5.6, we present the results of the parameter estimation process under conditions that allow for exact parameter estimation even when the PE condition is not satisfied. The following graphs illustrate the performance of the adaptive controller using the DREM technique with a gradient estimator.

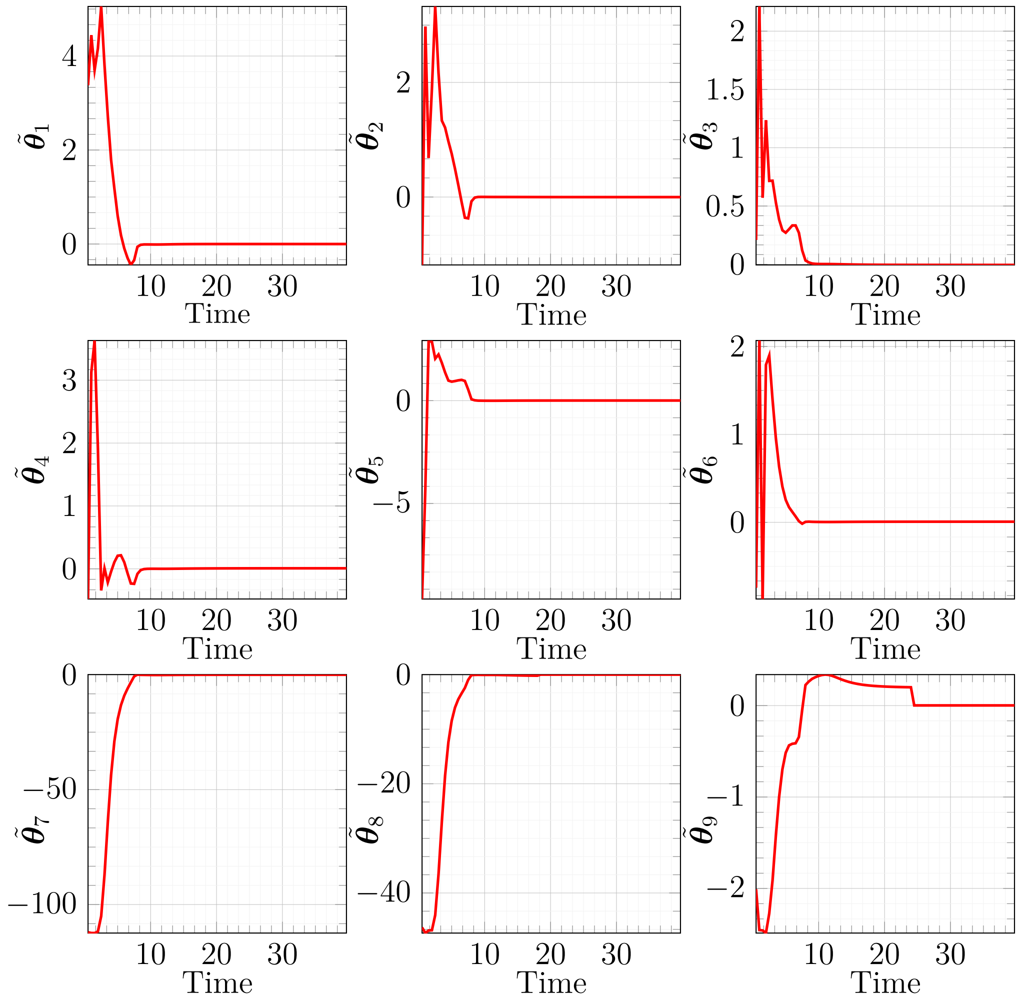

Figure 5.6: Case 1: MREM Nonlinear Adaptive $\mathcal{H}_\infty$ - Parameter estimation.

It is worth highlighting that the system successfully tracks the desired trajectory while concurrently achieving parameter estimation. This confirms the effectiveness of the control strategy in environments where the specified conditions for exact parameter estimation are met. The graphs in Figure 5.6 provide a clear visualization of how the estimated parameters converge to their true values over time.

5.2.2 Case 2: Determinant Condition Violation

The nonlinear adaptive $\mathcal{H}_\infty$ controller was implemented considering (3.64) along with (3.63), and synthesized with the tuning parameters $\boldsymbol{Q} = 0.9\boldsymbol{I}$, $\boldsymbol{R} = (0.01)\boldsymbol{I}$, $\rho = 0.2$, with the estimator gain $\boldsymbol{\Gamma} = 5\boldsymbol{I}$. The results of the numerical experiment are presented in Figures 5.7-5.10. In this scenario, the condition (3.68) is violated resulting in a non-exact parameter estimation. Nevertheless, trajectory tracking could still be ensured, as seen in Figure 5.7.

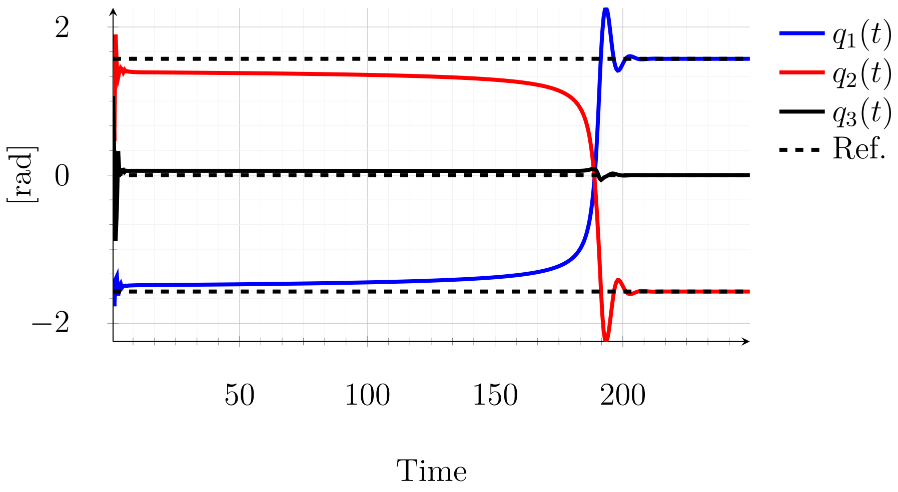

Figure 5.7: Case 2: MREM Nonlinear Adaptive $\mathcal{H}_\infty$ - Generalized coordinates.

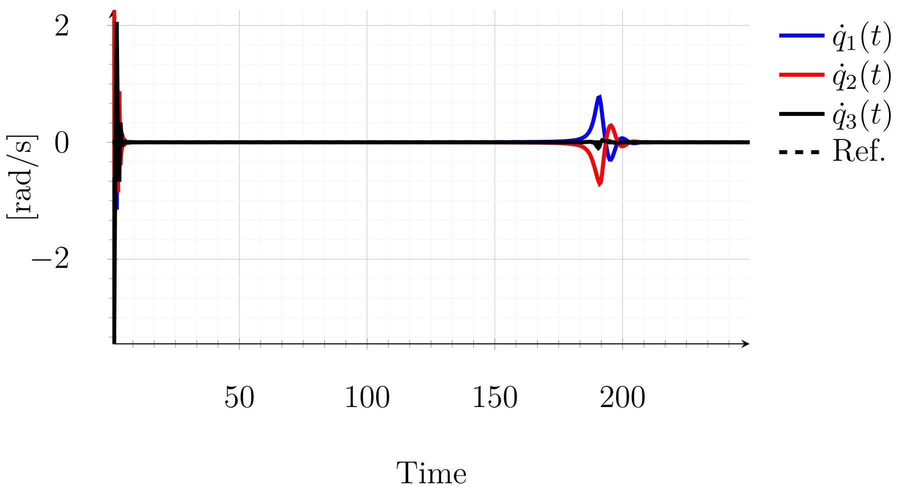

Figure 5.8: Case 2: MREM Nonlinear Adaptive $\mathcal{H}_\infty$ - Generalized velocities.

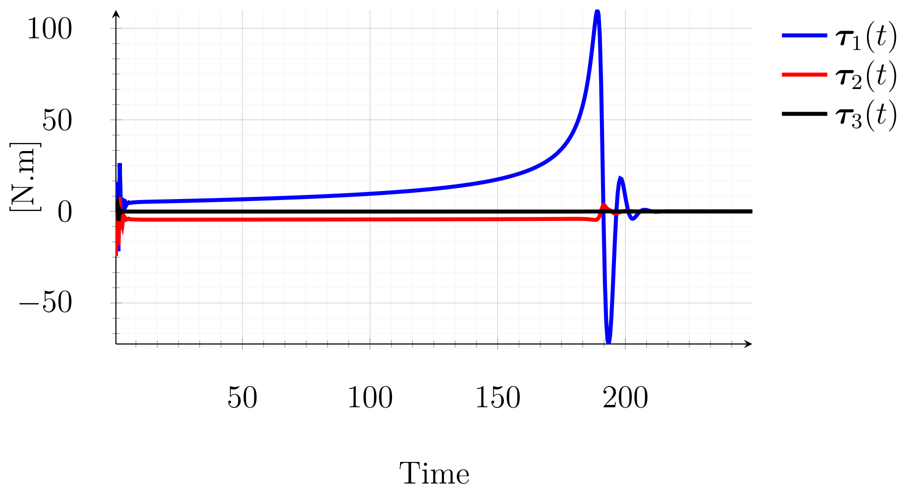

Figure 5.9: Case 2: MREM Nonlinear Adaptive $\mathcal{H}_\infty$ - Control inputs.

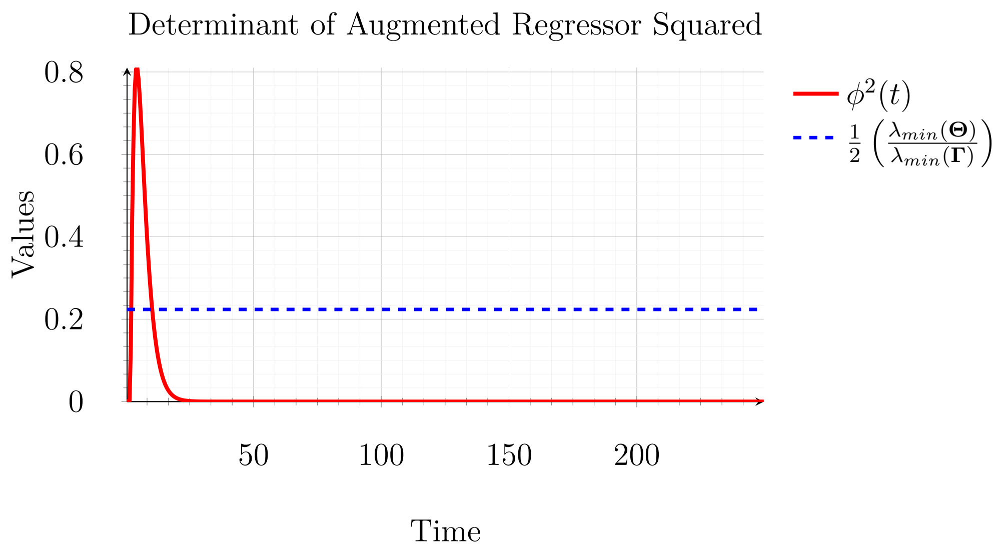

Figure 5.10: Case 2: MREM Nonlinear Adaptive $\mathcal{H}_\infty$ - Determinant condition.

In Figure 5.11, we present the results of the parameter estimation process when the conditions (3.68) do not hold. In this case, the estimation error remains bounded and the following graph illustrates the performance of the adaptive controller using the DREM technique with a gradient estimator.

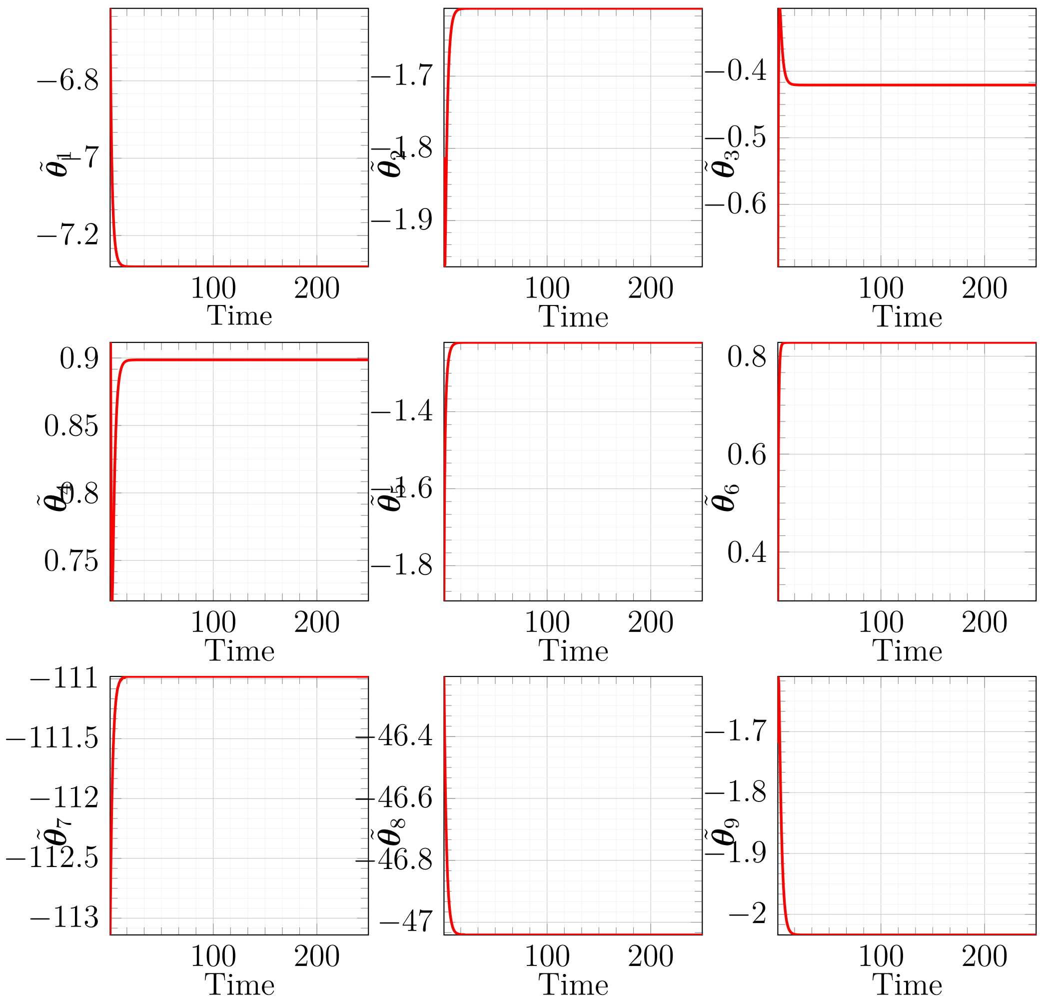

Figure 5.11: Case 2: MREM Finite-Time Nonlinear Adaptive $\mathcal{H}_\infty$ - Parameter Estimation.

5.3 Experiments - MREM based Finite-Time Nonlinear Adaptive $\mathcal{H}_\infty$

In this numerical experiment, the robot manipulator started at the initial condition $\boldsymbol{q}(0) = [0\ 0\ 90]'(\text{deg})$ and $\dot{\boldsymbol{q}}(0) = \mathbf{0}$, with $\hat{\boldsymbol{\theta}}(0) = \mathbf{0}$. The system was requested to track the desired non PE trajectory $\boldsymbol{q}_r(t) = [90\ \ -90\ 0](\text{deg})$, with $\dot{\boldsymbol{q}}_r(t) = \ddot{\boldsymbol{q}}_r(t) = \mathbf{0}$. The filter parameters in (3.14) are given by $a = 0.22$ and $b = 0.05$. The nonlinear adaptive $\mathcal{H}_\infty$ controller, based on the DREM technique using the finite-time estimator, is evaluated in two scenarions. In the first scenario, the conditions specified by (3.108) are satisfied, allowing for both exact parameter estimation and trajectory tracking. In the second scenario, these conditions are violated. Therefore, we can only guarantee the boundedness of the parameter estimation errors, while trajectory tracking is ensured.

5.3.1 Case 1: Determinant Condition Satisfaction

The nonlinear adaptive $\mathcal{H}_\infty$ controller was implemented considering (3.102) along with (3.101), and synthesized with the tuning parameters $\boldsymbol{Q} = \boldsymbol{I}$, $\boldsymbol{R} = (0.8)\boldsymbol{I}$, $\rho = 0.9$, with the estimator gain $\boldsymbol{\Gamma} = 5\boldsymbol{I}$. The results of the numerical experiment are presented in Figs. 5.12-5.15. Considering this tuning is possible to ensure that condition (3.108) is satisfied during a sufficient long time interval, ensuring exact parameter estimation.

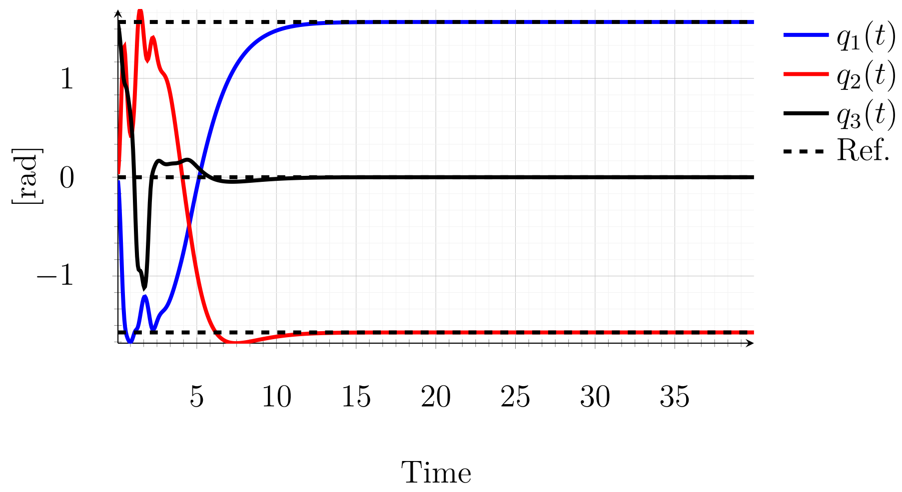

Figure 5.12: Case 1: MREM Finite-Time Nonlinear Adaptive $\mathcal{H}_\infty$ - Generalized coordinates.

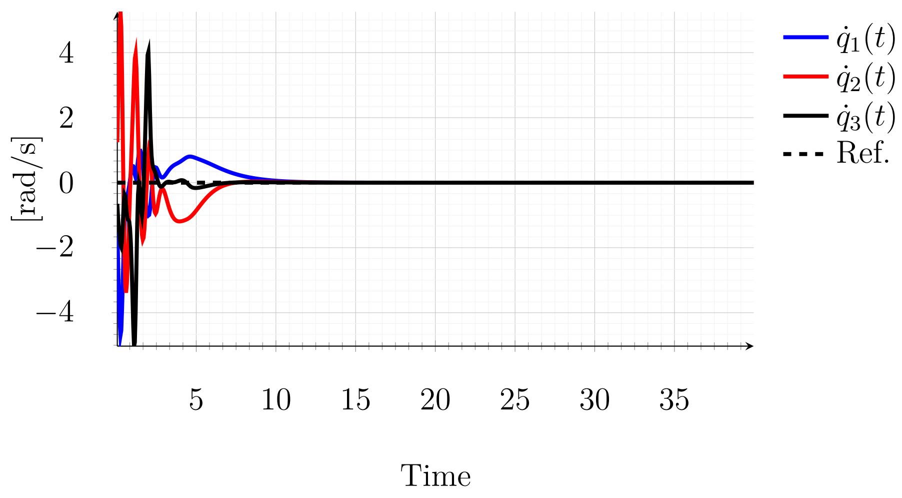

Figure 5.13: Case 1: MREM Finite-Time Nonlinear Adaptive $\mathcal{H}_\infty$ - Generalized velocities.

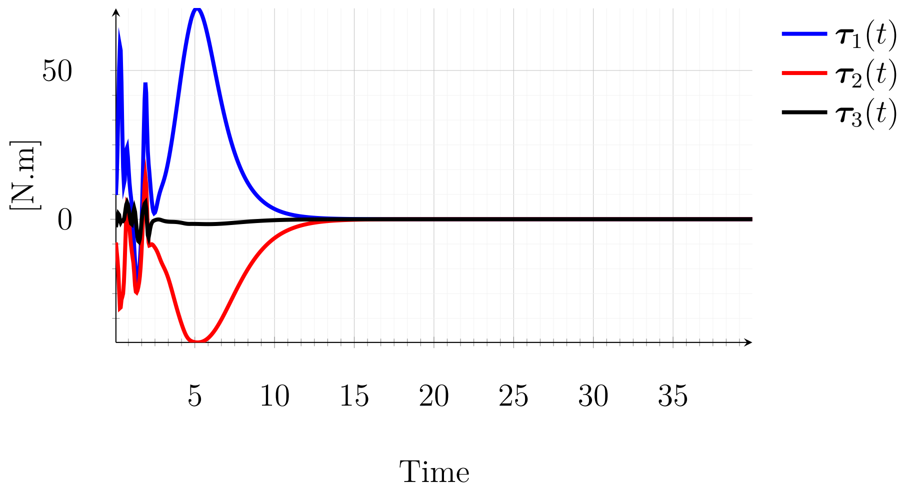

Figure 5.14: Case 1: MREM Finite-Time Nonlinear Adaptive $\mathcal{H}_\infty$ - Control inputs.

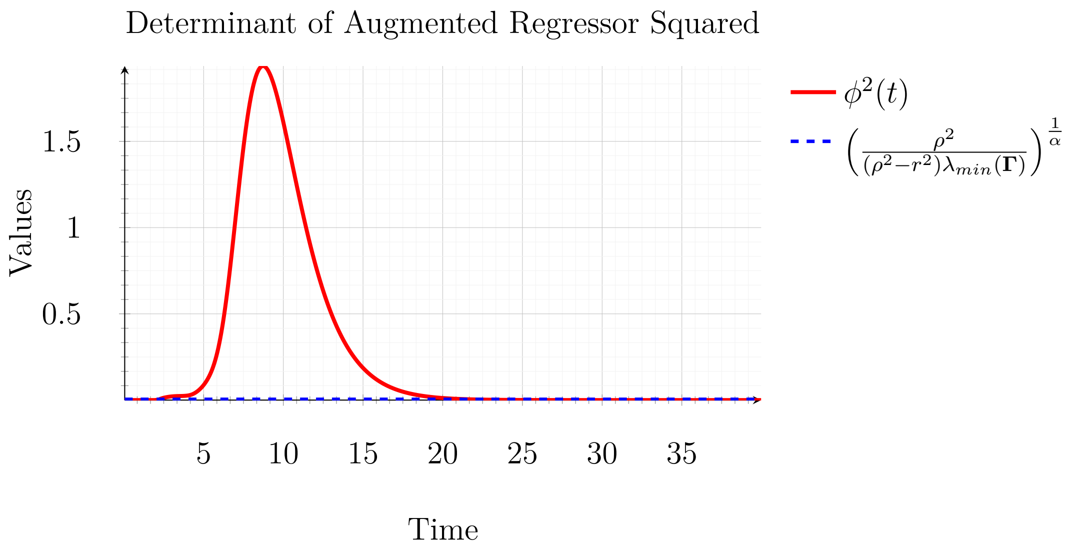

Figure 5.15: Case 1: MREM Finite-time Nonlinear Adaptive $\mathcal{H}_\infty$ - Determinant condition.

In Figure 5.16, we present the results of the parameter estimation process under conditions that allow for exact parameter estimation. The following graphs illustrate the performance of the adaptive controller using the DREM technique with a gradient estimator.

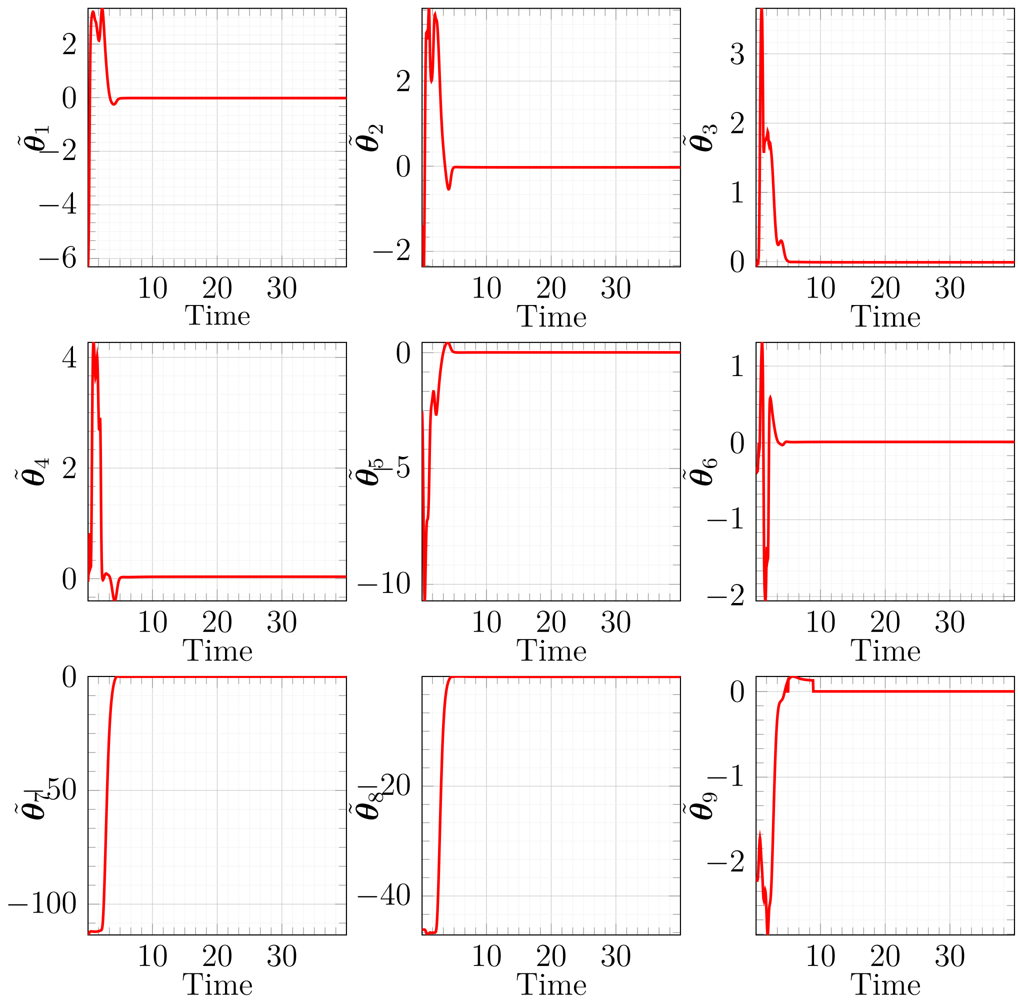

Figure 5.16: Case 1: MREM Finite-Time Nonlinear Adaptive $\mathcal{H}_\infty$ - Parameter estimation.

It is worth noting that the system successfully tracks the desired trajectory while concurrently achieving parameter estimation. This confirms the effectiveness of the control strategy in environments where the specified conditions for exact parameter estimation are satisfied.

5.3.2 Case 2: Determinant Condition Violation

The nonlinear adaptive $\mathcal{H}_\infty$ controller was implemented considering (3.102) along with (3.101), and synthesized with the tuning parameters $\boldsymbol{Q} = 0.9\boldsymbol{I}$, $\boldsymbol{R} = (0.8)\boldsymbol{I}$, $\rho = 0.9$, with the estimator gain $\Gamma = 5\boldsymbol{I}$. The filter parameter in (3.14) are given by $a = 0.34$ and $b = 0.07$. The results of the numerical experiment are presented in Figures 5.17-5.20. Considering this tuning, condition (3.108) does not hold and exact parameter estimation is not achieved. Nevertheless, trajectory tracking could still be ensured, as seen in Figure 5.17.

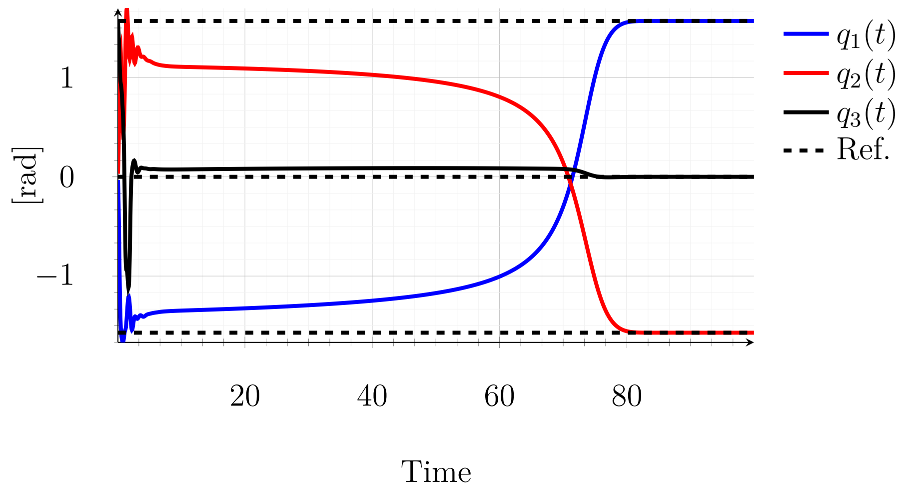

Figure 5.17: Case 2: MREM Finite-Time Nonlinear Adaptive $\mathcal{H}_\infty$ - Generalized coordinates.

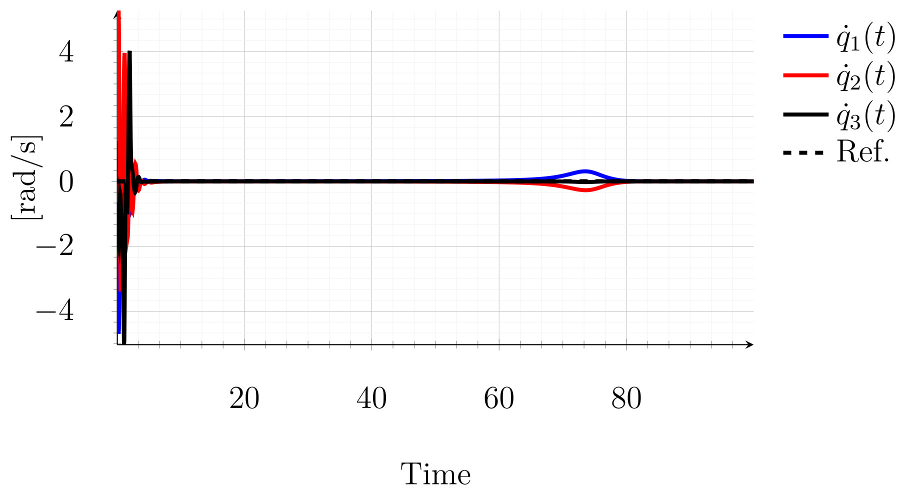

Figure 5.18: Case 2: MREM Finite-Time Nonlinear Adaptive $\mathcal{H}_\infty$ - Generalized velocities.

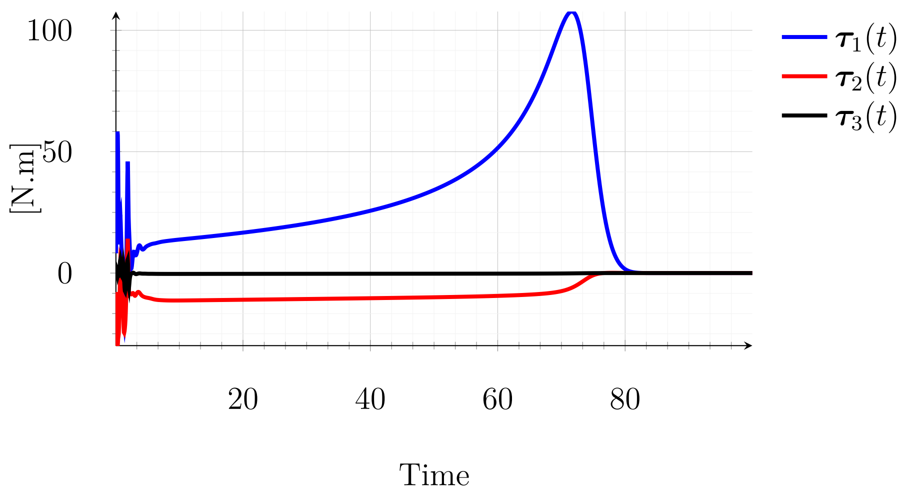

Figure 5.19: Case 2: MREM Finite-Time Nonlinear Adaptive $\mathcal{H}_\infty$ - Control inputs.

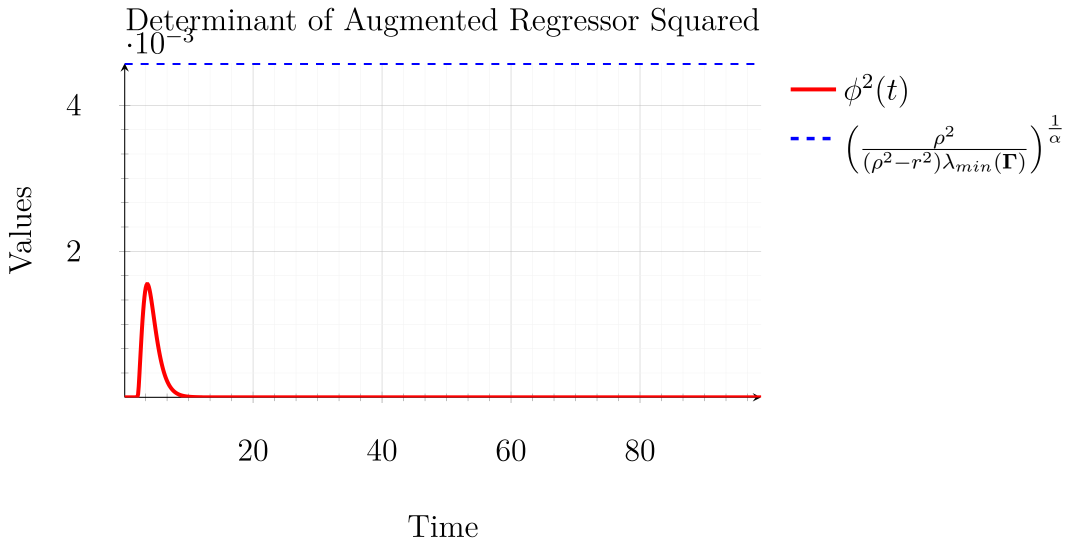

Figure 5.20: Case 2: MREM Finite-time Nonlinear Adaptive $\mathcal{H}_\infty$ - Determinant condition.

In Figure 5.21, we present the results of the parameter estimation process when the conditions (3.108) are violated.

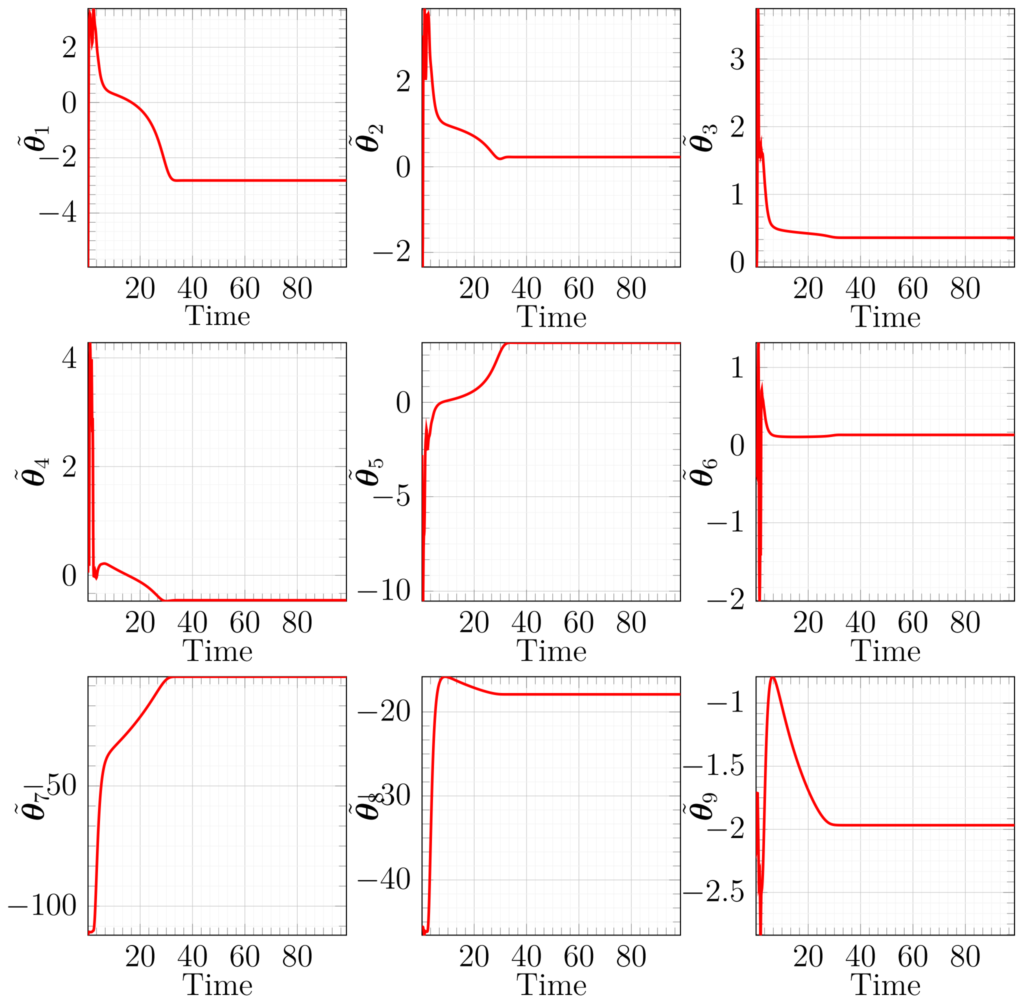

Figure 5.21: Case 2: MREM Finite-Time Nonlinear Adaptive $\mathcal{H}_\infty$ - Parameter estimation.

In this case, the system successfully tracks the desired trajectory while maintaining the estimation error bounded.

5.4 Experiments - MREM based Nonlinear Adaptive $\mathcal{W}_\infty$

In this numerical experiment, the robot manipulator started at the initial conditions $\boldsymbol{q}(0) = [0\ 0\ 90]'(\text{deg})$ and $\dot{\boldsymbol{q}}(0) = \mathbf{0}$, with $\hat{\boldsymbol{\theta}}(0) = \mathbf{0}$. The system was requested to track the desired non PE trajectory $\boldsymbol{q}_r(t) = [90\ \ -90\ 0](\text{deg})$, with $\dot{\boldsymbol{q}}_r(t) = \ddot{\boldsymbol{q}}_r(t) = \mathbf{0}$. The filter parameters in (3.14) are given by $a = 1000$ and $b = 0.195$. The nonlinear adaptive $\mathcal{W}_\infty$ controller based on the DREM technique using the gradient estimator, was implemented considering (4.35) along with (4.24), and synthesized with the tuning parameters $\boldsymbol{\Psi}_0 = \boldsymbol{I}$, $\boldsymbol{\Psi}_1 = 10\boldsymbol{I}$, $\boldsymbol{\Psi}_2 = \boldsymbol{I}$, and the estimator gain $\boldsymbol{\Gamma} = 0.05\boldsymbol{I}$. The results of the numerical experiment are presented in Figures 5.22-5.25.

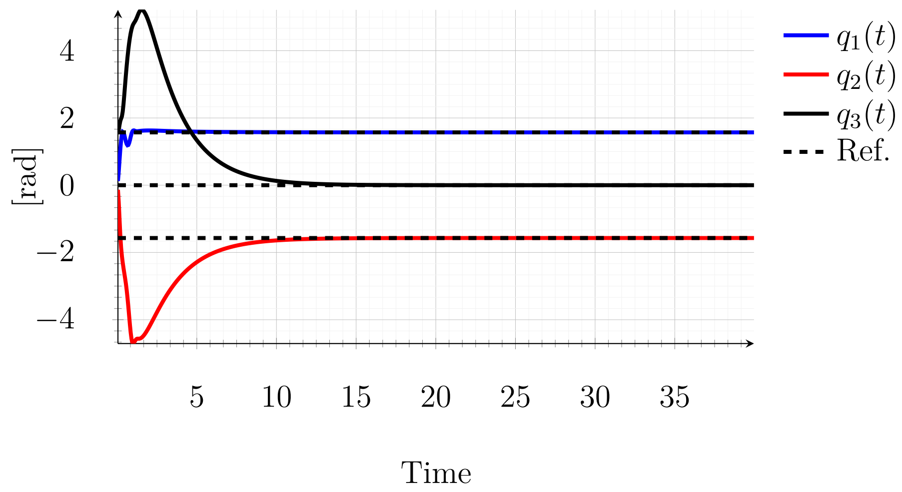

Figure 5.22: MREM Nonlinear Adaptive $\mathcal{W}_\infty$ - Generalized coordinates.

In Figure 5.22, it is worth highlighting the transient response improvement reached by the proposed controller. In addition, Figure 5.24 shows that the DREM based adaptive nonlinear $\mathcal{W}_\infty$ controller achieved the desired positions with bounded control inputs.

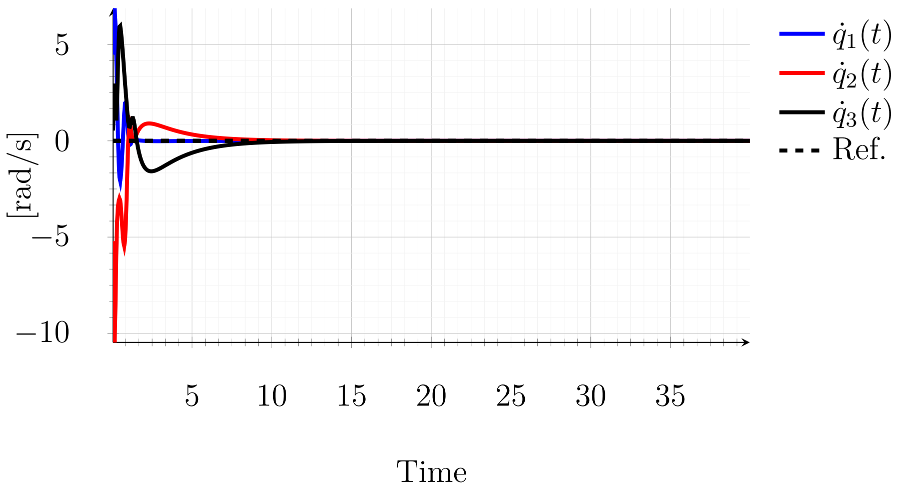

Figure 5.23: MREM Nonlinear Adaptive $\mathcal{W}_\infty$ - Generalized velocities.

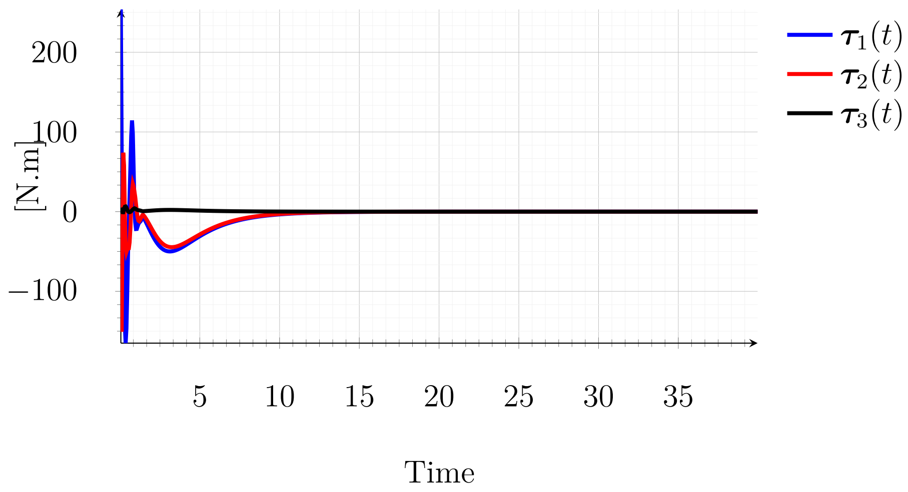

Figure 5.24: MREM Nonlinear Adaptive $\mathcal{W}_\infty$ - Control inputs.

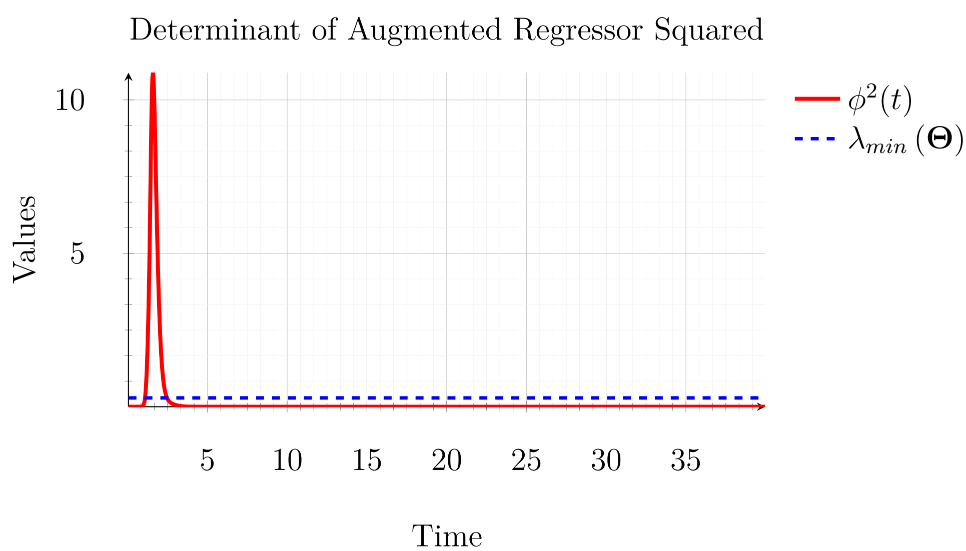

Figure 5.25: MREM Nonlinear Adaptive $\mathcal{W}_\infty$ - Determinant condition.

In Figure 5.27, we present the results of the parameter estimation process. In this case, since we can only ensure ultimate bound (see Figure 5.26), the estimation error remains bounded. Accordingly, the system successfully tracks the desired trajectory with minimum error, improved transient response, and maintaining the estimation error bounded.

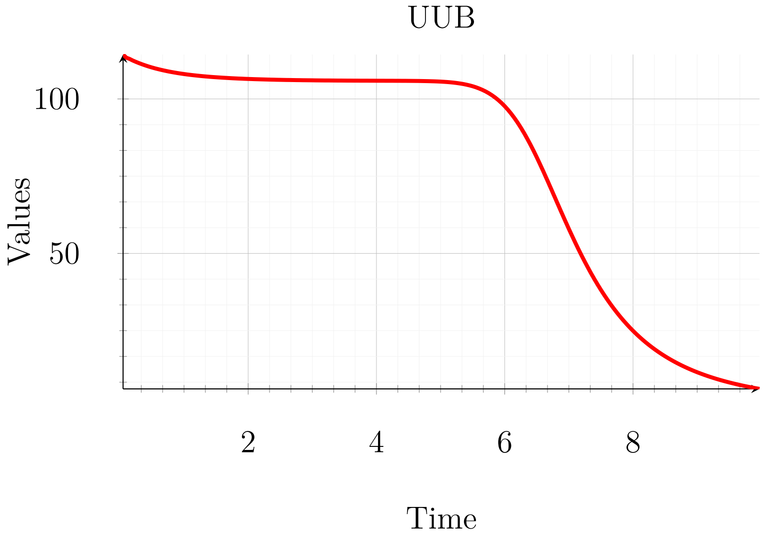

Figure 5.26: MREM Nonlinear Adaptive $\mathcal{W}_\infty$ - UUB.

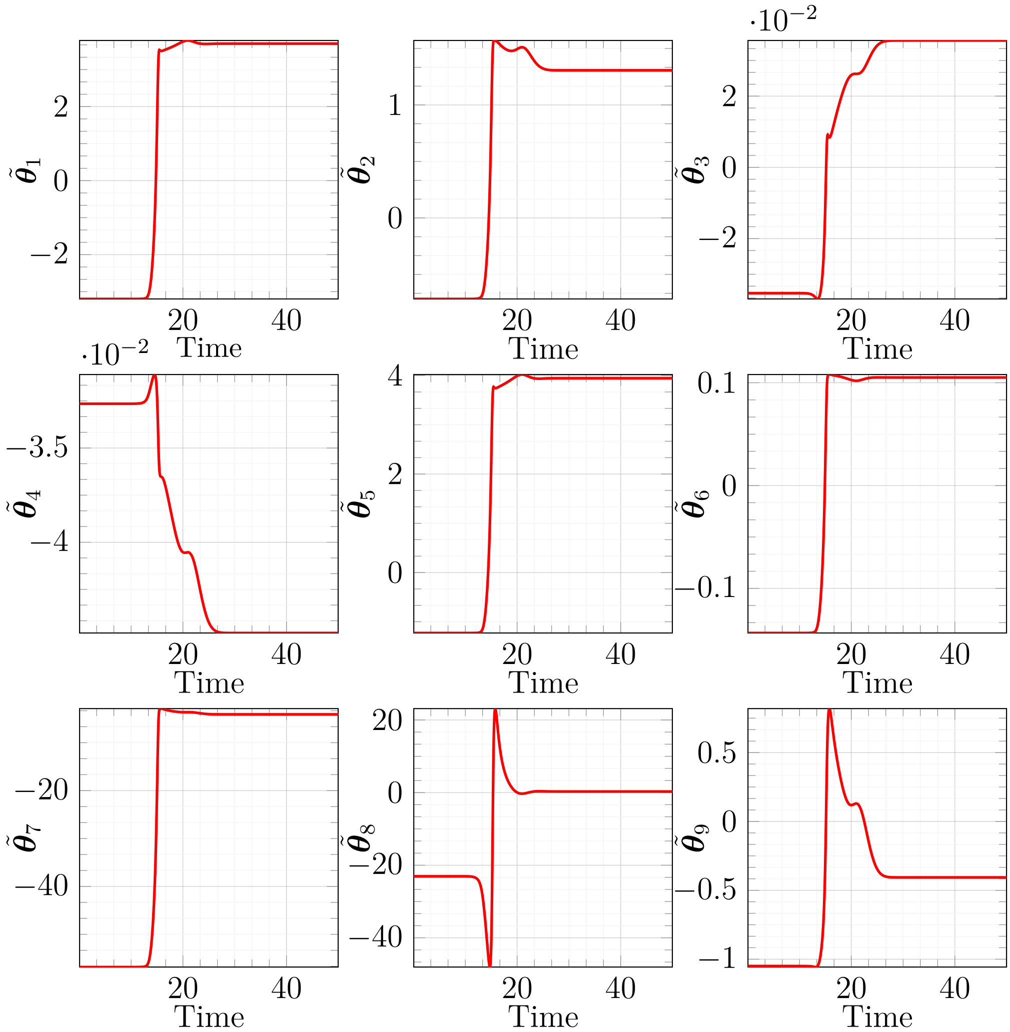

Figure 5.27: MREM Nonlinear Adaptive $\mathcal{W}_\infty$ - Parameter estimation.

5.5 Final Remarks

In this chapter, we have corroborated the efficacy of the adaptive $\mathcal{H}_\infty$ controller using the DREM gradient estimator in both scenarios: when the conditions for exact parameter estimation are satisfied and when they are not. The results indicated that under the ideal conditions, the controller achieved precise parameter estimation while maintaining accurate trajectory tracking. When the conditions are violated, this controller still ensures trajectory tracking, with the parameter estimation error remaining bounded. Similarly, the adaptive $\mathcal{H}_\infty$ controller using the finite-time DREM estimator also showed good performance. In scenarios where the conditions for exact parameter estimation were satisfied, the controller effectively converged to the true parameter values while ensuring trajectory tracking. In cases where these conditions were violated, the controller achieved trajectory tracking with bounded parameter estimation errors. Additionally, the results obtained for the adaptive $\mathcal{W}_\infty$ controller corroborated the presented theoretical developments, providing improved transient response.

6

Conclusions

This chapter summarizes the main contributions obtained in this thesis, and concludes the text. Future work proposals are also presented and detailed at the end of this chapter.

6.1 Discussion

One of the main challenges in modern control applications is managing systems with uncertainties. Control design is usually based on mathematical models, which cannot fully capture the complexities of real-world phenomena. Mathematical models are often approximations that introduce unmodeled dynamics and parameter uncertainties. In addition, real systems are frequently subjected to external disturbances, further complicating the problem of designing controllers that can maintain performance under uncertain condition. Robust and adaptive control approaches have emerged as promising solutions. Robust control is designed to maintain performance despite model uncertainties and external disturbances, providing a high level of reliability and stability. However, robust controllers can be overly conservative, since they are designed to handle worst-case scenarios. On the other hand, adaptive control adjusts its parameters online in response to changes in system dynamics and external conditions. This adaptability allows for improved performance and efficiency as the controller continuously optimizes its behavior. However, adaptive control can struggle with stability and convergence issues, particularly in the presence of significant uncertainties and rapid changes in system dynamics. This work proposed the integration of the advantages of both robust and adaptive control approaches by designing optimal nonlinear adaptive controllers based on the $\mathcal{H}_\infty$ and $\mathcal{W}_\infty$ control. These controllers can offer enhanced stability, performance, and resilience, making them an ideal choice for complex, real-world systems.

In Chapter 2 fundamental concepts for the development of this thesis were introduced. It begins with the Euler-Lagrange systems and its properties relevant to control theory. Additionally, it was presented the nonlinear $\mathcal{W}_2$ and $\mathcal{W}_\infty$ control strategies, highlighting their benefit of enhancing the transient performance of the $\mathcal{H}_2$ and $\mathcal{H}_\infty$ controllers. The concept of persistency of excitation condition was explained, and finally, the chapter detailed the Dynamic Regressor Extension and Mixing (DREM) technique, which is responsible to achieve exact parameter estimation by satisfying the DREM condition, a less stringent condition than the PE one.

Regarding nonlinear robust adaptive controllers, Chapter 3 outlined a method for transforming matrix regressors into vector regressors using the Euler-Lagrange first integral, allowing the direct use of DREM-based techniques. Additionally, the Memory Regressor Extension (MRE) technique was discussed, which is a commonly used approach in adaptive control for extending dynamics while maintaining excitation. This method, based on the often overlooked work of Kreisselmeier (1977), offers an alternative to the DREM technique, which can be limited by poor filter choices that may hinder convergence even when the original regressor is PE. Building upon foundational research by Chen et al. (1997), which initially proposed the adaptive $\mathcal{H}_\infty$ control without exact parameter estimation, we integrated advancements from Aranovskiy et al. (2017). These improvements enable us to obtain precise parameter estimation, state tracking, and incorporate modifications for finite-time estimation. Two estimation laws were presented: the classic DREM gradient estimator and a modified version designed to ensure finite-time estimation. The proposed $\mathcal{H}_\infty$ controllers were modified accordingly, with stability proofs grounded in Lyapunov theory.

Aiming at improved transient response, in Chapter 4, the nonlinear adaptive $\mathcal{W}_\infty$ controller was proposed based on the DREM technique. The controller was analysed using Lyapunov stability theory, ensuring uniform ultimate boundedness.

In Chapter 5, numerical results were presented to corroborate the efficacy of the proposed adaptive nonlinear $\mathcal{H}_\infty$ and $\mathcal{W}_\infty$ control strategies. The numerical experiment were conducted considering a simplified version of the CRS-A465 robot model. The $\mathcal{H}_\infty$ controllers were tested for the cases when the conditions (3.68) and (3.108) hold and when they do not. In the first case both controller achieved trajectory tracking and exact parameter estimation. For the second case, as expected, only trajecoty tracking is attained. During the experiments it was also clear that the adaptive nonlinear $\mathcal{W}_\infty$ presented overall better transient performance, corroborating the developed theory.

6.2 Contributions

The main contribution of this master thesis are:

- **Proposition of a Method to Transform Matrix Regressors into Vector Regressors Based on the Euler-Lagrange First Integral:**

  (i) This method generalizes the approach, allowing the use of Dynamic Regressor Extension and Mixing (DREM) techniques in a broader range of applications.

  (ii) The transformation leverages the properties of the Euler-Lagrange first integral, ensuring that the regressor transformation maintains the essential dynamics of the original system.

- **Proposition of the Adaptive Nonlinear $\mathcal{H}_\infty$ Controller Based on the DREM Technique:**

  (i) The adaptive nonlinear $\mathcal{H}_\infty$ controller ensures exact parameter estimation under less stringent conditions than the Persistent Excitation (PE) requirement.

  (ii) This controller is designed as a robust adaptive controller, capable of maintaining performance and stability in the presence of system uncertainties and external disturbances.

- **Proposition of the Adaptive Nonlinear $\mathcal{W}_\infty$ Controller Based on the DREM Technique:**

  (i) The adaptive nonlinear $\mathcal{W}_\infty$ controller guarantees uniform ultimate boundedness (UUB) with a computable ultimate bound, providing a clear measure of the system's performance.

  (ii) The controller enhances the transient response of the system, leading to less oscilations.

6.3 Future Works

Some future work guidelines are:

- **Handling Noise in Linear Regression Equations:**

  (i) Develop and implement robust techniques to mitigate the effects of noise in linear regression models.

  (ii) Explore advanced filtering and noise reduction methods to enhance the accuracy of parameter estimation.

   (iii) Conduct simulations and experiments to validate the effectiveness of these noise handling techniques in real-world scenarios.

- **Development of Strategies for the Underactuated Case:**
   (i) Extend the current models and control strategies to address the challenges posed by underactuated systems.
   (ii) Validate the proposed strategies through theoretical analysis and practical implementations on prototype systems.

- **Controllers with Finite-Time Parameter Estimation and Tracking:**
   (i) Investigate the design and implementation of finite time controllers that can achieve both accurate parameter estimation and trajectory tracking within a finite time horizon.
   (ii) Analyze the theoretical foundations and stability properties of these controllers.
   (iii) Perform simulation studies and experimental validations to demonstrate the practical applicability of the proposed controllers.

- **Improvement of DREM Estimators:**
   (i) Enhance the existing Dynamic Regressor Extension and Mixing (DREM) estimators to increase the minimal amount of excitation necessary for exact parameter estimation in finite-time, similar to Arteaga (2024).
   (ii) Develop methods to ensure that the required level of excitation is maintained throughout the estimation process.
   (iii) Test and validate the improved DREM estimators through simulations and real-time experiments to ensure their reliability and robustness.

- **Relax the Nonlinear Adaptive $\mathcal{W}_\infty$ Controller Assumptions:**
   (i) Remove the requirement on the assumptions regarding bounds of the Euler-Lagrange matrices.
   (ii) Evaluate how restrictive it is the assumption that the norm of the uncertainty is bounded by a continuos scalar function and propose alternatives to it.

Bibliography

R. A. Adams and J. J. Fournier. *Sobolev Spaces (Pure and Applied Mathematics; V. 140)*. Elsevier, 2003.

L. T. Aguilar, Y. Orlov, and L. Acho. Nonlinear $\mathcal{H}_\infty$-control of nonsmooth time-varying systems with application to friction mechanical manipulators. *Automatica*, 39(9):1531–1542, 2003.

A. Alessandri and M. Sanguineti. Input-output stability for optimal estimation problems. In *Int'l Math. Forum*, volume 2, pages 593–617, 2007.

M. Aliyu and E. K. Boukas. Extending nonlinear $\mathcal{H}_2$, $\mathcal{H}_\infty$ optimisation to $\mathcal{W}_{1,2}$, $\mathcal{W}_{1,\infty}$ spaces - part I: optimal control. *International Journal of Systems Science*, 42(5):889–906, 2011a.

M. Aliyu and E. K. Boukas. Extending nonlinear $\mathcal{H}_2$, $\mathcal{H}_\infty$ optimisation to $\mathcal{W}_2$ and $\mathcal{W}_\infty$ spaces-part II: optimal estimation and ouput-feedback control. *International Journal of Systems Science*, 42(5):907–920, 2011b.

A. M. Annaswamy, A. Guha, Y. Cui, S. Tang, P. A. Fisher, and J. E. Gaudio. Integration of adaptive control and reinforcement learning for real-time control and learning. *IEEE Transactions on Automatic Control*, 68(12):7740–7755, 2023.

S. Aranovskiy, A. Bobtsov, R. Ortega, and A. Pyrkin. Performance enhancement of parameter estimators via dynamic regressor extension and mixing. *IEEE Transactions on Automatic Control*, 62(7):3546–3550, 2017.

S. Aranovskiy, R. Ushirobira, M. Korotina, and A. Vedyakov. On preserving-excitation properties of a dynamic regressor extension scheme. *IEEE Transactions on Automatic Control*, 68(2):1296–1302, 2023.

M. A. Arteaga. On the exact parameter estimation for robot manipulators without persistence of excitation. *IEEE Transactions on Automatic Control*, 2023.

M. A. Arteaga. On the exact parameter estimation of robot manipulators with a predefined minimal amount of excitation. *International Journal of Robust and Nonlinear Control*, 2024.

A. M. Bersani and P. Caressa. Lagrangian descriptions of dissipative systems: a review. *Mathematics and Mechanics of Solids*, 26(6):785–803, 2021.

S. Boyd and S. Sastry. On parameter convergence in adaptive control. *Systems & control letters*, 3(6):311–319, 1983.

S. Boyd and S. S. Sastry. Necessary and sufficient conditions for parameter convergence in adaptive control. *Automatica*, 22(6):629–639, 1986.

J. M. Campos, D. N. Cardoso, and G. V. Raffo. A robust nonlinear flight control in the weighted sobolev space for a quadtiltrotor uav. In *International Conference Series on Climbing and Walking Robots and the Support Technologies for Mobile Machines, (CLAWAR)*, 2023a.

J. M. Campos, D. N. Cardoso, and G. V. Raffo. Adaptive nonlinear $\mathcal{W}_\infty$ control for fully actuated mechanical systems. In *Simposio Brasileiro de Automacao Inteligente, SBAI*, 2023b.

J. M. Campos, D. N. Cardoso, S. Esteban, and G. V. Raffo. Enhanced robust adaptive flight control for a convertible vtol uav. *Journal of the Franklin Institute*, 361(5):106663, 2024a.

J. M. Campos, D. N. Cardoso, and G. V. Raffo. A nonlinear adaptive $\mathcal{H}_\infty$ control with finite-time stability and exact parameter estimation. In *Conference on Decision and Control, CDC*, 2024b.

J. M. Campos, D. N. Cardoso, and G. V. Raffo. An adaptive nonlinear $\mathcal{H}_\infty$ control with exact parameter estimation for mechanical systems. In *European Control Conference, ECC*, 2024c.

C. Cao and N. Hovakimyan. Design and analysis of a novel $\mathcal{L}_1$ adaptive control architecture with guaranteed transient performance. *IEEE Transactions on Automatic Control*, 53 (2):586–591, 2008.

D. N. Cardoso, S. Esteban, and G. V. Raffo. A robust optimal control approach in the weighted sobolev space for underactuated mechanical systems. *Automatica*, 125:109474, 2021a.

D. N. Cardoso, S. Esteban, and G. V. Raffo. A robust nonlinear controller in the weighted sobolev space for trajectory tracking throughout the full flight envelope of a tilt-rotor UAV. *To be submitted*, pages 1–14, 2021b.

B. S. Chen, T. S. Lee, and J. H. Feng. A nonlinear $\mathcal{H}_\infty$ control design in robotic systems under parameter perturbation and external disturbance. *International Journal of Control*, 59(2):439–461, 1994a.

B.-S. Chen, T.-S. Lee, and J.-H. Feng. A nonlinear $\mathcal{H}_\infty$ control design in robotic systems under parameter perturbation and external disturbance. *International Journal of Control*, 59(2):439–461, 1994b.

B.-S. Chen, T.-S. Lee, and W.-S. Chang. A robust $\mathcal{H}_\infty$ model reference tracking design for non-holonomic mechanical control systems. *International Journal of Control*, 63(2): 283–306, 1996.

B.-S. Chen, Y.-C. Chang, and T.-C. Lee. Adaptive control in robotic systems with $\mathcal{H}_\infty$ tracking performance. *Automatica*, 33(2):227–234, 1997.

M. Chilali and P. Gahinet. $\mathcal{H}_\infty$ design with pole placement constraints: An LMI approach. *IEEE Transactions on Automatic Control*, 41(3):358–367, 1996.

A. Datta and P. A. Ioannou. Performance analysis and improvement in model reference adaptive control. *IEEE Transactions on Automatic Control*, 39(12):2370–2387, 1994.

J. G. De Jalon and E. Bayo. *Kinematic and dynamic simulation of multibody systems: the real-time challenge*. Springer Science & Business Media, 2012.

T. Dlotko. Sobolev spaces and embedding theorems. Technical report, Citeseer, 2014.

J. C. Doyle, K. Glover, P. P. Khargonekar, and B. A. Francis. State-space solutions to standard $\mathcal{H}_2$ and $\mathcal{H}_\infty$ control problems. *IEEE Transactions on Automatic Control*, 34 (8):831–847, 1989.

J. C. Doyle, B. A. Francis, and A. R. Tannenbaum. *Feedback control theory*. Courier Corporation, 2013.

M. A. Duarte and K. S. Narendra. Combined direct and indirect approach to adaptive control. *IEEE Transactions on Automatic Control*, 34(10):1071–1075, 1989.

G. E. Dullerud and F. Paganini. *A course in robust control theory: a convex approach*, volume 36. Springer Science & Business Media, 2013.

Z. T. Dydek, A. M. Annaswamy, and E. Lavretsky. Adaptive control and the nasa x-15-3 flight revisited. *IEEE Control Systems Magazine*, 30(3):32–48, 2010.

B. Egardt. *Stability of adaptive controllers*. Springer, 1979.

W. Feng and I. Postlethwaite. Robust nonlinear $\mathcal{H}_\infty$/adaptative control of robot manipulator motion. *IFAC Proc. Vol.*, 26(2):31–34, 1993.

B. A. Francis and J. C. Doyle. Linear control theory with an $\mathcal{H}_\infty$ optimality criterion. *SIAM Journal on Control and Optimization*, 25(4):815–844, 1987.

P. Gahinet and P. Apkarian. A linear matrix inequality approach to $\mathcal{H}_\infty$ control. *International Journal of Robust and Nonlinear Control*, 4(4):421–448, 1994.

D. N. Gerasimov and V. O. Nikiforov. On key properties of the lion's and kreisselmeier's adaptation algorithms. *International Journal of Adaptive Control and Signal Processing*, 36(6):1285–1304, 2022.

J. C. Geromel, J. Bernussou, and M. C. Oliveira. $\mathcal{H}_2$-norm optimization with constrained dynamic output feedback controllers: decentralized and reliable control. *IEEE Transactions on Automatic Control*, 44(7):1449–1454, 1999.

V. Goldshtein and A. Ukhlov. Weighted sobolev spaces and embedding theorems. *Transactions of the American Mathematical Society*, 361(7):3829–3850, 2009.

H. Goldstein, C. Poole, and J. Safko. *Classical mechanics*. American Association of Physics Teachers, 2002.

R. B. González De Paz. On a variational principle for shape optimization and elliptic free boundary problems. *Revista de Matemática: Teoría y Aplicaciones*, Vol. 6(1), 2009.

G. Goodwin, P. Ramadge, and P. Caines. Discrete-time multivariable adaptive control. *IEEE Transactions on Automatic Control*, 25(3):449–456, 1980.

G. C. Goodwin and K. S. Sin. *Adaptive filtering prediction and control*. Courier Corporation, 1984.

R. A. Horn and C. R. Johnson. *Matrix analysis*. Cambridge university press, 2012.

L.-S. Hu, J. Lam, Y.-Y. Cao, and H.-H. Shao. A linear matrix inequality (LMI) approach to robust $\mathcal{H}_2$ sampled-data control for linear uncertain systems. *IEEE Transactions on Systems, Man, and Cybernetics, Part B: Cybernetics*, pages 149–155, 2003.

J. T. Huang. Sufficient conditions for parameter convergence in linearizable systems. *IEEE Transactions on Automatic Control*, 48(5):878–880, 2003.

P. Ioannou and J. Sun. Theory and design of robust direct and indirect adaptive-control schemes. *International Journal of Control*, 47(3):775–813, 1988.

P. A. Ioannou and P. V. Kokotovic. *Adaptive systems with reduced models*. Springer, 1983.

P. A. Ioannou and J. Sun. *Robust adaptive control*, volume 1. PTR Prentice-Hall Upper Saddle River, NJ, 1996.

P. Johan, J. T. Gravdahl, K. Y. Pettersen, et al. *Vehicle-manipulator systems*. Springer, 2014.

R. Johansson. Quadratic optimization of motion coordination and control. *IEEE Transactions on Automatic Control*, (11):1197–1208, 1990.

R. E. Kalman. Design of a self-optimizing control system. *Transactions of the American Society of Mechanical Engineers*, 80(2):468–477, 1958.

R. Kamalapurkar, P. Walters, and W. E. Dixon. Model-based reinforcement learning for approximate optimal regulation. *Automatica*, 64:94–104, 2016.

R. Kelly, V. Santibáñez, and A. Loría. *Control of robot manipulators in joint space*, volume 693. Springer, 2005.

M. Khalaf, J. Huang, and F. Lewis. Nonlinear $\mathcal{H}_2/\mathcal{H}_\infty$ constrained feedback control: a practical design approach using neural networks (advances in industrial control), 2006.

H. Khalil. Nonlinear systems, printice-hall. *Upper Saddle River, NJ*, 3, 1996.

P. P. Khargonekar and M. A. Rotea. Mixed $\mathcal{H}_2/\mathcal{H}_\infty$ control: a convex optimization approach. *IEEE Transactions on Automatic Control*, 36(7):824–837, 1991.

T. Kilpeläinen. Weighted sobolev spaces and capacity. *Ann. Acad. Sci. Fenn. Ser. AI Math*, 19(1):95–113, 1994.

D. E. Kirk. *Optimal control theory: an introduction*. Courier Corporation, 2004.

M. Korotina, S. Aranovskiy, R. Ushirobira, and A. Vedyakov. On parameter tuning and convergence properties of the drem procedure. In *2020 European Control Conference (ECC)*, pages 53–58. IEEE, 2020.

G. Kreisselmeier. Adaptive observers with exponential rate of convergence. *IEEE transactions on automatic control*, 22(1):2–8, 1977.

A. Kufner. *Weighted sobolev spaces*, volume 31. John Wiley & Sons Incorporated, 1985.

C. Lanczos. *The variational principles of mechanics*. University of Toronto press, 2020.

Y. D. Landau. Adaptive control: the model reference approach. *IEEE Transactions on Systems, Man, and Cybernetics*, (1):169–170, 1984.

E. Lavretsky. Combined/composite model reference adaptive control. *IEEE Transactions on Automatic Control*, 54(11):2692–2697, 2009.

F. L. Lewis and D. Vrabie. Reinforcement learning and adaptive dynamic programming for feedback control. *IEEE circuits and systems magazine*, 9(3):32–50, 2009.

J.-S. Lin and I. Kanellakopoulos. Nonlinearities enhance parameter convergence in output-feedback systems. *IEEE Transactions on Automatic Control*, 43(2):204–222, 1998.

A. Loria. Explicit convergence rates for mrac-type systems. *Automatica*, 40(8):1465–1468, 2004.

A. Loría, R. Kelly, and A. R. Teel. Uniform parametric convergence in the adaptive control of mechanical systems. *European Journal of Control*, 11(2):87–100, 2005.

J. R. Magnus and H. Neudecker. *Matrix differential calculus with applications in statistics and econometrics*. John Wiley & Sons, 2019.

I. M. Mareels, B. D. Anderson, R. R. Bitmead, M. Bodson, and S. S. Sastry. Revisiting the mit rule for adaptive control. In *Adaptive Systems in Control and Signal Processing 1986*, pages 161–166. Elsevier, 1987.

V. Maz'ya. *Sobolev spaces*. Springer, 2013.

A. Morse. Global stability of parameter-adaptive control systems. *IEEE Transactions on Automatic Control*, 25(3):433–439, 1980.

K. Narendra, Y.-H. Lin, and L. Valavani. Stable adaptive controller design, part ii: Proof of stability. *IEEE Transactions on Automatic Control*, 25(3):440–448, 1980.

S. K. Nguang and P. Shi. $\mathcal{H}_\infty$ fuzzy output feedback control design for nonlinear systems: an LMI approach. *IEEE Transactions on Fuzzy Systems*, 11(3):331–340, 2003.

R. A. Nichols, R. T. Reichert, and W. J. Rugh. Gain scheduling for H-infinity controllers: A flight control example. *IEEE Transactions on Control systems technology*, 1(2):69–79, 1993.

R. Olfati-Saber. *Nonlinear control of underactuated mechanical systems with application to robotics and aerospace vehicles*. PhD thesis, Massachusetts Institute of Technology, 2001.

M. G. Ortega, M. Vargas, C. Vivas, and F. R. Rubio. Robustness Improvement of a Nonlinear $\mathcal{H}_\infty$ Controller for Robot Manipulators via Saturation Functions. *Journal of Robotic Systems*, 22(8):421–437, 2005.

R. Ortega, V. Nikiforov, and D. Gerasimov. On modified parameter estimators for identification and adaptive control. a unified framework and some new schemes. *Annual Reviews in Control*, 50:278–293, 2020.

A. W. Osburn, P.V. and A. Kezer. New developments in the design of model reference adaptive control systems. *Institute of the Aerospace Sciences*, pages 61–39, 1961.

Y. Pan and H. Yu. Composite learning robot control with guaranteed parameter convergence. *Automatica*, 89:398–406, 2018.

E. Panteley, A. Loria, and A. Teel. Relaxed persistency of excitation for uniform asymptotic stability. *IEEE Transactions on Automatic Control*, 46(12):1874–1886, 2001.

P. Parks. Liapunov redesign of model reference adaptive control systems. *IEEE Transactions on Automatic Control*, 11(3):362–367, 1966.

L. Pavel. Classical solutions in sobolev spaces for a class of hyperbolic lotka–volterra systems. *SIAM Journal on Control and Optimization*, 51(3):2132–2151, 2013.

A. Petronilho, A. A. Siqueira, and M. H. Terra. Adaptive $\mathcal{H}_\infty$ tracking control design via neural networks of a constrained robot system. In *Proceedings of the 44th IEEE Conference on Decision and Control*, pages 5528–5533. IEEE, 2005.

G. V. Raffo. *Robust control strategies for a quadrotor helicopter: An underactuated mechanical system*. PhD thesis, Univ. de Sevilla, 2011.

G. V. Raffo, M. G. Ortega, and F. R. Rubio. Path Tracking of a UAV via an Underactuated $\mathcal{H}_\infty$ Control Strategy. *European J. of Control*, 17(2):194–213, 2011a.

G. V. Raffo, M. G. Ortega, and F. R. Rubio. Nonlinear $\mathcal{H}_\infty$ controller for the quad-rotor helicopter with input coupling. *IFAC Proc. Vol.*, 44(1):13834–13839, 2011b.

G. V. Raffo, M. G. Ortega, V. Madero, and F. R. Rubio. Two-wheeled self-balanced pendulum workspace improvement via underactuated robust nonlinear control. *Control Eng. Practice*, 44:231–242, 2015.

C. Rohrs, L. Valavani, M. Athans, and G. Stein. Robustness of continuous-time adaptive control algorithms in the presence of unmodeled dynamics. *IEEE Transactions on Automatic Control*, 30(9):881–889, 1985.

H. Sage, M. De Mathelin, and E. Ostertag. Robust control of robot manipulators: a survey. *International Journal of control*, 72(16):1498–1522, 1999.

S. Sastry, M. Bodson, and J. F. Bartram. Adaptive control: stability, convergence, and robustness, 1990.

B. E. Sedhom, M. M. El-Saadawi, A. Y. Hatata, and E. E. Abd-Raboh. A multistage H-infinity-based controller for adjusting voltage and frequency and improving power quality in islanded microgrids. *International Transactions on Electrical Energy Systems*, 30(1):e12143, 2020.

D. Simon. *Optimal state estimation: Kalman, $\mathcal{H}_\infty$, and nonlinear approaches.* John Wiley & Sons, 2006.

A. A. Siqueira and M. H. Terra. Nonlinear and markovian $\mathcal{H}_\infty$ controls of underactuated manipulators. *IEEE Transactions on Control Systems Technology*, 12(6):811–826, 2004.

A. A. Siqueira, M. H. Terra, and B. C. Maciel. Nonlinear mixed $\mathcal{H}_2/\mathcal{H}_\infty$ control applied to manipulators via actuation. *Control engineering practice*, 14(4):327–335, 2006.

J.-J. E. Slotine and W. Li. Composite adaptive control of robot manipulators. *Automatica*, 25(4):509–519, 1989.

J.-J. E. Slotine, W. Li, et al. *Applied nonlinear control*, volume 199. Prentice hall Englewood Cliffs, NJ, 1991.

M. W. Spong, S. Hutchinson, and M. Vidyasagar. *Robot modeling and control.* John Wiley & Sons, 2020.

G. Tao. *Adaptive control design and analysis*, volume 37. John Wiley & Sons, 2003.

F. Treves. *Topological Vector Spaces, Distributions and Kernels: Pure and Applied Mathematics*, volume 25. Elsevier, 2016.

A. Trofino, D. Coutinho, and K. A. Barbosa. Sistemas multivariáveis: Uma abordagem via lmis. *Santa Catarina*, 2003.

G.-W. Van der Linden and P. F. Lambrechts. $\mathcal{H}_\infty$ control of an experimental inverted pendulum with dry friction. *IEEE Control Systems Magazine*, 13(4):44–50, 1993.

Van der Schaft. On a state space approach to nonlinear $\mathcal{H}_\infty$ control. *Systems & Control Letters*, 16(1):1–8, 1991.

Van Der Schaft. $\mathcal{L}_2$-gain analysis of nonlinear systems and nonlinear state-feedback $\mathcal{H}_\infty$ control. *IEEE Transactions on Automatic Control*, 37(6):770–784, 1992.

D. Vrabie, O. Pastravanu, M. Abu-Khalaf, and F. L. Lewis. Adaptive optimal control for continuous-time linear systems based on policy iteration. *Automatica*, 45(2):477–484, 2009.

J. Wang, D. Efimov, and A. A. Bobtsov. On robust parameter estimation in finite-time without persistence of excitation. *IEEE Transactions on Automatic Control*, 65(4): 1731–1738, 2019.

H. Whitaker, J. Yamron, A. Kezer, and M. I. of Technology. Instrumentation Laboratory. *Design of Model Reference Adaptive Control Systems for Aircraft.* Report Massachusetts

Institute of Technology Instrumentation Laboratory R. M.I.T. Instrumentation Laboratory, 1958. URL https://books.google.com.br/books?id=3V-jtgAACAAJ.

J. C. Willems. Dissipative dynamical systems. *European Journal of Control*, 13(2-3): 134–151, 2007.

A. Zemouche and M. Boutayeb. Unknown input observer synthesis method with modified $\mathcal{H}_\infty$ criteria for nonlinear systems using sobolev norms. *IFAC Proc. Vol.*, 41(2):8588–8593, 2008.

A

Miscellaneous Proofs and Derivations

A.1 A Calculus of Variations approach to the Euler-Lagrange Equations

Let $\boldsymbol{q}(t)$ denote the configuration of a system in the space $\mathcal{Q} \subset \mathbb{R}^n$. Hamilton's principle claims that the path $\boldsymbol{q}(t)$ between two configurations $\boldsymbol{q_1}$ and $\boldsymbol{q_2}$ minimizes the following action functional,

$$S = \int_{t_1}^{t_2} \boldsymbol{\mathcal{L}}(\boldsymbol{q}, \dot{\boldsymbol{q}}) dt, \tag{A.1}$$

where $\boldsymbol{\mathcal{L}}(\boldsymbol{q}, \dot{\boldsymbol{q}}) \in \mathbb{R}$ is the Lagrangian function[1]. The minimization of this action functional leads to the Euler-Lagrange equation. Nevertheless, the consideration of external forces are outside the realm of that formulation (Lanczos, 2020). Therefore, a modification to the action functional must be made to comply with external forces. This modification is done by considering the Lagrange-D'Alembert principle in order to take into account the work done by nonconservative forces (De Jalon and Bayo, 2012),$\boldsymbol{W}_{ext}$, which leads to the

[1] It is noteworthy that the Lagrangian can be in fact also dependent explicitly in time without impacting the derivation that follows in this chapter. However, for the sake of simplicity this explicit dependence is ommited. In addition, explicit dependence on time would prevent the use of the Euler-Lagrange First Integral used in the following chapters.

following problem

$$S_a = \min_{\boldsymbol{q}(t)\in\mathcal{Q}} \int_{t_1}^{t_2} \Big(\boldsymbol{\mathcal{L}}(\boldsymbol{q}, \dot{\boldsymbol{q}}) + \boldsymbol{W}_{ext}\Big)dt. \tag{A.2}$$

In addition, consider the following definitions and theorem.

Definition A.1. (Kirk, 2004) If $\boldsymbol{x}$ and $\boldsymbol{x} + \delta\boldsymbol{x}$ are functions for which the functional J is defined, then the increment of J, denoted by ΔJ, is

$$\Delta J \triangleq J(\boldsymbol{x} + \delta\boldsymbol{x}) - J(\boldsymbol{x}). \tag{A.3}$$

Q.E.D

Definition A.2. (Kirk, 2004) The increment of a functional can be written as

$$\Delta J = \delta J(\boldsymbol{x}, \delta\boldsymbol{x}) + \boldsymbol{g}(\boldsymbol{x}, \delta\boldsymbol{x})||\delta\boldsymbol{x}||, \tag{A.4}$$

where δJ is linear in $\delta\boldsymbol{x}$. If

$$\lim_{||\delta\boldsymbol{x}||\to 0} \boldsymbol{g}(\boldsymbol{x}, \delta\boldsymbol{x}) = 0, \tag{A.5}$$

then J is said to be differentiable on $\boldsymbol{x}$, and δJ is the variation of J evaluated for the function $\boldsymbol{x}$. Q.E.D

Theorem A.3. *Kirk (2004). [Fundamental Theorem of the Calculus of Variations]: Let $\boldsymbol{x}$ be a function of t in the class Ω, and $J(\boldsymbol{x})$ be a differentiable functional of $\boldsymbol{x}$. Assume that functions in Ω are not constrained by any boundaries. If $\boldsymbol{x}^*$ is an extremal, the variation of J must vanish on $\boldsymbol{x}^*$; that is,*

$$\delta J(\boldsymbol{x}^*, \delta\boldsymbol{x}) = 0, \ \textit{for all admissible } \delta\boldsymbol{x}.^2 \tag{A.6}$$

In what follows, the Euler-Lagrange equation is computed taking into account (A.2), Definitions A.1 and A.2, and Theorem A.3. Firstly, the increment of the action functional (A.2) is computed through Definition A.1. Then, it is approximated by (A.4), according to Definition A.2. Finally, using the Fundamental Theorem of the Calculus of Variations, from Theorem A.3, the Euler-Lagrange equation is obtained.

Therefore, considering (A.2), we have that

$$S_a = \min_{\boldsymbol{q}(t)\in\mathcal{Q}} \int_{t_1}^{t_2} \boldsymbol{\mathcal{L}}_a(\boldsymbol{q}, \dot{\boldsymbol{q}}, \boldsymbol{W}_{ext})dt. \tag{A.7}$$

Then, assuming $\boldsymbol{\mathcal{L}}_a(\boldsymbol{q}, \dot{\boldsymbol{q}}, \boldsymbol{W}_{ext})$ has continuous first and second order partial derivatives

[2] By admissible $\delta\boldsymbol{x}$ it is meant that $\boldsymbol{x} + \delta\boldsymbol{x}$ must be a member of class Ω; thus, if Ω is the class of continuous functions, $\boldsymbol{x}$ and $\delta\boldsymbol{x}$ are required to be continuous.

with respect to its arguments, the increment of the action functional (A.7) is computed as

$$\begin{aligned}\Delta S_a &= S_a(\boldsymbol{q}+\delta\boldsymbol{q}, \boldsymbol{W}_{ext}+\delta\boldsymbol{W}_{ext}) - S_a(\boldsymbol{q}, \boldsymbol{W}_{ext}),\\ &= \int_{t_1}^{t_2}\Big(\boldsymbol{\mathcal{L}}_a(\boldsymbol{q}+\delta\boldsymbol{q}, \dot{\boldsymbol{q}}+\delta\dot{\boldsymbol{q}}, \boldsymbol{W}_{ext}+\delta\boldsymbol{W}_{ext}) - \boldsymbol{\mathcal{L}}_a(\boldsymbol{q}, \dot{\boldsymbol{q}}, \boldsymbol{W}_{ext})\Big)dt. \end{aligned} \tag{A.8}$$

Note that, the dependency of the terms $\dot{\boldsymbol{q}}(t)$ and $\delta\dot{\boldsymbol{q}}(t)$ in the increment (A.8) is omitted, because they can be expressed in terms of $\boldsymbol{q}(t)$ and $\delta\boldsymbol{q}(t)$, respectively.

Therefore, by expanding the integrand of (A.8) in a Taylor series about $\boldsymbol{q}(t)$, $\dot{\boldsymbol{q}}(t)$ and $\boldsymbol{W}_{ext}$, we have that

$$\begin{aligned}\Delta \boldsymbol{S}_a = \int_{t_1}^{t_2}\Bigg\{&\boldsymbol{\mathcal{L}}_a(\boldsymbol{q}, \dot{\boldsymbol{q}}, \boldsymbol{W}_{ext}) + \left[\frac{\partial\boldsymbol{\mathcal{L}}_a(\boldsymbol{q}, \dot{\boldsymbol{q}}, \boldsymbol{W}_{ext})}{\partial\boldsymbol{q}}\right]'\delta\boldsymbol{q}\\ &+\left[\frac{\partial\boldsymbol{\mathcal{L}}_a(\boldsymbol{q}, \dot{\boldsymbol{q}}, \boldsymbol{W}_{ext})}{\partial\dot{\boldsymbol{q}}}\right]'\delta\dot{\boldsymbol{q}} + \left[\frac{\partial\boldsymbol{\mathcal{L}}_a(\boldsymbol{q}, \dot{\boldsymbol{q}}, \boldsymbol{W}_{ext})}{\partial\boldsymbol{W}_{ext}}\right]'\delta\boldsymbol{W}_{ext}\\ &+\frac{1}{2}\Bigg(\delta\boldsymbol{q}'\left[\frac{\partial^2\boldsymbol{\mathcal{L}}_a(\boldsymbol{q}, \dot{\boldsymbol{q}}, \boldsymbol{W}_{ext})}{\partial\boldsymbol{q}^2}\right]\delta\boldsymbol{q} + 2\delta\boldsymbol{q}'\left[\frac{\partial^2\boldsymbol{\mathcal{L}}_a(\boldsymbol{q}, \dot{\boldsymbol{q}}, \boldsymbol{W}_{ext})}{\partial\boldsymbol{q}\partial\dot{\boldsymbol{q}}}\right]\delta\dot{\boldsymbol{q}}\\ &+2\delta\boldsymbol{q}'\left[\frac{\partial^2\boldsymbol{\mathcal{L}}_a(\boldsymbol{q}, \dot{\boldsymbol{q}}, \boldsymbol{W}_{ext})}{\partial\boldsymbol{q}\partial\boldsymbol{W}_{ext}}\right]\delta\boldsymbol{W}_{ext} + \delta\dot{\boldsymbol{q}}'\left[\frac{\partial^2\boldsymbol{\mathcal{L}}_a(\boldsymbol{q}, \dot{\boldsymbol{q}}, \boldsymbol{W}_{ext})}{\partial\dot{\boldsymbol{q}}^2}\right]\delta\dot{\boldsymbol{q}}\\ &+2\delta\dot{\boldsymbol{q}}'\left[\frac{\partial^2\boldsymbol{\mathcal{L}}_a(\boldsymbol{q}, \dot{\boldsymbol{q}}, \boldsymbol{W}_{ext})}{\partial\dot{\boldsymbol{q}}\partial\boldsymbol{W}_{ext}}\right]\delta\boldsymbol{W}_{ext} + \delta\boldsymbol{W}_{ext}'\left[\frac{\partial^2\boldsymbol{\mathcal{L}}_a(\boldsymbol{q}, \dot{\boldsymbol{q}}, \boldsymbol{W}_{ext})}{\partial\boldsymbol{W}_{ext}^2}\right]\delta\boldsymbol{W}_{ext}\Bigg)\\ &+\mathcal{R}(.) - \boldsymbol{\mathcal{L}}_a(\boldsymbol{q}, \dot{\boldsymbol{q}}, \boldsymbol{W}_{ext})\Bigg\}dt, \end{aligned} \tag{A.9}$$

in which $\mathcal{R}(.)$ denotes terms in the Taylor series of order three and greater, and they approach zero when $\delta\boldsymbol{q}$, $\delta\dot{\boldsymbol{q}}$ and $\delta\boldsymbol{W}_{ext}$ tend to zero. Note that, (A.9) can be written as

$$\Delta\boldsymbol{S}_a = \int_{t_1}^{t_2}\left(\nabla\boldsymbol{\mathcal{L}}_a(\boldsymbol{q}, \dot{\boldsymbol{q}}, \boldsymbol{W}_{ext})\delta\boldsymbol{x} + \frac{1}{2}\delta\boldsymbol{x}'\boldsymbol{H}_{\mathcal{L}_a}\delta\boldsymbol{x}\right)dt, \tag{A.10}$$

with $\delta\boldsymbol{x} \triangleq \begin{bmatrix}\delta\boldsymbol{q}' & \delta\dot{\boldsymbol{q}}' & \delta\boldsymbol{W}_{ext}'\end{bmatrix}'$, $\nabla\boldsymbol{\mathcal{L}}_a(\boldsymbol{q}, \dot{\boldsymbol{q}}, \boldsymbol{W}_{ext}, t) \triangleq \begin{bmatrix}\dfrac{\partial\boldsymbol{\mathcal{L}}_a}{\partial\boldsymbol{q}}' & \dfrac{\partial\boldsymbol{\mathcal{L}}_a}{\partial\dot{\boldsymbol{q}}}' & \dfrac{\partial\boldsymbol{\mathcal{L}}_a}{\partial\boldsymbol{W}_{ext}}'\end{bmatrix}$, and

$$\boldsymbol{H}_{\mathcal{L}_a} \triangleq \begin{bmatrix}\dfrac{\partial^2\boldsymbol{\mathcal{L}}_a(\boldsymbol{q}, \dot{\boldsymbol{q}}, \boldsymbol{W}_{ext}, t)}{\partial\boldsymbol{q}^2} & \dfrac{\partial^2\boldsymbol{\mathcal{L}}_a(\boldsymbol{q}, \dot{\boldsymbol{q}}, \boldsymbol{W}_{ext}, t)}{\partial\boldsymbol{q}\partial\dot{\boldsymbol{q}}} & \dfrac{\partial^2\boldsymbol{\mathcal{L}}_a(\boldsymbol{q}, \dot{\boldsymbol{q}}, \boldsymbol{W}_{ext}, t)}{\partial\boldsymbol{q}\partial\boldsymbol{W}_{ext}}\\ * & \dfrac{\partial^2\boldsymbol{\mathcal{L}}_a(\boldsymbol{q}, \dot{\boldsymbol{q}}, \boldsymbol{W}_{ext}, t)}{\partial\dot{\boldsymbol{q}}\partial\dot{\boldsymbol{q}}} & \dfrac{\partial^2\boldsymbol{\mathcal{L}}_a(\boldsymbol{q}, \dot{\boldsymbol{q}}, \boldsymbol{W}_{ext}, t)}{\partial\dot{\boldsymbol{q}}\partial\boldsymbol{W}_{ext}}\\ * & * & \dfrac{\partial^2\boldsymbol{\mathcal{L}}_a(\boldsymbol{q}, \dot{\boldsymbol{q}}, \boldsymbol{W}_{ext}, t)}{\partial\boldsymbol{W}_{ext}\partial\boldsymbol{W}_{ext}}\end{bmatrix}.$$

Then, we can relate (A.10) with (A.4), as follows

$$\delta S_a = \int_{t_1}^{t_2} \nabla \boldsymbol{\mathcal{L}}_a(\boldsymbol{q}, \dot{\boldsymbol{q}}, \boldsymbol{W}_{ext}) \delta \boldsymbol{x} dt, \tag{A.11}$$

$$\boldsymbol{g}(\boldsymbol{x}, \delta\boldsymbol{x}) ||\delta\boldsymbol{x}||_{\mathcal{L}_2} = \frac{1}{2} \int_{t_1}^{t_2} \delta\boldsymbol{x}' \boldsymbol{H}_{\mathcal{L}_a} \delta\boldsymbol{x} dt. \tag{A.12}$$

According to Definition A.2, if δS_a is the variation of S_a, then $\lim_{||\delta \boldsymbol{x}|| \to 0} \boldsymbol{g}(\boldsymbol{x}, \delta\boldsymbol{x}) = 0$. To show that holds for (A.10), we consider the following assumption.

Assumption A.4. The Hessian matrix $\boldsymbol{H}_{\mathcal{L}_a}$ is positive definite. Q.E.D

Remark A.5. Assumption A.4 is true if S_a has a local minimum on $\boldsymbol{x} = [\boldsymbol{q}' \ \ \dot{\boldsymbol{q}}' \ \ \boldsymbol{W}_{ext}']'$. Q.E.D

Accordingly, from (A.12) and Assumption A.4, we have that

$$\begin{aligned}
\boldsymbol{g}(\boldsymbol{x}, \delta\boldsymbol{x}) ||\delta\boldsymbol{x}||_{\mathcal{L}_2} &= \int_{t_1}^{t_2} \delta\boldsymbol{x}' \boldsymbol{H}_{\mathcal{L}_a} \delta\boldsymbol{x} dt \geq 0, \\
\int_{t_1}^{t_2} \delta\boldsymbol{x}' \boldsymbol{H}_{\mathcal{L}_a} \delta\boldsymbol{x} dt &\leq \Psi(\boldsymbol{H}_{\mathcal{L}_a})^2 \int_{t_1}^{t_2} \delta\boldsymbol{x}' \delta\boldsymbol{x} dt, \\
\int_{t_1}^{t_2} \delta\boldsymbol{x}' \boldsymbol{H}_{\mathcal{L}_a} \delta\boldsymbol{x} dt &\leq \Psi(\boldsymbol{H}_{\mathcal{L}_a})^2 ||\delta\boldsymbol{x}||_{\mathcal{L}_2}^2,
\end{aligned} \tag{A.13}$$

where $\Psi(\boldsymbol{H}_{\mathcal{L}_a})$ stands for the highest singular value of $\boldsymbol{H}_{\mathcal{L}_a}$ at the interval $[t_1, t_2]$. Consequently,

$$\Psi(\boldsymbol{H}_{\mathcal{L}_a})^2 ||\delta\boldsymbol{x}||_{\mathcal{L}_2} \geq \boldsymbol{g}(\boldsymbol{x}, \delta\boldsymbol{x}) \geq 0. \tag{A.14}$$

Therefore, assuming $\Psi(\boldsymbol{H}_{\mathcal{L}_a}) \in \mathbb{R}$, and since

$$\lim_{||\delta\boldsymbol{x}||_{\mathcal{L}_2} \to 0} \Psi(\boldsymbol{H}_{\mathcal{L}_a})^2 ||\delta\boldsymbol{x}||_{\mathcal{L}_2} = 0, \tag{A.15}$$

one can infer that

$$\lim_{||\delta\boldsymbol{x}||_{\mathcal{L}_2} \to 0} \boldsymbol{g}(\boldsymbol{x}, \delta\boldsymbol{x}) = 0. \tag{A.16}$$

Leading to

$$\begin{aligned}
\delta S_a &= \int_{t_1}^{t_2} \nabla \boldsymbol{\mathcal{L}}_a(\boldsymbol{q}, \dot{\boldsymbol{q}}, \boldsymbol{W}_{ext}) \delta\boldsymbol{x} dt, \\
&= \int_{t_1}^{t_2} \Big(\frac{\partial \boldsymbol{\mathcal{L}}_a(\boldsymbol{q}, \dot{\boldsymbol{q}}, \boldsymbol{W}_{ext})'}{\partial \boldsymbol{q}} \delta\boldsymbol{q} + \frac{\partial \boldsymbol{\mathcal{L}}_a(\boldsymbol{q}, \dot{\boldsymbol{q}}, \boldsymbol{W}_{ext})'}{\partial \dot{\boldsymbol{q}}} \delta\dot{\boldsymbol{q}} + \frac{\partial \boldsymbol{\mathcal{L}}_a(\boldsymbol{q}, \dot{\boldsymbol{q}}, \boldsymbol{W}_{ext})'}{\partial \boldsymbol{W}_{ext}} \delta\boldsymbol{W}_{ext} \Big) dt.
\end{aligned} \tag{A.17}$$

Note that $\delta\dot{\boldsymbol{q}}$ and $\delta\boldsymbol{q}$ are related by

$$\delta\boldsymbol{q}(t) = \int_{t_1}^{t} \delta\dot{\boldsymbol{q}}(\tau)d\tau + \delta\boldsymbol{q}(t_1). \tag{A.18}$$

Thus, selecting $\delta\boldsymbol{q}(t)$ uniquely determines $\delta\dot{\boldsymbol{q}}(t)$.

To express (A.17) entirely in terms containing $\delta\boldsymbol{q}(t)$, we integrate by part the term containing $\delta\dot{\boldsymbol{q}}(t)$ to obtain

$$\begin{aligned}\delta S_a = &\int_{t_1}^{t_2} \left(\left[\frac{\partial \boldsymbol{\mathcal{L}}_a(\boldsymbol{q},\dot{\boldsymbol{q}},\boldsymbol{W}_{ext})}{\partial \boldsymbol{q}}\right]'\delta\boldsymbol{q} + \left[\frac{\partial \boldsymbol{\mathcal{L}}_a(\boldsymbol{q},\dot{\boldsymbol{q}},\boldsymbol{W}_{ext})}{\partial \boldsymbol{W}_{ext}}\right]'\delta\boldsymbol{W}_{ext}\right)dt\\ &+ \left[\frac{\partial \boldsymbol{\mathcal{L}}_a(\boldsymbol{q},\dot{\boldsymbol{q}},\boldsymbol{W}_{ext})}{\partial \dot{\boldsymbol{q}}}\right]'\delta\boldsymbol{q}\Bigg|_{t_1}^{t_2} - \int_{t_1}^{t_2}\left(\frac{d}{dt}\left[\frac{\partial \boldsymbol{\mathcal{L}}_a(\boldsymbol{q},\dot{\boldsymbol{q}},\boldsymbol{W}_{ext})}{\partial \dot{\boldsymbol{q}}}\right]'\delta\boldsymbol{q}\right)dt.\end{aligned} \tag{A.19}$$

Since $\boldsymbol{q}(t_1)$ and $\boldsymbol{q}(t_2)$ are specified, all admissible curves must pass through these points. Therefore, $\delta\boldsymbol{q}(t_1) = \delta\boldsymbol{q}(t_2) = 0$, and the terms outside the integral vanish. Consequently, (A.19) becomes

$$\begin{aligned}\delta S_a = &\int_{t_1}^{t_2} \left(\frac{\partial \boldsymbol{\mathcal{L}}_a(\boldsymbol{q},\dot{\boldsymbol{q}},\boldsymbol{W}_{ext})}{\partial \boldsymbol{q}} - \frac{d}{dt}\left[\frac{\partial \boldsymbol{\mathcal{L}}_a(\boldsymbol{q},\dot{\boldsymbol{q}},\boldsymbol{W}_{ext})}{\partial \dot{\boldsymbol{q}}}\right]\right)'\delta\boldsymbol{q}dt\\ &+ \int_{t_1}^{t_2}\left(\frac{\partial \boldsymbol{\mathcal{L}}_a(\boldsymbol{q},\dot{\boldsymbol{q}},\boldsymbol{W}_{ext})}{\partial \boldsymbol{W}_{ext}}'\delta\boldsymbol{W}_{ext}\right)dt.\end{aligned} \tag{A.20}$$

Then, the partial derivatives in (A.20) are expanded, taking into account (A.2), as

$$\frac{\partial \boldsymbol{\mathcal{L}}_a(\boldsymbol{q},\dot{\boldsymbol{q}},\boldsymbol{W}_{ext})}{\partial \boldsymbol{q}} = \frac{\partial \boldsymbol{\mathcal{L}}(\boldsymbol{q},\dot{\boldsymbol{q}})}{\partial \boldsymbol{q}}, \quad \frac{\partial \boldsymbol{\mathcal{L}}_a(\boldsymbol{q},\dot{\boldsymbol{q}},\boldsymbol{W}_{ext})}{\partial \dot{\boldsymbol{q}}} = \frac{\partial \boldsymbol{\mathcal{L}}(\boldsymbol{q},\dot{\boldsymbol{q}})}{\partial \dot{\boldsymbol{q}}}, \quad \frac{\partial \boldsymbol{\mathcal{L}}_a(\boldsymbol{q},\dot{\boldsymbol{q}},\boldsymbol{W}_{ext})}{\partial \boldsymbol{W}_{ext}} = \boldsymbol{I},$$

which yields

$$\delta S_a = \int_{t_1}^{t_2} \left(\frac{\partial \boldsymbol{\mathcal{L}}(\boldsymbol{q},\dot{\boldsymbol{q}})}{\partial \boldsymbol{q}} - \frac{d}{dt}\left[\frac{\partial \boldsymbol{\mathcal{L}}(\boldsymbol{q},\dot{\boldsymbol{q}})}{\partial \dot{\boldsymbol{q}}}\right]\right)'\delta\boldsymbol{q}dt + \int_{t_1}^{t_2}\delta\boldsymbol{W}_{ext}dt. \tag{A.21}$$

Before conclude the development of the Euler-Lagrange equation, the following assumptions are posed.

Assumption A.6. The coordinates of all k bodies in a system can be expressed in terms of the vector of generalized coordinates,

$$\boldsymbol{r}_i(\boldsymbol{q}), \quad i = 1, ..., k, \tag{A.22}$$

where r_i is the coordinate of the i-th body and $\boldsymbol{q}(t) = [q_1(t), ..., q_n(t)]$ is the vector of generalized coordinates, in which $q_1(t), ..., q_n(t)$ are all independent. Q.E.D

Assumption A.7. The orientation of all k bodies in a system can be expressed in terms of the vector of generalized coordinates,

$$\boldsymbol{\eta}_i(\boldsymbol{q}), \quad i = 1, ..., k, \tag{A.23}$$

where $\boldsymbol{\eta}_i$ is the coordinate of the i-th body and $\boldsymbol{q}(t) = [q_1(t), ..., q_n(t)]$ is the vector of generalized coordinates, in which $q_1(t), ..., q_n(t)$ are all independent. Q.E.D

It's noteworthy that if Assumption A.6 and A.7 hold then by means of the total differential one can write the so-called Jacobian matrices, $\boldsymbol{J}_v$ and $\boldsymbol{J}_\omega$, used in the following sections to map the derivative of generalized coordinates to the linear and angular velocity respectively

$$\dot{\boldsymbol{r}} = \frac{\partial \boldsymbol{r}(\boldsymbol{q})}{\partial \boldsymbol{q}} \dot{\boldsymbol{q}}(t) = \boldsymbol{J}_v(\boldsymbol{q}) \dot{\boldsymbol{q}}(t). \tag{A.24}$$

Note that essentially $\dot{\boldsymbol{r}} = \boldsymbol{f}(\boldsymbol{q}(t), \dot{\boldsymbol{q}}(t))$, meaning that the velocity is a function of $\boldsymbol{q}(t)$ and $\dot{\boldsymbol{q}}(t)$.[3] Thus, one can write the following equivalence

$$\frac{\partial \dot{\boldsymbol{r}}}{\partial \dot{\boldsymbol{q}}} = \frac{\partial \boldsymbol{v}^{\mathcal{I}}}{\partial \dot{\boldsymbol{q}}} = \frac{\partial \boldsymbol{r}(\boldsymbol{q})}{\partial \boldsymbol{q}} = \boldsymbol{J}_v(\boldsymbol{q}). \tag{A.25}$$

The same development can be taken for the orientation,

$$\dot{\boldsymbol{\eta}} = \frac{\partial \boldsymbol{\eta}(\boldsymbol{q})}{\partial \boldsymbol{q}} \dot{\boldsymbol{q}}(t) = \boldsymbol{J}_\omega(\boldsymbol{q}) \dot{\boldsymbol{q}}(t), \tag{A.26}$$

which implies

$$\frac{\partial \dot{\boldsymbol{\eta}}}{\partial \dot{\boldsymbol{q}}} = \frac{\partial \boldsymbol{\omega}^{\mathcal{I}}}{\partial \dot{\boldsymbol{q}}} = \frac{\partial \boldsymbol{\eta}(\boldsymbol{q})}{\partial \boldsymbol{q}} = \boldsymbol{J}_\omega(\boldsymbol{q}). \tag{A.27}$$

Therefore, if Assumption A.6 holds, a virtual displacement, $\delta \boldsymbol{r}$, can be written in terms of infinitesimal displacement of the generalized coordinates, as follows

$$\delta \boldsymbol{r} = \frac{\partial \boldsymbol{r}}{\partial \boldsymbol{q}} \delta \boldsymbol{q}, \tag{A.28}$$

where $\boldsymbol{r} = [\boldsymbol{r}_1, ...\boldsymbol{r}_k]'$. Besides, if Assumption A.7 holds, $\delta \boldsymbol{\eta}$ can be written in terms of infinitesimal displacement of the generalized coordinates, as follows

$$\delta \boldsymbol{\eta} = \frac{\partial \boldsymbol{\eta}}{\partial \boldsymbol{q}} \delta \boldsymbol{q}, \tag{A.29}$$

where $\boldsymbol{\eta} = [\boldsymbol{\eta}_1, ...\boldsymbol{\eta}_k]'$.

With these assumptions, we can proceed with the development. The external forces

[3] More precisely, $\dot{\boldsymbol{r}}$ is at least a function of the derivative of the generalized coordinates.

and dissipative forces are included in the term $\boldsymbol{W}_{ext}$ such that

$$\boldsymbol{W}_{ext} = \boldsymbol{W}_f + \boldsymbol{W}_{diss}, \tag{A.30}$$

where $\boldsymbol{W}_f$ contain the contributions forces not derived from a potential, and $\boldsymbol{W}_{diss}$ contains the contribution of the dissipative forces.

The next subsections detail how to incorporate the external and dissipative forces into the vector of generalized forces.

To comply with external forces if one applies a fictitious external force f_i and a fictitious external torque τ_i on the i-th body belonging to the system, the variation of the work done by these force and torque can be computed as

$$\delta W_f = \sum_{i=1}^{k} f_i \delta r_i + \tau_i \delta \eta_i. \tag{A.31}$$

From Assumption A.6 and A.7, and considering (A.28) and (A.29), we have that

$$\begin{aligned} \delta W_f &= \sum_{i=1}^{k}\sum_{j=1}^{n} \left(f_i \frac{\partial r_i}{\partial q_j}\delta q_j + \tau_i \frac{\partial \eta_i}{\partial q_j}\delta q_j \right), \\ &= \sum_{i=1}^{k}\sum_{j=1}^{n} \left(f_i \frac{\partial r_i}{\partial q_j} + \tau_i \frac{\partial \eta_i}{\partial q_j} \right)\delta q_j, \\ &= \Big(\underbrace{\boldsymbol{J}_v' \boldsymbol{f}(t)}_{\boldsymbol{\vartheta}_{force}} + \underbrace{\boldsymbol{J}_\omega' \boldsymbol{\tau}(t)}_{\boldsymbol{\vartheta}_{torque}} \Big)' \delta \boldsymbol{q}, \\ &= \left(\boldsymbol{\vartheta}_{force} + \boldsymbol{\vartheta}_{torque}\right)' \delta \boldsymbol{q} \end{aligned} \tag{A.32}$$

where $\boldsymbol{f}(t) \triangleq [f_1 \ \cdots \ f_k]$, $\boldsymbol{\tau}(t) \triangleq [\tau_1 \ \cdots \ \tau_k]$, $\boldsymbol{J}_v' \triangleq [\frac{\partial \boldsymbol{r}}{\partial q_1} \ \cdots \ \frac{\partial \boldsymbol{r}}{\partial q_n}]$ and $\boldsymbol{J}_\omega' \triangleq [\frac{\partial \boldsymbol{\eta}}{\partial q_1} \ \cdots \ \frac{\partial \boldsymbol{\eta}}{\partial q_n}]$.

So far we are trying to show that the variational approach can be extended beyond simple conservative systems. Generally, dissipative forces are included in the Euler-Lagrange formulation in two manners. The first one involves explicitly multiplying the Lagrangian by an exponential time-dependent "damping term" and the second one, which is more general, involves a dissipation function (Bersani and Caressa, 2021). For the sake of generality, consider the following dissipation function:

$$\boldsymbol{\mathcal{D}}(\boldsymbol{v}) = \frac{1}{m+1}\sum_{i=1}^{k} c_i \left(\boldsymbol{v}_i\right)^{m+1}, \tag{A.33}$$

where c_i is some coefficient of friction, $\boldsymbol{v}_i$ is the velocity of the i-th body, and $m \in \mathbb{N}_0$ determines the behavior of the dissipative. We assume the dissipative forces can be written as

$$\boldsymbol{f}_i^{(diss)}(t) = -\frac{\partial \boldsymbol{\mathcal{D}}}{\partial \boldsymbol{v}_i}. \tag{A.34}$$

By using a general dissipation function, several friction forces can be included in the Lagrangian formalism. Notably, it becomes possible to include quadratic velocity-dependent friction, for example, by simply considering $m = 2$.

To show this, consider a single object moving in the x direction on a incompressible fluid. Then, by defining $m = 2$, $v = \dot{x}$ and $c = \frac{1}{2}\rho C_d A$, the drag equation can be obtained as shown

$$D = \frac{1}{6}\rho C_d A v^3. \tag{A.35}$$

Thus, by using (A.34), one can obtained the drag equation,

$$f^{drag} = -\frac{1}{2}\rho C_d A v^2. \tag{A.36}$$

The variation of the work done by these forces can be computed as

$$\delta W_{diss} = \sum_{i=1}^{k} f_i^{(diss)} \delta r_i. \tag{A.37}$$

From Assumption A.6,

$$\delta W_{diss} = \sum_{i=1}^{k}\sum_{j=1}^{n} f_i^{(diss)} \frac{\partial r_i}{\partial q_j}\delta q_j. \tag{A.38}$$

Since the position is only a function of the generalized coordinates and by substituting (A.34), the contribution of the dissipative forces can be stated as

$$\delta W_{diss} = -\sum_{i=1}^{k}\sum_{j=1}^{n} \frac{\partial \boldsymbol{\mathcal{D}}}{\partial v_i}\frac{\partial v_i}{\partial \dot{q}_j}\delta q_j = -\overbrace{\left(\frac{\partial \boldsymbol{\mathcal{D}}}{\partial \dot{\boldsymbol{q}}}\right)'}^{\boldsymbol{\vartheta}'_{diss}} \delta \boldsymbol{q} = (\boldsymbol{\vartheta}_{diss})' \,\delta \boldsymbol{q}. \tag{A.39}$$

Finally, one can write the contributions of nonconservative forces by substituting (A.32) and (A.39) into (A.30)

$$\delta \boldsymbol{W}_{ext} = (\boldsymbol{\vartheta}_{forces} + \boldsymbol{\vartheta}_{torques} + \boldsymbol{\vartheta}_{diss})' \,\delta \boldsymbol{q}. \tag{A.40}$$

Therefore, by considering Theorem A.3, if $\boldsymbol{q}(t)$ is an extremal of S_a, then $\delta S_a = 0$ for all admissible $\delta \boldsymbol{q}$. Accordingly, equation (A.21) reduces to

$$\delta S_a = \int_{t_1}^{t_2} \left(\frac{\partial \boldsymbol{\mathcal{L}}(\boldsymbol{q}, \dot{\boldsymbol{q}})}{\partial \boldsymbol{q}} - \frac{d}{dt} \left[\frac{\partial \boldsymbol{\mathcal{L}}(\boldsymbol{q}, \dot{\boldsymbol{q}})}{\partial \dot{\boldsymbol{q}}} \right] + (\boldsymbol{\vartheta}_{forces} + \boldsymbol{\vartheta}_{torques} + \boldsymbol{\vartheta}_{diss}) \right)' \delta \boldsymbol{q} dt = 0,$$

which leads to the following Euler-Lagrange equation considering external forces,

$$\frac{d}{dt} \left[\frac{\partial \boldsymbol{\mathcal{L}}(\boldsymbol{q}, \dot{\boldsymbol{q}})}{\partial \dot{\boldsymbol{q}}} \right] - \frac{\partial \boldsymbol{\mathcal{L}}(\boldsymbol{q}, \dot{\boldsymbol{q}})}{\partial \boldsymbol{q}} = \boldsymbol{\vartheta}(\boldsymbol{q}, \dot{\boldsymbol{q}}, \boldsymbol{u}). \tag{A.41}$$

where $\boldsymbol{\vartheta}(\boldsymbol{q}, \dot{\boldsymbol{q}}, \boldsymbol{u}) = \boldsymbol{\vartheta}_{forces} + \boldsymbol{\vartheta}_{torques} + \boldsymbol{\vartheta}_{diss}$, with $\boldsymbol{\vartheta} \in \mathbb{R}^n$, being the vector of generalized forces composed of terms regarding external forces, torques, and dissipative forces.

In conclusion, while using Newton's approach the behavior os a system is described by forces, in Hamilton's approach the behavior is described by a function involving energies, the Lagrangian. Since energy is scalar quantity one advantage of the Lagrangian formulation is the absence of the need to consider direction of vectors. Another advantage of Hamilton's approach appears when dealing with constraints. Lagrange's method allows to encapsulate information about the constraints through the use of Lagrangian multipliers. Moreover, by choosing appropriate generalized coordinates the notion of constraints could be implicitly contained in the model. Since Lagrangian mechanics is built upon the notion of energy, the forces involved are of conservative nature. This is a drawback when comparing with Newton's approach that can deal more easily with nonconservative forces. Nevertheless, nonconservative forces can be included into the Euler-Lagrange formulation as have been shown. With everything presented one can argue that the principle of least action is a more elegant procedure to derive equations of motion. In the words of Lanczos, "the idea of enlarging reality by including "tentative" possibilities and then selecting one of these by the condition that it minimizes a certain quantity, seems to bring a purpose to the flow of natural events" (Lanczos, 2020).

A.2 DREM Estimator Properties

First, define

$$\Phi(t, r) \triangleq e^{-\gamma_j \int_r^t \phi^2(s) ds}, \tag{A.42}$$

such that $\Phi(t, r) \in \mathbb{R}_{>0}$. Therefore, (2.45) can be rewritten as

$$\tilde{\theta}_j(t) = \Phi(t, t_0) \tilde{\theta}_j(t_0).$$

Since by assumption we have $\phi(t) \notin \mathcal{L}_2[t_0, \infty)$, then $\int_{t_0}^{\infty} \phi^2(s)ds \to \infty$. As a result, the following properties hold

$$0 < \Phi(t, r) \leq 1, \ \forall t \geq r, \tag{A.43}$$

$$\Phi(t, r) \to 0 \ as \ t \to \infty, \tag{A.44}$$

$$\Phi(t, r) \leq \Phi(t, r + \delta), \ \forall t \geq r + \delta, \ \delta \geq 0. \tag{A.45}$$

From (A.44), it is clear that $\Phi(t, t_0)\tilde{\theta}_j(t_0) \to 0$ as $t \to \infty$, thus showing the validity of (i). Furthermore, if $\phi(t)$ is PE, i.e $\int_0^\infty \phi^2(t) \geq \epsilon$, where $\epsilon \in \mathbb{R}_{>0}$, then consequently

$$\left(\Phi(t, r) \leq e^{-\gamma_j \epsilon} (t - t_0)\right) \implies \left(\tilde{\theta}_j(t) \leq e^{-\gamma_j \epsilon (t - t_0)} \tilde{\theta}_j(t_0)\right), \tag{A.46}$$

completing the proof of (ii).

To demonstrate (iii) is true, note that for (A.42) it is easy to show that its inverse is given by $\Phi^{-1}(t, r) = \Phi(r, t)$. Therefore, in view of (A.45),

$$\left((\Phi(t_0, t_2))^{-1} \tilde{\theta}_j(t_0) \leq (\Phi(t_0, t_1))^{-1} \tilde{\theta}_j(t_0) \right) \implies \left(\tilde{\theta}_j(t_2) \leq \tilde{\theta}_j(t_1) \right), \ \forall t_2 \geq t_1 \geq 0, \tag{A.47}$$

which proves allegation (iii).

The remaining property (iv) follows directly by inspection of (2.45).

A.3 Nonlinear Adaptive $\mathcal{H}_\infty$ Control

The proof follows the same steps as presented in Chen et al. (1997). Given (3.32) and from the fact that $\boldsymbol{u}^*(t) = -\boldsymbol{R}^{-1}\boldsymbol{B}'\boldsymbol{T}_0\tilde{\boldsymbol{x}}$ one has

$$\boldsymbol{\tau}^*(t) = \boldsymbol{Y}\boldsymbol{\theta} + \boldsymbol{T}_{11}^{-1}\boldsymbol{u}^*(t). \tag{A.48}$$

Note that from (3.34)-(3.35) evaluated at $\boldsymbol{\tau}^*(t)$ yields

$$\frac{\partial V(\tilde{\boldsymbol{x}}, t)}{\partial t} + (\mathcal{L})_{\boldsymbol{\tau}^*} + \left(\frac{\partial V(\tilde{\boldsymbol{x}}, t)'}{\partial \tilde{\boldsymbol{x}}} \dot{\tilde{\boldsymbol{x}}} \right)_{\boldsymbol{\tau}^*} = \left(\dot{V}(\tilde{\boldsymbol{x}}, t) \right)_{\boldsymbol{\tau}^*} + (\mathcal{L})_{\boldsymbol{\tau}^*} = 0 \implies \left(\dot{V}(\tilde{\boldsymbol{x}}, t) \right)_{\boldsymbol{\tau}^*} = -(\mathcal{L})_{\boldsymbol{\tau}^*}. \tag{A.49}$$

Next consider the following candidate Lyapunov function for the augmented state space vector $\boldsymbol{\mathcal{X}} = [\tilde{\boldsymbol{x}}' \ \ \tilde{\boldsymbol{\theta}}']'$:

$$V(\boldsymbol{\mathcal{X}}, t) \triangleq V(\tilde{\boldsymbol{x}}, t) + V(\tilde{\boldsymbol{\theta}}) = \frac{1}{2}\tilde{\boldsymbol{x}}'\boldsymbol{T}_0' \begin{bmatrix} \boldsymbol{M}(\boldsymbol{q}) & \boldsymbol{0} \\ * & \boldsymbol{K} \end{bmatrix} \boldsymbol{T}_0\tilde{\boldsymbol{x}} + \frac{1}{2}\tilde{\boldsymbol{\theta}}'\boldsymbol{K}_{\tilde{\theta}}\tilde{\boldsymbol{\theta}} \tag{A.50}$$

In addition, it is noteworthy that

$$\dot{V}(\boldsymbol{\mathcal{X}}, t) = \left(\dot{V}(\tilde{\boldsymbol{x}}, t)\right)_{\tau} + \tilde{\boldsymbol{\theta}}' \boldsymbol{K}_{\tilde{\boldsymbol{\theta}}} \dot{\tilde{\boldsymbol{\theta}}}. \tag{A.51}$$

Furthermore, it can be verified that

$$\left(\dot{V}(\tilde{\boldsymbol{x}}, t)\right)_{\tau} = \left(\dot{V}(\tilde{\boldsymbol{x}}, t)\right)_{\tau^*} + \tilde{\boldsymbol{x}}' \boldsymbol{T}_0 \boldsymbol{B}' \boldsymbol{Y} \tilde{\boldsymbol{\theta}}. \tag{A.52}$$

By direct substitution of (3.50) and (A.52) in (A.51) produces

$$\dot{V}(\boldsymbol{\mathcal{X}}, t) = \left(\dot{V}(\tilde{\boldsymbol{x}}, t)\right)_{\tau^*} = -\left(\mathcal{L}\right)_{\boldsymbol{\tau}^*} \leq 0, \tag{A.53}$$

where (A.49) has been used. Integrating both sides renders,

$$V(\boldsymbol{\mathcal{X}}, \infty) - V(\boldsymbol{\mathcal{X}}, t_0) = -\int_{t_0}^{\infty} \left(\frac{1}{2}\tilde{\boldsymbol{x}}' \boldsymbol{Q} \tilde{\boldsymbol{x}} + \frac{1}{2}\boldsymbol{u}' \boldsymbol{R} \boldsymbol{u}\right) ds + \int_{t_0}^{\infty} \rho^2 \boldsymbol{d}' \boldsymbol{d} ds. \tag{A.54}$$

Since, $V(\boldsymbol{\mathcal{X}}, \infty) \geq 0$, then

$$\begin{aligned} \int_{t_0}^{\infty} \left(\frac{1}{2}\tilde{\boldsymbol{x}}' \boldsymbol{Q} \tilde{\boldsymbol{x}} + \frac{1}{2}\boldsymbol{u}' \boldsymbol{R} \boldsymbol{u}\right) ds \leq V(\boldsymbol{\mathcal{X}}, t_0) + \rho^2 \int_{t_0}^{\infty} \boldsymbol{d}' \boldsymbol{d} ds, \\ ||\boldsymbol{z}(t)||_{\mathcal{L}_2} \leq V(\boldsymbol{\mathcal{X}}, t_0) + \rho^2 ||\boldsymbol{d}(t)||_{\mathcal{L}_2}. \end{aligned} \tag{A.55}$$

and therefore we guarantee the $\mathcal{H}_\infty$ criteria completing the proof.

A.4 MREM Excitation Propagation

Consider the solution of (3.14) presented bellow

$$\boldsymbol{Y}_f(t) = e^{-at} \boldsymbol{Y}_f(t_0) + \int_{t_0}^{t} \boldsymbol{\Phi}(t, s) ds \tag{A.56}$$

with

$$\boldsymbol{\Phi}(t, s) \triangleq e^{-a(t-s)} \boldsymbol{Y}_{\mathcal{I}}(s) \boldsymbol{Y}_{\mathcal{I}}'(s). \tag{A.57}$$

For $t \geq \Delta T$ and for a $k \geq 1$ a positive number such that $t \geq k\Delta T$. Then, considering a positive integer $j \leq k$, the integral term can be rewritten as

$$\int_{t_0}^{t} \boldsymbol{\Phi}(t, s) ds = \int_{t_0}^{t-k\Delta T} \boldsymbol{\Phi}(t, s) ds + \sum_{j=1}^{k} \int_{t-j\Delta T}^{t-j\Delta T+\Delta T} \boldsymbol{\Phi}(t, s) ds, \tag{A.58}$$

which in turn implies

$$\int_{t-j\Delta T}^{t-j\Delta T+\Delta T} \boldsymbol{\Phi}(t,s)ds = e^{-at}\int_{t-j\Delta T}^{t-j\Delta T+\Delta T} e^{as}\boldsymbol{Y}_{\mathcal{I}}(s)\boldsymbol{Y}_{\mathcal{I}}(s)'ds = e^{-at}\left(e^{as}\boldsymbol{\Xi}(t)\right)\Big|_{t-j\Delta T}^{t-j\Delta T+\Delta T}$$
$$- e^{-at}\int_{t-j\Delta T}^{t-j\Delta T+\Delta T} \frac{d}{dt}(e^{as})\boldsymbol{\Xi}(t)ds \geq e^{-at}e^{a(t-j\Delta T+\Delta T)}\mu\boldsymbol{I} \geq e^{-at}e^{a(t-j\Delta T)}\mu\boldsymbol{I},$$
$$\int_{t-j\Delta T}^{t-j\Delta T+\Delta T} \boldsymbol{\Phi}(t,s)ds \geq e^{-aj\Delta T}\mu\boldsymbol{I} \tag{A.59}$$

where $\boldsymbol{\Xi}(t) \triangleq \int_{t-j\Delta T}^{t}\boldsymbol{Y}_{\mathcal{I}}(s)\boldsymbol{Y}_{\mathcal{I}}(s)'ds$, the assumption $\boldsymbol{Y}_{\mathcal{I}} \in PE$ has been used and integration by parts has been carried out to proof the inequality above. Thus,

$$\boldsymbol{Y}_f(t) \geq e^{-at}\boldsymbol{Y}_f(t_0) + \int_{t_0}^{t-k\Delta T} \boldsymbol{\Phi}(t,s)ds + \mu\sum_{j=1}^{k} e^{-aj\Delta T}\boldsymbol{I}. \tag{A.60}$$

Next, since $\boldsymbol{Y}_f(t_0) \geq 0$ and $\boldsymbol{Y}_{\mathcal{I}}(t) \in PE$ implies $\boldsymbol{Y}_{\mathcal{I}}(t)\boldsymbol{Y}_{\mathcal{I}}(t)' \geq 0$, then

$$e^{-at}\boldsymbol{Y}_f(t_0) + \int_{t_0}^{t-k\Delta T} \boldsymbol{\Phi}(t,s)ds \geq 0, \tag{A.61}$$

and, consequently,

$$\boldsymbol{Y}_f(t) \geq \mu\sum_{j=1}^{k} e^{-aj\Delta T}\boldsymbol{I}. \tag{A.62}$$

From (A.60), one can conclude that for $t \geq k\Delta T$ the smallest eigenvalue of $\boldsymbol{Y}_f(t)$ is

$$\lambda_i\left(\boldsymbol{Y}_f\right) \geq \lambda_{\min}\left(\boldsymbol{Y}_f\right) \geq \mu\sum_{j=1}^{k} e^{-aj\Delta T}, \ \forall i = 1, ...p, \tag{A.63}$$

where $\lambda_i(\boldsymbol{Y}_f(t))$ denotes the i-th eigenvalue of $\boldsymbol{Y}_f(t)$ and $\lambda_{\min}(\boldsymbol{Y}_f(t))$ its minimum eigenvalue. Then, the determinant of $\boldsymbol{Y}_f(t)$ can be inferred as

$$\phi \geq \prod_{i=1}^{p}\lambda_i\left(\boldsymbol{Y}_f\right) \geq \mu^p\left(\sum_{j=1}^{k} e^{-aj\Delta T}\right)^p, \tag{A.64}$$

which proves (3.21) and also that $\boldsymbol{Y}_{\mathcal{I}} \in PE \implies \phi \in PE$.

It is noteworthy that if k is chosen as the largest integer such that $t \geq k\Delta T$. Then, $k \to \infty$ as $t \to \infty$ and, consequently,

$$\lim_{k\to\infty}\sum_{j=1}^{k} e^{-aj\Delta T} = \frac{1}{e^{a\Delta T}-1}, \tag{A.65}$$

which proves allegation (3.22).

A.5 Swapping Lemma

Applying Laplace's transform into the filtered regressor equations (3.7) and (3.8) yields

$$\boldsymbol{Y}_{\mathcal{I}}(s) = \frac{1}{\bar{a}_j}\left(s\boldsymbol{I} + b_j\boldsymbol{I}\right)\boldsymbol{Y}_{\phi_j}(s), \tag{A.66}$$

$$\tau_{\phi_j}(s) = \left(s\boldsymbol{I} + b_j\boldsymbol{I}\right)^{-1}\bar{a}_j\boldsymbol{Y}_{\mathcal{I}}(s)\boldsymbol{\theta}, \tag{A.67}$$

where the relation $\tau_{\mathcal{I}} = \boldsymbol{Y}_{\mathcal{I}}(\boldsymbol{q}, \dot{\boldsymbol{q}})\boldsymbol{\theta}$ has been used. Then, by direct substitution of (A.66) into (A.67), we obtain

$$\tau_{\phi_j} = \boldsymbol{Y}_{\phi_j}\boldsymbol{\theta}, \tag{A.68}$$

which concludes the proof.

A.6 Nonlinear $\mathcal{W}_\infty$ Control

The proof is conducted by replacing the following Lyapunov candidate function:

$$V(\tilde{\boldsymbol{x}}, t) = \frac{1}{2}\tilde{\boldsymbol{x}}'\boldsymbol{P}\tilde{\boldsymbol{x}}, \tag{A.69}$$

into the Hamilton-Jacobi equation, (4.18), which results in

$$\tilde{\boldsymbol{x}}'\boldsymbol{P}\dot{\tilde{\boldsymbol{x}}} + \frac{1}{2}\tilde{\boldsymbol{x}}'\begin{bmatrix}\boldsymbol{\Psi}_1 & \boldsymbol{0}\\ \boldsymbol{0} & \boldsymbol{\Psi}_0\end{bmatrix}\tilde{\boldsymbol{x}} + \frac{1}{2}\ddot{\tilde{\boldsymbol{q}}}'\boldsymbol{\Psi}_2\ddot{\tilde{\boldsymbol{q}}} - \frac{1}{2}\gamma^2\boldsymbol{\tau}_l^{*\prime}\boldsymbol{\tau}_l^{*} = 0. \tag{A.70}$$

In addition, considering (A.69) and substituting (4.13), (4.14) in (4.9), the acceleration error dynamics is given by

$$\ddot{\tilde{\boldsymbol{q}}} = \begin{bmatrix}-\boldsymbol{\Psi}_2^{-1} & \boldsymbol{0}\end{bmatrix}\boldsymbol{P}\tilde{\boldsymbol{x}}. \tag{A.71}$$

From (4.17), the closed-loop state-space dynamics is

$$\dot{\tilde{\boldsymbol{x}}} = \begin{bmatrix}\boldsymbol{0} & \boldsymbol{0}\\ \boldsymbol{I} & \boldsymbol{0}\end{bmatrix}\tilde{\boldsymbol{x}} - \begin{bmatrix}\boldsymbol{\Psi}_2^{-1} & \boldsymbol{0}\\ \boldsymbol{0} & \boldsymbol{0}\end{bmatrix}\boldsymbol{P}\tilde{\boldsymbol{x}}. \tag{A.72}$$

Then, replacing (A.71) and (A.72) into (A.70) yields

$$\boldsymbol{P}\begin{bmatrix}\boldsymbol{0} & \boldsymbol{0}\\ \boldsymbol{I} & \boldsymbol{0}\end{bmatrix} + \begin{bmatrix}\boldsymbol{0} & \boldsymbol{I}\\ \boldsymbol{0} & \boldsymbol{0}\end{bmatrix}\boldsymbol{P} - \boldsymbol{P}\begin{bmatrix}\boldsymbol{\Psi}_2^{-1} & \boldsymbol{0}\\ \boldsymbol{0} & \boldsymbol{0}\end{bmatrix}\boldsymbol{P} + \begin{bmatrix}\boldsymbol{\Psi}_1 & \boldsymbol{0}\\ \boldsymbol{0} & \boldsymbol{\Psi}_0\end{bmatrix} = 0, \tag{A.73}$$

which is the Riccati equation (4.19).

From (4.18) it is possible to infer that

$$\dot{V}(\tilde{\boldsymbol{x}}) = -\frac{1}{2}\tilde{\boldsymbol{x}}'\begin{bmatrix}\boldsymbol{\Psi}_1 & \boldsymbol{0}\\ \boldsymbol{0} & \boldsymbol{\Psi}_0\end{bmatrix}\tilde{\boldsymbol{x}} - \frac{1}{2}\ddot{\tilde{\boldsymbol{q}}}'\boldsymbol{\Psi}_2\ddot{\tilde{\boldsymbol{q}}} + \frac{1}{2}\gamma^2\boldsymbol{\tau}_l^{*'}\boldsymbol{\tau}_l^*. \tag{A.74}$$

Substituting the worst-case disturbance, (4.14), and (A.71) into (A.74) yields,

$$\dot{V}(\tilde{\boldsymbol{x}}) = -\frac{1}{2}\tilde{\boldsymbol{x}}'\left(\begin{bmatrix}\boldsymbol{\Psi}_1 & \boldsymbol{0}\\ \boldsymbol{0} & \boldsymbol{\Psi}_0\end{bmatrix} + \boldsymbol{P}\begin{bmatrix}\boldsymbol{\Psi_2}^{-1} & \boldsymbol{0}\\ \boldsymbol{0} & \boldsymbol{0}\end{bmatrix}\boldsymbol{P}\right)\tilde{\boldsymbol{x}} < 0, \tag{A.75}$$

which ensure asymptotically stability for system (4.3) in closed loop with the control law (4.13) for the worst case disturbance (4.14).

In addition, from (A.74) and $\mathbb{H}(\tilde{\boldsymbol{x}}, \boldsymbol{\tau}^*, \boldsymbol{\tau}_l) \leq \mathbb{H}(\tilde{\boldsymbol{x}}, \boldsymbol{\tau}^*, \boldsymbol{\tau}_l^*) \leq \mathbb{H}(\tilde{\boldsymbol{x}}, \boldsymbol{\tau}, \boldsymbol{\tau}_l^*)$, we have

$$\dot{V}(\tilde{\boldsymbol{x}}) \leq -\frac{1}{2}\tilde{\boldsymbol{x}}'\begin{bmatrix}\boldsymbol{\Psi}_1 & \boldsymbol{0}\\ \boldsymbol{0} & \boldsymbol{\Psi}_0\end{bmatrix}\tilde{\boldsymbol{x}} - \frac{1}{2}\ddot{\tilde{\boldsymbol{q}}}'\boldsymbol{\Psi}_2\ddot{\tilde{\boldsymbol{q}}} + \frac{1}{2}\gamma^2\boldsymbol{\tau}_l'\boldsymbol{\tau}_l.$$

Integrating both sides renders

$$\begin{aligned} V(\tilde{\boldsymbol{x}}(\infty)) - V(\tilde{\boldsymbol{x}}(t_0)) &\leq -\int_{t_0}^{\infty}\left(\frac{1}{2}\tilde{\boldsymbol{q}}'\boldsymbol{\Psi_0}\tilde{\boldsymbol{q}} + \frac{1}{2}\dot{\tilde{\boldsymbol{q}}}'\boldsymbol{\Psi_1}\dot{\tilde{\boldsymbol{q}}} + \frac{1}{2}\ddot{\tilde{\boldsymbol{q}}}'\boldsymbol{\Psi}_2\ddot{\tilde{\boldsymbol{q}}}\right)dt + \int_{t_0}^{\infty}\left(\frac{1}{2}\gamma^2\boldsymbol{\tau}_l'\boldsymbol{\tau}_l\right)dt, \\ &\leq -||\boldsymbol{z}(t)||^2_{\mathcal{W}_{2,2,\boldsymbol{\Psi}}} + \gamma^2||\boldsymbol{\tau}_l(t)||^2_{\mathcal{L}_2}. \end{aligned} \tag{A.76}$$

Therefore, since $\lim_{t\to\infty} V(\tilde{\boldsymbol{x}}(t)) = 0$, the closed-loop system (4.3) with the control law (4.20) ensures

$$||\boldsymbol{z}(t)||^2_{\mathcal{W}_{2,2,\boldsymbol{\Psi}}} \leq V(\tilde{\boldsymbol{x}}(t_0)) + \gamma^2||\boldsymbol{\tau}_l(t)||^2_{\mathcal{L}_2}. \tag{A.77}$$

Thus, concluding the proof.